

# Quantitative CT of the lungs: technical aspects and clinical studies

Citation for published version (APA):

Lamers, R. J. S. (1998). *Quantitative CT of the lungs: technical aspects and clinical studies*. [Doctoral Thesis, Maastricht University]. Maastricht University. <https://doi.org/10.26481/dis.19981218rl>

## Document status and date:

Published: 01/01/1998

## DOI:

[10.26481/dis.19981218rl](https://doi.org/10.26481/dis.19981218rl)

## Document Version:

Publisher's PDF, also known as Version of record

## Please check the document version of this publication:

- A submitted manuscript is the version of the article upon submission and before peer-review. There can be important differences between the submitted version and the official published version of record. People interested in the research are advised to contact the author for the final version of the publication, or visit the DOI to the publisher's website.
- The final author version and the galley proof are versions of the publication after peer review.
- The final published version features the final layout of the paper including the volume, issue and page numbers.

[Link to publication](#)

## General rights

Copyright and moral rights for the publications made accessible in the public portal are retained by the authors and/or other copyright owners and it is a condition of accessing publications that users recognise and abide by the legal requirements associated with these rights.

- Users may download and print one copy of any publication from the public portal for the purpose of private study or research.
- You may not further distribute the material or use it for any profit-making activity or commercial gain
- You may freely distribute the URL identifying the publication in the public portal.

If the publication is distributed under the terms of Article 25fa of the Dutch Copyright Act, indicated by the "Taverne" license above, please follow below link for the End User Agreement:

[www.umlib.nl/taverne-license](http://www.umlib.nl/taverne-license)

## Take down policy

If you believe that this document breaches copyright please contact us at:

[repository@maastrichtuniversity.nl](mailto:repository@maastrichtuniversity.nl)

providing details and we will investigate your claim.

## Quantitative CT of the lungs

© R.J.S. Lamers, Maastricht 1998  
ISBN 90 9012277 x

Vormgeving en druk: Datawyse boekproducties Maastricht

# **Quantitative CT of the lungs**

Technical aspects and clinical studies

## PROEFSCHRIFT

ter verkrijging van de graad van doctor  
aan de Universiteit Maastricht  
op gezag van de Rector Magnificus,  
Prof. Dr. A.C. Nieuwenhuijzen Kruseman  
volgens het besluit van het College van Decanen  
in het openbaar te verdedigen  
op vrijdag 18 december 1998 om 12.00 uur

door

R.J.S. Lamers

*Promotores:*

Prof. Dr. J.M.A. van Engelshoven

Prof. Dr. E.F.M. Wouters

*Co-promotor:*

Dr. G.J. Kemerink

*Beoordelingscommissie:*

Prof. Dr. J.W. Arends (voorzitter)

Prof. Dr. C.L.A. van Herwaarden (Katholieke Universiteit Nijmegen)

Prof. Dr. S.C.M. Luijendijk

Prof. Dr. J.A. Verschakelen (Katholieke Universiteit Leuven)

The publication of this thesis was financially supported by:

Astra Pharmaceutica Benelux, GlaxoWellcome, Nycomed, Schering, Siemens, Zambon.

*Aan: mijn ouders  
Gerti  
Michiel, Jeroen, Stephan*



---

# Table of contents

CHAPTER 1	
General introduction	9
CHAPTER 2	
Chronic obstructive pulmonary disease: a review	15
CHAPTER 3	
CT lung densitometry: a review	29
CHAPTER 4	
Scanner conformity in CT densitometry of the lungs	41
CHAPTER 5	
On segmentation of lung parenchyma in quantitative computed tomography of the lung	51
CHAPTER 6	
Reproducibility of spirometrically controlled CT lung densitometry in a clinical setting	69
CHAPTER 7	
Chronic obstructive pulmonary disease: evaluation with spirometrically controlled CT lung densitometry	79
CHAPTER 8	
Emphysema and airflow limitation in patients with advanced chronic obstructive pulmonary disease: a CT study	93
CHAPTER 9	
CT lung densitometry and visual assessment of thin-section CT in the diagnosis of coal worker's pneumoconiosis	111



## CHAPTER 10

Summary and conclusions 127

Samenvatting 133

Acknowledgments 139

Curriculum vitae 141

## CHAPTER 1

# General introduction

Attenuation of an X-ray beam is caused by coherent scattering, the photo-electric effect and Compton scattering. The contribution of each these effects depends on the photon energy as well as the atomic numbers and the density of the exposed tissue. For the X-rays commonly used in computed tomography (CT), the photo-electric effect prevails for iodine or barium containing contrast media while the Compton effect is dominant for soft tissues. For bone both effects contribute significantly to the attenuation.

A CT scanner has the unique property that it accurately measures the X-ray attenuation in a cross-section of the body. The map of these attenuation values is the CT image. However, it is common practice not to present the linear attenuation coefficient ( $\mu$ ) itself, but a derived quantity that is called the CT number. The definition is:  $CT\ number_{tissue} = 1000 (\mu_{tissue} - \mu_{water}) / \mu_{water}$ . Its unit is the Hounsfield or Hounsfield unit (HU). The CT image is generally evaluated by visual inspection, but the CT number can also be used in a quantitative way. Soon after the introduction of CT, applications were developed to quantify bone mineral content, diffuse lung pathology, and brain perfusion using inhalation of xenon. Diffuse lung pathology was quantified by the density of the lung, which has a linear relationship to the CT number.

CT densitometry of the lungs has been proposed as a sensitive tool to diagnose a wide variety of pulmonary disorders. Applications range from assessing pulmonary emphysema (1-14), sarcoidosis (15), panbronchiolitis (16), coal worker's pneumoconiosis (17), radiation induced pneumonitis (18), pulmonary edema (19), characterization of pulmonary nodules (20), to bleomycin-related lung damage (21,22).

Despite favorable reports (4,5,12,13), CT densitometry of the lungs has not been yet applied as a clinical tool. Comparison of densitometric results obtained on different scanners and/or for different patients is difficult for various reasons. Most early CT scanners were not optimized for densitometry in the low density range. A large variability in absolute CT numbers between scanners of various manufacturers has been observed (23,24). Moreover, internationally accepted protocols for CT lung densitometry were not available. CT numbers were affected by the reconstruction algorithm, slice thickness, object size and variations in the tube high voltage (24-29). Reproducibility errors due to the operator's intervention in the evaluation process may exceed 10 HU (30). An additional problem in CT densitometry of the lungs (compared to bone and brain) is the influence of the level of inspiration. At inspiration

the lung contains more air compared to expiration which results in a considerable variation in lung density between in- and expiration (31). Patients will generally not be able to exhale to some fixed level. Control of the level of inspiration, especially when intermediate respiratory levels are required, is therefore mandatory to obtain reproducible results of lung density.

Modern CT scanners are much better optimized for densitometry in the low density range. The stability of our system for measuring air density is for example within 1 HU and for water density within 2 HU (32). The accuracy and reproducibility for densities found in the lung are within 2-3 percent (32). Spirometric gating to control the respiratory level of the patient during data acquisition has increased the reproducibility of this method enormously (33), and so has semiautomated evaluation procedures that extract the relevant densitometric parameters from the CT data (30,34).

Densitometry has the potential to diagnose and quantify pulmonary emphysema, chronic bronchitis, or interstitial lung disorders. Densitometry of the lungs can provide an objective quantification of changes in lung density over time and may determine at what level the airway obstruction may be occurring (35). Results may be useful for epidemiologic, transverse and longitudinal studies. It is not easy but nevertheless critical to distinguish chronic bronchitis from emphysematous patients with chronic obstructive lung disease because they have a different treatment and prognosis (36). In epidemiologic studies this distinction is important to discover risk factors. CT densitometry may be of help in lung reduction surgery in case of advanced emphysema by determining the site of greatest severity prior to operation that aims at reducing breathlessness (37). It may become possible to quantitatively assess the morphologic changes in the lungs after therapeutic interventions (38).

In spite of this large potential, CT densitometry of the lungs will not find broad introduction into clinical practice until all variables affecting densitometry are under control and scan protocols have been developed that give comparable results on all CT scanners.

## Outline of the thesis

Chapter 2 focuses on several important aspects of chronic obstructive pulmonary disease: definition, pathologic characterization, clinical features, pulmonary function tests and radiological diagnosis. In chapter 3 the relevant literature on CT densitometry of the lung is reviewed. The technique of respiratory gating of the CT scanner, the technical parameters used in CT densitometry of the lung, as well as the method used in this thesis for extracting density information from CT scans are described. Subsequently, dosimetrical aspects of our CT densitometry protocol are discussed. In chapter 4 inter- and intrascanner conformity in CT densitometry of the lung is quantified.

In chapter 5 the influence of scan protocol and post-processing on estimated lung density is evaluated as a contribution to the standardization of the technique. In chapter 6 the issue of reproducibility of spirometric gated CT lung densitometry at defined levels of inspiration is addressed. In chapter 7 the potential of quantitative CT to distinguish between patients with emphysema, chronic bronchitis and healthy individuals is studied. In chapter 8 we assessed the association of emphysema with airflow limitation in patients with chronic obstructive pulmonary disease and studied the point of debate whether the single breath carbon monoxide diffusing capacity can be used as an indicator for emphysema in these patients. In chapter 9 the usefulness of CT lung densitometry in interstitial lung disease is investigated and the most suitable level of inspiration to assess severity and extent of interstitial lung disease is defined in a population of coal miners. Chapter 10 contains a summary and conclusions of this thesis.

## REFERENCES

1. Goddard PR, Nicholson EM, Laszlo G, Watt I. Computed tomography in pulmonary emphysema. *Clin Radiol* 1982; 33:379-387.
2. Hayhurst MD, Flenley DC, McLean A, et al. Diagnosis of emphysema by computerised tomography. *Lancet* 1984; 2:320-322.
3. Bergin C, Müller N, Nichols DM, et al. The diagnosis of emphysema: a computed tomographic-pathologic correlation. *Am Rev Respir Dis* 1986; 133:541-546.
4. Gould GA, Macnee W, McLean A, et al. CT measurements of lung density in life can quantitate distal airspace enlargement: an essential defining feature of human emphysema. *Am Rev Respir Dis* 1988; 137:380-392.
5. Müller NL, Staples CA, Miller RR, Abboud RT. "Density mask": an objective method to quantitate emphysema using computed tomography. *Chest* 1988; 94:782-787.
6. Biernacki W, Gould GA, Whyte KF, Flenley DC. Pulmonary hemodynamics, gas exchange, and the severity of emphysema as assessed by quantitative CT scan in chronic bronchitis and emphysema. *Am Rev Respir Dis* 1989; 139:1509-1515.
7. Kinsella M, Müller NL, Abboud RT, Morrison NJ, DyBuncio A. Quantification of emphysema by computed tomography using a "density mask" program and correlation with pulmonary function tests. *Chest* 1990; 97:315-321.
8. Knudson RJ, Standen JR, Kaltenborn WT, et al. Expiratory computed tomography for assessment of suspected pulmonary emphysema. *Chest* 1991; 99:1357-1366.
9. Gould GA, Redpath AT, Ryan M, et al. Lung CT density correlates with measurements of airflow limitation and the diffusing capacity. *Eur Respir J* 1991; 4:141-146.
10. Guenard H, Mamadou H, Diallo HH, Laurent F, Vergeret J. Lung density and lung mass in emphysema. *Chest* 1992; 102:198-203.
11. Gould GA, Redpath AT, Ryan M, et al. Parenchymal emphysema measured by CT lung density correlates with lung function in patients with bullous disease. *Eur Respir J* 1993; 6:698-704.
12. Gevenois PA, de Maertelaer V, De Vuyst P, Zanen J, Yernault JC. Comparison of computed density and macroscopic morphometry in pulmonary emphysema. *Am J Respir Crit Care Med* 1995; 152:653-657.

13. Gevenois PA, De Vuyst P, Sy M, et al. Pulmonary emphysema: quantitative CT during expiration. *Radiology* 1996; 199:825-829.
14. Eda S, Kubo K, Fujimoto K, Matsuzawa Y, Sekiguchi M, Sakai F. The relations between expiratory chest CT using helical CT and pulmonary function tests in emphysema. *Am J Respir Crit Care Med* 1997; 155:1290-1294.
15. Gilman MJ, Laurens RG, Somogyi, Honig EG. CT attenuation values of lung density in sarcoidosis. *J Comput Assist Tomogr* 1983; 7:407-410.
16. Murata K, Itoh H, Senda M, et al. Stratified impairment of pulmonary ventilation in "diffuse panbronchiolitis:" PET and CT studies. *J Comput Assist Tomogr* 1989; 13:48-53.
17. Bergin CJ, Müller NL, Vedal S, Chan-Yeung M. CT in silicosis: correlation with plain films and pulmonary function tests *AJR* 1986; 146:477-4833.
18. van Dyk J, Keane TJ, Rider WD. Lung density as measured by computerized tomography: implications for radiotherapy. *Int J Radiol Oncol Biol Phys.* 1982; 8:1363-1372.
19. Hedlund LW, Effmann E, Bates WM, Beck JW, Goulding PL, Putman CE. Pulmonary edema: a CT study of regional changes in lung density following oleic acid injury. *J Comput Assist Tomogr* 1982; 6:939-946.
20. Siegelman SS, Zerhouni EA, Leo FP, Khouri NF, Stitik FP. CT of the pulmonary solitary nodule. *AJR* 1980; 135:1-13.
21. Bellamy EA, Husband JE, Blaquiére RM, Law MR. Bleomycin-related lung damage: CT evidence. *Radiology* 1985; 156:155-158.
22. Bellamy EA, Nicholas D, Husband JE. Quantitative assessment of lung damage due to bleomycin using computed tomography. *Br J Radiol* 1987; 60:1205-1209.
23. Levi C, Gray JE, McCullough EC, Hattery RR. The unreliability of CT numbers as absolute values. *AJR* 1982; 139:443-447.
24. Zerhouni EA, Spivey JF, Morgan RH, Leo FP, Stitik FP, Siegelman SS. Factors influencing quantitative CT measurements of solitary pulmonary nodules. *J Comput Assist Tomogr* 1982; 6:1075-1087.
25. McCullough EC, Morin RL. CT-number variability in thoracic geometry. *AJR* 1983; 141:135-140.
26. Adams H, Bernard MS, McConnochie K. An appraisal of CT pulmonary density mapping in normal subjects. *Clin Radiol* 1991; 43:238-242.
27. Kemerink GJ, Kruize HH, Lamers RJS. Density resolution in quantitative computed tomography of foam and lung. *Med Phys* 1996; 23:1697-1708.
28. Kemerink GJ, Kruize HH, Lamers RJS, van Engelshoven JMA. CT lung densitometry: dependence of CT number histograms on sample volume and consequences for scan protocol comparability. *J Comput Assist Tomogr* 1997; 21:948-954.
29. Kemerink GJ, Kruize HH, Lamers RJS. The CT's sample volume as an approximate, instrumental measure for density resolution in densitometry of the lung. *Med Phys* 1997; 24:1615-1620.
30. Kalender WA, Fichte H, Bautz W, Skalej M. Semiautomatic evaluation procedures for quantitative CT of the lung. *J Comput Assist Tomogr* 1991; 15:248-255.
31. Robinson PJ, Kreel L. Pulmonary tissue attenuation with computed tomography: comparison of inspiration and expiration scans. *J Comput Assist Tomogr* 1979; 3:740-748.
32. Kemerink GJ, Lamers RJS, Thelissen GRP, van Engelshoven JMA. CT densitometry of the lungs: scanner performance. *J Comput Assist Tomogr* 1996; 20:24-33.
33. Kalender WA, Rienmüller R, Seissler W, Behr J, Welke M, Fichte H. Measurement of pulmonary parenchymal attenuation: use of spirometric gating with quantitative CT. *Radiology* 1990; 175:265-268.
34. Archer DC, Coblenz CL, deKemp RA, Nahmias C, Norman G. Automated in vivo quantification of emphysema. *Radiology* 1993; 188:835-838.
35. Müller NL, Thurlbeck WM. Thin-section CT, emphysema, air trapping, and airway obstruction. *Radiology* 1996; 199:621-622.
36. Burrows B, Bloom JW, Traver GA, Cline MG. The course and prognosis of different forms of chronic airways obstruction in a sample from the general population. *N Engl J Med* 1987; 317:1309-1314.

37. Bae KT, Slone RM, Gierada DS, Yusem RD, Cooper JD. Patients with emphysema: quantitative CT analysis before and after lung volume reduction surgery. *Radiology* 1997; 203:705-714.
38. Holbert JM, Brown ML, Sciurba FC, Keenan RJ, Landreneau RJ, Holzer AD. Changes in lung volume and volume of emphysema after unilateral lung reduction surgery: analysis with CT lung densitometry. *Radiology* 1996; 201:793-797.



## CHAPTER 2

---

# Chronic obstructive pulmonary disease: a review



## 2.1 Introduction

Chronic obstructive pulmonary disease (COPD), a relatively common form of chronic lung disease, is defined as a disease state characterized by the presence of airflow obstruction due to emphysema or chronic bronchitis (1). The airflow obstruction is generally progressive. The major risk factor is cigarette smoking and 15% of all cigarette smokers develop clinically significant COPD (2). Knowledge of the prevalence of COPD in the Netherlands is incomplete. In the United States it is estimated that about 4-6% of adult white males and about 1-3% of adult white females suffer from COPD (1). In 1991, in the United States, the associated death rate was 18.6 per 100,000 persons per year. Age of starting, total pack-years and current smoking status are predictive of COPD mortality. COPD ranked as the fourth leading cause of death in the United States (1). It is essential to distinguish emphysematous from chronic bronchitis forms of COPD since they have such a different prognosis (3).

## 2.2 Definitions

Emphysema is a pathological entity defined by the American Thoracic Society in strictly morphologic terms as a condition of the lung characterized by abnormal permanent enlargement of airspaces distal to the terminal bronchioles accompanied by destruction of their walls and without obvious fibrosis (4).

Chronic bronchitis is a poorly defined condition. In contrast to emphysema, chronic bronchitis is defined on clinical criteria as recurrent excess of secretion in the bronchial tree occurring on most days for at least three months of the year for at least two successive years in a patient in whom other causes of cough have been excluded (5). Although not included in the definition of chronic bronchitis, chronic airflow obstruction is commonly present.

## 2.3 Pathologic characterization of COPD

Emphysema is classified by the way the acinus is involved (1,6,7). Three patterns are recognized, each having a characteristic distribution within the lung. The most common type is proximal acinar emphysema which characteristically destroys the proximal portion of the acinus with a predominance in the upper zones of the lungs. It is the most frequent type of emphysema among cigarette smokers (6,8). The second type of emphysema, panacinar emphysema, destroys the acinus more or less uniformly. It is more common in the lower zones of the lungs, and is the predominant type of emphysema in patients with  $\alpha_1$ -antitrypsin deficiency. The third type of emphysema, distal

acinar emphysema, dominantly involves the peripheral part of the acinus. Distal acinar emphysema is almost always seen in the periphery of the lung, along interlobular fibrous septa or beneath the pleura. The remainder of the lung is often spared. Proximal acinar emphysema and panacinar emphysema may coexist (8).

Pathologic findings in the bronchial walls of patients with chronic bronchitis are a chronic inflammatory reaction in the small airways - airways less than 2-3 mm in diameter - consisting of cellular infiltration, goblet metaplasia, smooth muscle hyperplasia, accompanied by connecting tissue deposition (9,10). Mucus secretion and mucus gland hyperplasia are characteristic histological findings in the large airways (11).

## 2.4 Clinical features of COPD

Patients with COPD have usually been smoking more than 20 cigarettes per day for more than 20 years before symptoms develop (1). Symptoms commonly present in the fifth decade of life with productive cough or an acute chest illness (1). Sputum production is insidious, initially occurring in the morning. Sputum is usually mucoid but becomes purulent with exacerbation. With progression, the intervals between acute exacerbation grow shorter. Dyspnea on effort usually does not occur until the sixth or seventh decade. It is clinically difficult to distinguish emphysema from chronic bronchitis because of the similar symptoms of wheezing, cough and shortness of breath (12,13).

## 2.5 Pulmonary function tests in COPD

A decrease in maximal expiratory flow is a functional hallmark of COPD. Abnormalities in the small airways function tests are related to the inflammatory process in these small airways (14-17), the most important site of increased resistance in the lungs of patients with established COPD (18-21). The mechanisms by which the inflammatory changes in the airways lead to excessive airway narrowing remains unclear. Forced expiratory volume in one second ( $FEV_1$ ) is the most useful test of airflow dynamics. In this thesis, patients with fixed airway obstruction were considered to have COPD if the prebronchodilator  $FEV_1$  was less than 70% of the predicted value, if this  $FEV_1$  did not change over several months and if a difference between prebronchodilator and post-bronchodilator values of  $FEV_1$  did not exceed 10% of predicted.

Airflow limitation at spirometry and disturbance of gas exchange, manifested by reduced single-breath carbon monoxide diffusing capacity ( $DL_{CO}$ ), have been proposed as the most accurate and specific pulmonary function tests for pulmonary em-

physema (22). Correlations between various pulmonary function tests and the pathologic extent of emphysema range from 0.4 to 0.7 (23). The mechanism of airflow limitation in emphysema involves emphysematous destruction of parenchymal support of the peripheral airways and/or loss of elastic recoil force driving air out of the lung (24,25). Although emphysema is considered part of the spectrum of chronic obstructive pulmonary diseases, expiratory air-flow obstruction is not invariably present (26). Patients with severe emphysema may have few symptoms and little evidence of airflow obstruction, while patients with moderate grades of emphysema may have significant disabling pulmonary dysfunction (27). Patients may have up to 30 percent of their lung function involved with emphysema and no evidence of functional impairment (28). Many authors agree that emphysema has a dominant role in causing airflow limitation (25,26,28), whereas others state the opposite (2,30,31).

The  $DL_{CO}$ , whether measured using a single breath or a steady state method, expressed in absolute terms, as percent predicted, or as function of the alveolar volume, has constantly been the best predictor of emphysema (22,32). The impairment of  $DL_{CO}$  present in emphysema may arise from breakdown of alveolo-capillary surface area, the concomitant loss of pulmonary arteries leading to impairment in diffusion in the enlarged airspaces and decreased diffusion of carbon monoxide into the pulmonary blood. Patients are considered to have emphysema if they meet the ATS criteria for functional emphysema:  $DL_{CO}$  less than 80% of the predicted value and  $FEV_1$  less than 80% of the predicted value (4). However,  $DL_{CO}$  is decreased in a number of pulmonary disorders (33).  $DL_{CO}$  provides only a very imprecise quantification of the grade of macroscopic emphysema (26). The upper zones of the lungs are a relatively silent region where extensive destruction may occur before functional abnormalities become evident (34). Therefore there may be an apparent discrepancy between the radiologic extent of emphysema and the physiologic measurements of emphysema.

## 2.6 Radiologic diagnosis of COPD

### *Chest radiography*

Findings indicative of emphysema on a chest radiograph are overinflation and pulmonary vascular abnormalities (13,28). Overinflation is represented by a low and flat diaphragm and an enlarged retrosternal air-space. Pulmonary vascular abnormalities are indicated by excessive rapid tapering of vascular shadows, local areas of oligemia and prominent hilar vascular shadows (13). However, these findings are difficult to detect before the disease is severe (6). The diagnosis of emphysema from the chest radiograph is neither very accurate nor specific (35). There are no criteria which permit more than an approximate estimate of the severity of emphysema from the chest ra-

diograph. The chest radiograph diagnosis is usually 'yes-no' which is in contradiction with the natural behavior of the disease which is slowly progressive and of insidious onset. It is thus hardly possible to quantitate the severity and extent of emphysema by chest radiography. Chest radiographs are useful for making a diagnosis of moderate to severe emphysema.

Radiographic abnormalities in patients with chronic bronchitis generally reflect bronchial wall thickening (36). However, bronchial wall thickening has no fixed definitions and abnormalities are non-specific. The diagnosis of bronchial wall thickening is very subjective and is influenced by the degree of inspiration. Up to 50% of patients with clinically defined chronic bronchitis have a normal chest film (37).

### *Computed tomography*

It is generally conceded that CT is superior to chest radiography in assessing the presence and extent of parenchymal abnormalities (23,38). Emphysema is diagnosed on CT by hypodense areas of pulmonary parenchyma without clear margins, usually associated with pruning, obliteration, or abnormal course of the adjacent pulmonary vessels. In the past CT scans were obtained with long scan times and 1-cm collimation. However, thick sections resulted in volume averaging within the plane of section and a decreased resolution so that the anatomic detail provided was insufficient. Modern CT scanners provide 1-mm collimation and scan times of 1 second with high spatial resolution, enabling recognition of normal and diseased lobular structures. With optimal technical parameters, namely large matrix size, small field of view, thin-sections, and use of an ultra-high resolution filter, spatial resolution is reported to be 0.5 to 0.8 mm (39). High-resolution CT (HRCT) has shown to be superior to conventional CT in evaluating chronic diffuse lung disease (23), and the overall extent of emphysema is more conspicuous and more reliably diagnosed (40). HRCT is recognized as a powerful technique for the identification of the type of emphysema (41). Proximal emphysema of mild to moderate severity appears as a localized area of abnormally low attenuation located near the vessels in the center of a secondary lobule, approximately 0.5 cm in diameter (Figure 1). Panacinar emphysema is characterized by extensive areas of uniform low attenuation and a predominant lower lobe distribution (Figure 2). Distal acinar emphysema may be recognized by bullae, with a tendency to subpleural localizations (Figure 3). As emphysema becomes more severe, classification into subtypes becomes difficult. Different types of emphysema may coexist in the same person. A disadvantage of HRCT is that it is not so good at showing the vascular changes (42).

Specific HRCT findings of chronic bronchitis are usually lacking. Possible manifestations of chronic bronchitis on HRCT are thickening of the bronchial wall and some small airway abnormalities. A nodular branching structure resembling a bud-



**Figure 1.** Proximal acinar emphysema: HRCT scan through the upper zones of the lungs shows multiple localized areas of low attenuation, 2-10 mm in diameter.



**Figure 2.** Advanced panacinar emphysema: HRCT scan through the upper zones of the lungs demonstrates widespread areas of low attenuation and diminished vascular markings.

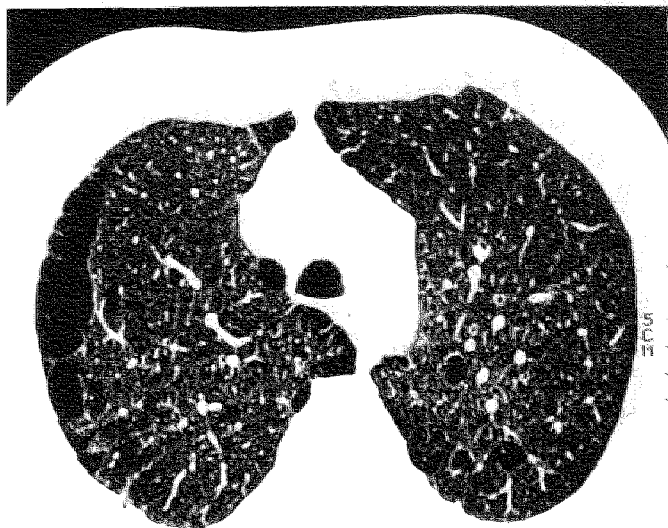


**Figure 3.** Distal acinar emphysema: HRCT scan through the upper zones of the lungs shows areas of subpleural emphysema most appropriately termed bullae.

ding tree in the lung periphery representing bronchiolar dilatation and filling of the lumen by mucus, pus, or fluid may be observed (42). At full inspiration, intervening lung parenchyma is normal. Expiratory CT scans may be useful to identify the subtle airway abnormalities indicative of air trapping in the evaluation of COPD (43).

## 2.7 Quantification of emphysema on CT

There are two ways to quantify the extent of emphysema using CT; subjectively by visual inspection for areas of emphysematous destruction, and objectively, by quantitative analysis of the density of the lung.

### *Visual assessment of emphysema*

CT compares favorably to pathological specimens and may be considered the gold standard for diagnosing emphysema *in vivo* (40,44-47). Emphysema is identified as non-peripheral unmarginated low-attenuation areas usually associated with vascular pruning or pulmonary vascular distortion. Three visual scoring methods have been employed to estimate the degree of emphysema: a grid method, a panel grading method, and a direct observational method introduced by Goddard.

The grid method is an accurate method of assessing emphysema on CT according to a pathological grid scoring system (45,46). A grid with squares corresponding to 1 cm<sup>2</sup> is placed on the CT image and the extent and severity of emphysema in each square is determined. Approximately 50 boxes per lung field, and 500 boxes per patient have to be analyzed. The CT emphysema score is expressed in the percentage of squares containing emphysema. The grid method is complex and extremely time-consuming and therefore not suitable for clinical application.

The panel grading scoring method (40,46) is a modification of the application of a panel of 16 standard photographs of parasagittal whole lung sections established by Thurlbeck et al (48). The grading panel of standards is based on recurring patterns of emphysematous lung destruction. Five CT slices are graded separately on a scale of zero to 100 by comparing the destructive changes seen radiographically to the grading panel according to the percentage that demonstrated changes suggestive of emphysema. Mild, moderate, and severe emphysema are scored 20, 50 and 80, respectively. The most severely emphysematous lung is given a score of 100. The standards in this system are allocated at intervals of 5 from zero to 50 and at intervals of 10 from 60 to 100. The mean of CT scores for the CT slices is calculated. Comparison of horizontal CT slices against the parasagittal sections of the panel is observer dependent.

The method introduced by Goddard et al is a direct observational method of assessing the extent of emphysema (47). The left and right lung in each CT slice are graded separately according to the percentage area that demonstrates changes suggestive of emphysema. A grade of 0 is given if there was no abnormality. If less than 25% of the pulmonary parenchyma in a slice is considered to show vascular disruption and low attenuation compared with the remaining lung parenchyma, the score is 1; between 25-50%, the score is 2; between 50-75%, the score is 3; up to a maximum of 4 if more than 75% of the lung parenchyma on one side shows changes suggestive of emphysema. The maximal emphysema score per CT slice is 8. Approximately 16-24 CT slices have to be evaluated. The CT emphysema score of each patient is calculated by adding the emphysema score for each level and dividing by the total possible maximal score for each individual.

In this thesis, assessment of emphysema was carried out to a visual score introduced by Sakai et al (49) which is in fact a modification of the method of Goddard (47). This method, contrary to the method of Goddard, also takes the severity of emphysema into account. It is a very useful method for application in clinical practice. Assessing severity and extent of pulmonary emphysema according to this method takes approximately three minutes per patient. The interobserver correlation is high ( $r = 0.89$ ,  $p < 0.001$ ). Grading emphysema on CT using this method is as precise as using the grid method (49). Each section of the lung is scored for the severity according to a four-point scale, as follows: 0, no emphysema; 1, low-attenuation areas smaller than 5 mm

in diameter; 2, circumscribed low-attenuation areas larger than 5 mm in diameter in addition to those smaller than 5 mm in diameter; and 3, diffuse low-attenuation areas without intervening normal lung of large, confluent low-attenuation areas. The extent of emphysema was scored for each section also according to a four point scale; 1, less than 25% cross-sectional area involvement; 2, 25%-50% cross-sectional involvement; 3, 50%-75% cross-sectional area involvement; and 4, more than 75% cross-sectional area involvement. The CT emphysema score is based on the evaluation of 5 CT sections. For each of the 10 lung sections, the score for severity of emphysema was multiplied by the score for the extent, and the resultant scores were subsequently summed to a final CT emphysema score which could range from zero to 120. The scoring method of Sakai is illustrated in the figures 4 to 6.

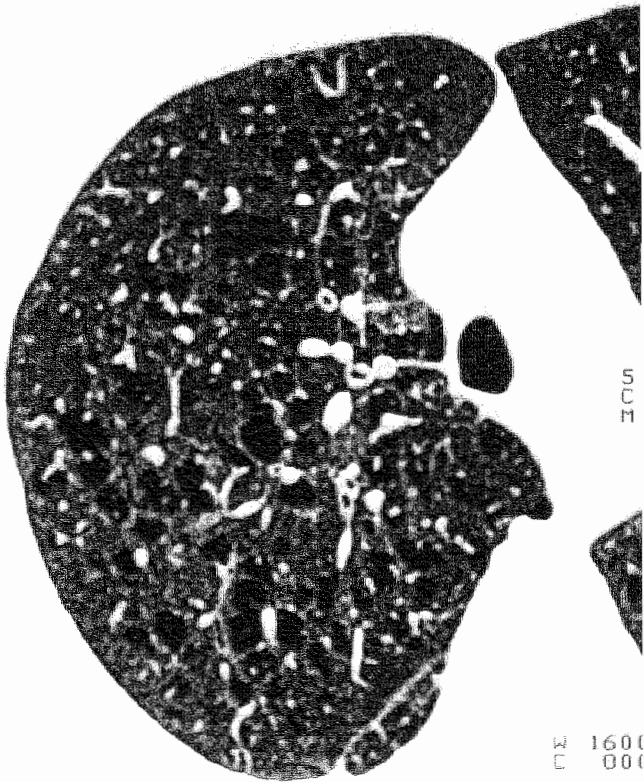


**Figure 4.** HRCT scan of the right lung demonstrates proximal acinar emphysema and normal vascular markings with a severity score of 1 and an extent score of 4.





**Figure 5.** HRCT scan of the right lung shows panacinar emphysema and diminished vascular markings with a severity score of 3 and an extent score of 2.

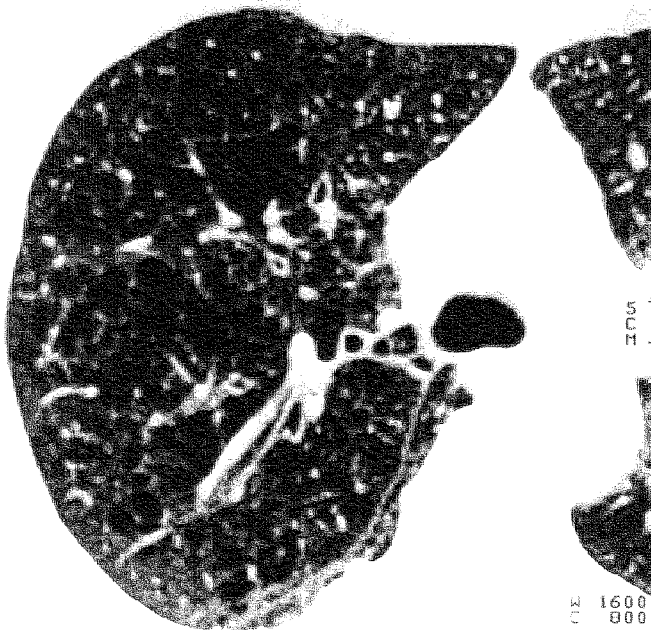


**Figure 6.** HRCT scan of the right lung shows panacinar emphysema and normal vascular markings with a severity score of 2 and an extent score of 4.

### *Quantitative assessment of emphysema*

Drawbacks of visual scoring techniques relate to the experience of the observer and the effort and time they require. Ultimate results are dependent on window settings. There is a 10% intra- and interobserver variability (50). The mildest forms of emphysema may be missed (45). To avoid subjectivity, methods have been developed to calculate objectively the relevant density characteristics from the CT sections. The value of CT densitometry in the assessment of parenchymal lung disease is discussed in chapter 3.

### **2.8 Correlation between visual assessment of emphysema by CT and pathologic grading**

Foster et al (50) tried to establish which CT sign is most valuable for the diagnosis of emphysema on CT. They evaluated the *in vivo* CT scans of 25 patients who later died. CT scans were obtained with 1-cm collimation at 1-cm intervals through the chest. The following signs were evaluated: nonperipheral low-attenuation areas, pulmonary vascular pruning, pulmonary vascular distortion, and visual density gradient. Post-mortem the lungs were fixed in the inflated state and assessed for the presence and severity of proximal acinar emphysema. Nonperipheral low-attenuation areas formed the CT sign which correlated best with the pathologic grade of emphysema (upper zones:  $r = 0.84$ , lower zones:  $r = 0.78$ ).

Bergin et al (44) assessed the accuracy of CT in the diagnosis of emphysema. One-cm collimated scans were obtained at 1-cm intervals from 32 patients prior to surgery for removal of suspected tumors. The extent of emphysema seen on CT was assessed using the method of Goddard (48). They found significant correlations between the CT score and the pathologic score for resected lobes ( $r = 0.57$ ,  $p < 0.001$ ) and for resected lungs ( $r = 0.64$ ,  $p < 0.001$ ). The authors concluded that CT was a useful adjunct in the assessment of severity and extent of emphysema.

Miller et al (45) analyzed 1-cm and 1.5-mm collimated scans obtained at 1-cm intervals from 38 patients, who underwent lobe or lung resection for malignancy, for the purpose of CT-pathologic correlation. The CT emphysema score was assessed using a grid method whereas the pathologic grade of emphysema was assessed using the grid method as well as the panel grading method. Correlations were better for the panel grading method than for the grid method. Correlation between the CT emphysema score and the pathologic grade was 0.81 for the 1-cm collimated and 0.85 for the 1.5-mm collimated scans. CT underestimated the extent of proximal acinar emphysema as well as panacinar emphysema because most lesions less than 0.5 cm were missed.

Hruban et al (46) assessed the accuracy of HRCT in the diagnosis of emphysema. Autopsied lungs were dried and fixed for the purpose of the radiologic study. Five 2-mm collimated scans were obtained of the lung specimens. Subsequently the pathologist sectioned the lung specimens along the planes of the CT scans. The extent of emphysema seen on CT was assessed using the panel-grading method for the purpose of CT - pathologic correlation. The authors found significant correlation between the CT emphysema score and the pathologic grade ( $r = 0.91$ ,  $p < 0.005$ ). They considered visual assessment of emphysema on HRCT, a reliable technique for the detection and quantification of emphysema even in its earliest stages.

Kuwano et al (40) determined the accuracy of CT scans in the assessment of clinically silent and mild emphysema. One- and 5-mm collimated scans were obtained from 42 patients who underwent surgery for removal of a pulmonary nodule. The extent of emphysema seen on CT was assessed using the panel grading method. The correlations between the CT emphysema score and the pathological grade were 0.68 for the 1-mm collimated scans and 0.75 for the 5-mm collimated scans. The authors concluded that HRCT scans can help to identify the presence and grading of mild emphysema. The detection of areas of low attenuation was more important in the diagnosis of emphysema than the evaluation of the vascular pattern.

## References

1. Standards for the diagnosis and care of patients with chronic obstructive pulmonary disease. *Am J Respir Crit Care Med* 1995; 152:S77-S120.
2. Hogg JC, Wright JL, Wiggs BR, Coxson HO, Opazo Saez A, Paré PD. Lung structure and function in cigarette smokers. *Thorax* 1994; 49:473-478.
3. Burrows B, Bloom JW, Traver GA, et al. The course and prognosis of different forms of chronic airways obstruction in a sample from the general population. *N Engl J Med* 1987; 317:1309-1314.
4. Snider GL, Kleinerman J, Thurlbeck WM, Bengali ZK. The definition of emphysema: report of a National Heart, Lung, and Blood Institute, Division of Lung Diseases Workshop. *Am Rev Respir Dis* 1985; 132:182-185.
5. American Thoracic Society. Chronic bronchitis, asthma, and pulmonary emphysema: Statement by the Committee on Diagnostic Standards for Nontuberculous Respiratory Diseases. *Am Rev Respir Dis* 1962; 85:762-768.
6. Snider GL. Emphysema: the first two centuries and beyond. *Am Rev Respir Dis* 1992; 146:1334-1344.
7. Stern EJ, Frank MS. CT of the lung in patients with pulmonary emphysema: diagnosis, quantification, and correlation with pathologic and physiologic findings. *AJR* 1994; 162:791-798.
8. Thurlbeck WM. Pathology of the lung. New York: Thieme Medical Publishers, 1987. 538-550.
9. Mullen JMB, Wright JL, Wiggs BR. Reassessment of airways in chronic bronchitis. *Br Med J* 1985; 291:1235-1239.
10. American Thoracic Society. Standards for the diagnosis and care of patients with chronic obstructive pulmonary disease (COPD) and asthma. *Am Rev Respir Dis* 1987; 136:225-243.
11. Reid L. The pathology of emphysema. London: Lloyd-Duke Ltd., 1967.
12. Snider GL. Distinguishing among asthma, chronic bronchitis, and emphysema. *Chest* 1985; 87:35S-39S.
13. Sanders C. The radiographic diagnosis of emphysema. *Radiol Clin North Am* 1991; 29:1019-1030.

14. Wright JL, Lawson LM, Paré PD, Kennedy S, Wiggs B, Hogg JC. The detection of small airways disease. *Am Rev Respir Dis* 1984; 129:989-994.
15. Cosio M, Ghezzi H, Hogg JC, et al. The relations between structural changes in small airways and pulmonary function tests. *N Engl J Med* 1978; 298:1277-1281.
16. Cosio MG, Hale KA, Niewoehner DE. Morphologic and morphometric effects of prolonged cigarette smoking on the small airways. *Am Rev Respir Dis* 1980; 122:265-271.
17. Berend N, Wright JL, Thurlbeck WM, Marlin GE, Woolcock AJ. Small airways disease: reproducibility of measurements and correlation with lung function. *Chest* 1981; 79:263-268.
18. Hogg JC, Macklem PT, Thurlbeck WM. Site and nature of airway obstruction in chronic obstructive lung disease. *N Engl J Med* 1968; 278:1355-1360.
19. Thurlbeck WM, Henderson JA, Fraser RG, Bates DV. Chronic obstructive lung disease: a comparison between clinical, roentgenologic, functional, and morphologic criteria in chronic bronchitis, emphysema, asthma, and bronchiectasis. *Medicine* 1970; 49:81-145.
20. Yanai M, Sekizawa K, Ohnishi T, Sasaki H, Takishima T. Site of airway obstruction in pulmonary disease: direct measurement of intrabronchial pressure. *J Appl Physiol* 1992; 72:1016-1023.
21. Petty TL, Silvers GW, Stanford RE. Mild emphysema is associated with reduced elastic recoil and increased lung size but not with airflow limitation. *Am Rev Respir Dis* 1987; 136:867-871.
22. Gelb AF, Gold WM, Wright R, Bruch HR, Nadel JA. Physiologic diagnosis of subclinical emphysema. *Am Rev Respir Dis* 1973; 107:50-64.
23. Müller NL. Clinical value of high-resolution CT in chronic diffuse lung disease. *AJR* 1991; 157:1163-1170.
24. Butler J, Caro C, Alkalé R, Dubois B. Physiologic factors affecting airway resistance in normal subjects and in patients with obstructive airways disease. *J Clin Invest* 1960; 39:584-591.
25. Demedts M, Aumann J. Early emphysema: ten years' evolution. *Chest* 1988; 94:337-342.
26. Nagai A, West WW, Thurlbeck WH. The National Institutes of Health Intermittent Positive Pressure Breathing Trial: pathology studies. II. Correlation between morphologic findings, clinical findings, and evidence of expiratory airflow obstruction. *Am Rev Respir Dis* 1985; 132:946-953.
27. Groskin SA. Emphysema: fact, fiction, or just a lot of hot air. *Radiology* 1992; 183:319-320.
28. Pratt PC. Role of conventional chest radiography in diagnosis and exclusion of emphysema. *Am J Med* 1987; 82:998-1006.
29. Miniati M, Filippi E, Falaschi F, et al. Radiologic evaluation of emphysema in patients with chronic obstructive pulmonary disease. *Am Rev Respir Crit Care Med* 1995; 151:1359-1367.
30. Gelb AF, Schein M, Kuei J, et al. Limited contribution of emphysema in advanced chronic obstructive pulmonary disease. *Am Rev Respir Dis* 1993; 147:1157-1161.
31. Gelb AF, Hogg JC, Müller NL, et al. Contribution of emphysema and small airways in COPD. *Chest* 1996; 109:353-359.
32. Thurlbeck WM. Overview of the pathology of pulmonary emphysema in the human. *Clin Chest Med* 1983; 4:337-350.
33. Klein JS, Gamsu G, Webb RW, Golden JA, Müller NL. High-resolution CT diagnosis of emphysema in symptomatic patients with normal chest radiographs and isolated low diffusing capacity. *Radiology* 1992; 182:817-821.
34. Gurney JW, Jones KK, Robbins RA, et al. Regional distribution of emphysema: correlation of high-resolution CT with pulmonary function tests in unselected smokers. *Radiology* 1992; 183:457-463.
35. Burki NK. Roentgenologic diagnosis of emphysema: accurate or not? *Chest* 1989; 95:1178-1179.
36. Fraser RG, Fraser RS, Renner JW, Bernard C, Fitzgerald PJ. The roentgenologic diagnosis of chronic bronchitis: a reassessment with emphasis on parahilar bronchi seen end-on. *Radiology* 1976; 120:1-9.
37. Simon G. Chronic bronchitis and emphysema: a symposium. III. Radiologic changes in chronic bronchitis. *Br J Radiol* 1959; 32:292-294.
38. Sanders C, Nath PH, Bailey WC. Detection of emphysema with computed tomography: correlation with pulmonary function tests and chest radiography. *Invest Radiol* 1988; 23:262-266.

39. Naidich DP, Zerhouni EA, Siegelman SS. Computed tomography of the thorax. New York: Raven Press, 1984.
40. Müller NL. CT diagnosis of emphysema: it may be accurate but is it relevant? *Chest* 1993; 103:329-330.
41. Webb WR, Müller NL, Naidich DP. High resolution CT of the lung. New York: Raven Press, 1992.
42. Müller NL, Miller RR. Diseases of the bronchioles: CT and histopathologic findings. *Radiology* 1995; 196:3-12.
43. Gevenois PA, De Vuyst P, Sy M, et al. Pulmonary emphysema: quantitative CT during expiration. *Radiology* 1996; 199:825-829.
44. Bergin C, Müller NL, Nichols DM, et al. The diagnosis of emphysema: a computed tomographic-pathologic correlation. *Am Rev Respir Dis* 1986; 133:541-546.
45. Miller RR, Müller NL, Vedal S, Morrison NJ, Staples CA. Limitations of computed tomography in the assessment of emphysema. *Am Rev Respir Dis* 1989; 139:980-983.
46. Hruban RH, Meziane MA, Zerhouni EA, et al. High resolution computed tomography of inflation-fixed lungs. Pathologic-radiologic correlation of centrilobular emphysema. *Am Rev Respir Dis* 1987; 136:935-940.
47. Goddard PR, Nicholson EM, Laszlo G, Watt I. Computed tomography in pulmonary emphysema. *Clin Radiol* 1982; 33:379-387.
48. Thurlbeck WM, Dunnill MS, Hartung WA, Heard BE, Heppleston AG, Ryder RC. A comparison of three methods of measuring emphysema. *Human Pathol* 1970; 1:215-226.
49. Sakai F, Gamsu G, Im JG, Ray CS. Pulmonary function abnormalities in patients with CT-determined emphysema. *J Comput Assist Tomogr* 1987; 11:963-968.
50. Morgan MDL. Detection and quantification of pulmonary emphysema by computed tomography: a window of opportunity. *Thorax* 1992; 47:1001-1004.
51. Foster WL, Pratt PC, Roggli VL, Godwin JD, Halvorsen RA, Putman CE. Centrilobular emphysema: CT-pathologic correlation. *Radiology* 1986; 159:27-32.

## CHAPTER 3

---

# CT lung densitometry: a review

### 3.1 Theoretical background

In computed tomography (CT) the X-ray attenuation values of tissue are calculated from X-ray transmissions in many directions through the human body. The reconstructed CT image is a two-dimensional representation of these x-ray attenuation coefficients in a cross-sectional body slice. The smallest unit composing a CT image is the individual picture element or pixel. The size of the image matrix is usually 256x256 or 512x512. In case of a 256 matrix, the CT image is made up of about 65000 pixels and in case of a 512 matrix of 260000 pixels. The area of a pixel depends on the field of view and the matrix size. For instance, for a typical field of view of 320 mm the pixel area is  $1.25 \times 1.25 \text{ mm}^2$  in a 256 matrix and  $0.625 \times 0.625 \text{ mm}^2$  in a 512 matrix.

The volume of tissue represented by a pixel is known as the voxel. The size of a voxel depends on the image matrix, slice thickness and the size of the field of view. For a slice thickness of 1 mm and a 320 mm diameter scanned field of view, the corresponding voxel volumes are  $1.56 \text{ mm}^3$  in a 256 matrix and  $0.39 \text{ mm}^3$  in a 512 matrix.

The X-ray attenuation values of the various tissues present in a single voxel are effectively averaged. They are presented as CT numbers expressed in Hounsfield units (HU). These Hounsfield units are established on a relative scale with the attenuation of water used as a reference and defined as 0 HU. The CT number of air is -1000 HU and that of bone of the order of 1000 HU. For a given soft tissue, CT numbers can be translated to density ( $\text{g/cm}^3$ ) using the formula: Physical density = (CT number)/1000 + 1 (1). It is easily seen that for instance a CT number of -800 HU corresponds to a tissue density of  $0.2 \text{ g/cm}^3$ .

### 3.2 Factors influencing quantitative CT density measurements of the lung

In theory, CT is a useful noninvasive method for evaluating the density of the lung. However, the use of absolute CT numbers for *in vivo* tissue characterization is compromised by a number of potential sources of errors: CT equipment, scan technique, image evaluation, the nonlinear partial volume effect and respiration.

#### *CT equipment*

CT scanners were traditionally not optimized for densitometry in the low density range that is of relevance for lung studies. Variation in the high voltage of the X-ray tube produced large changes in the CT numbers (2). Temporal drift in CT numbers was difficult to control. The CT numbers of water, in a standard water phantom, was seen to vary by 15 HU over an 18 month period (2). Beam hardening and reconstruction artefacts caused density shifts (2). CT numbers were also sensitive to thoracic ge-

ometry and to the position of the object in the scan field (3,4). Densitometric results could not be extrapolated to other circumstances because of significant intrascanner and interscanner variability (2-4).

The performance of newer CT equipment has been improved considerably. A CT scanner study showed that the linearity of Somatom Plus CT systems was quite adequate for the low attenuation studies that are relevant to investigations of lung disease (5). The temporal drift of the CT number for air over one day on the Somatom Plus scanner for instance, was found to be limited to within 1 HU. The long term stability was good. Thoracic geometry induced variations in CT numbers were limited to 3-4 HU (6). The reproducibility and accuracy for densities found for lung were within 2-3% (5).

### *Scan technique*

The mean lung density as determined with CT is the histogram related densitometric parameter most commonly used in published studies. The mean lung density is relatively insensitive to the scan technique used. The influence of the reconstruction filter on the average CT value is generally negligible, except when data truncation occurs as is possible for the ultra-high resolution reconstruction filter (5). This filter produces a very broad histogram that can be truncated at its lower end, resulting in a slight overestimation of the average CT lung density. Section thickness does not affect the estimated mean lung density, except when the local density varies strongly or air calibration is incorrect (5,6). The extent to which zoom factor and table height affect density measurements appears to be small (5). Density measurements are, of course, strongly affected by intravenous contrast administration. In 12 subjects receiving contrast a rise in mean lung density was noted from -813 to -789 HU (7).

The average density of the lung is thus a reasonable robust parameter. When histogram related parameters, other than the mean lung density are used for assessment of pulmonary disease, slice thickness and reconstruction filter will strongly affect the results. Narrower collimation and sharper reconstruction filters will broaden the CT number histogram (8). Consequently, the lowest 10th percentile of the frequency distribution will show a decrease, while the highest 10th percentile of the frequency distribution of CT numbers will show an increase in attenuation. A decrease from 10 to 2-mm slice thickness was accompanied by an increase of the cross-sectional percentage in the density range -900 HU to -1000 HU from 9.6% to 16.1% (7).

### *Image evaluation*

Manual analysis of lung tissue was time consuming and required considerable additional post-processing time. Reproducibility errors due to the operator's intervention



in the evaluation process may exceed 10 HU (9). At present, the lungs are automatically isolated using a suitable segmentation threshold in a contour tracking algorithm. Subsequently, outer pixels that are still affected by the thoracic wall or larger vessels have to be excluded by shrinking the contour to obtain truly parenchymal related data, a process called 'erosion'. Once the thoracic wall and the larger vessels are excluded, the mean lung density is nearly independent of additional erosions. The parameters that determine the thresholding and shrinking procedure can in principle be freely chosen but threshold and number of erosions have a substantial impact on the final densitometric outcome.

### *Nonlinear partial volume effect*

The nonlinear partial volume effect arises in heterogeneous materials such as lung or foam, having density variations on the scale of the CT's sample area. It leads to a higher transmission of the X-ray beam than expected on the basis of an object with constant attenuation characteristics. For lung it was found to cause a systematic underestimation of the density by less than 0.1 % (10). This density error is negligible and may be only of significance in calibration of CT scanners.

### *Respiration*

Lung density is a reflection of the relative distributions of air, pulmonary tissue, blood and interstitial fluid within the lung. Lung density changes substantially with levels of in- or expiration. In healthy subjects, lung attenuation was found to increase during exhalation by 150-300 HU (1,11-13). Therefore measurements should be interpreted with some knowledge of lung volume or respiratory level of inspiration. A spirometrically controlled CT technique has been developed offering the opportunity to obtain CT images at defined levels of inspiration (14).

## **3.3 Density patterns of the normal lung**

Approximately two thirds of the volume of a normal lung is taken up by air, and the rest by blood, pulmonary tissue and interstitial fluid (15). These components are not homogeneously distributed throughout the lungs. Gravitation accounts for a density gradient between the dependent and the nondependent parts of the lungs. The dependent lung has higher attenuation because there is a preferential distribution of the pulmonary blood volume to the dependent lung. Alveoli and distal airways in the dependent lung are smaller than those in the non-dependent.

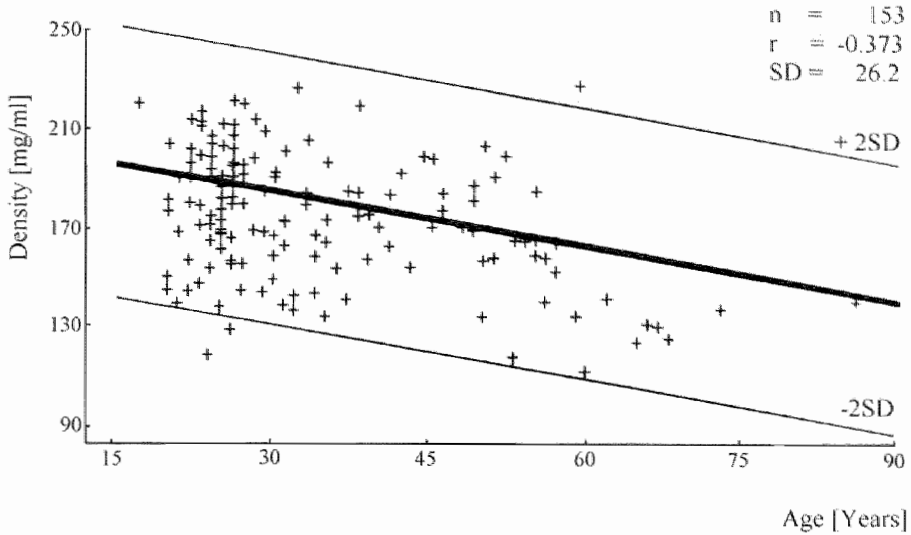


**Figure.** Relation of lung density to age in 153 healthy individuals.

To date, suitable reference data of lung density parameters of healthy subjects (normals) are still missing. Kalender et al (16) gathered normal data from 153 healthy individuals of various ages. Three spirometrically triggered scans at a trigger level of 50% vital capacity were obtained: one at the level of the carina, one 5 cm above and 5 cm below. The authors averaged the mean lung density of these three scans. They demonstrated a decrease in lung density as a function of age at a rate of about 0.7 mg/ml per year (Figure). However, subjects in the age range between 20 and 40 years were relatively over-represented in this study.

Webb et al (13) examined 10 healthy subjects to determine normal dynamic and expiratory findings. Scans were obtained in supine and in prone positions with 3-mm collimation and were reconstructed with an ultra-high reconstruction algorithm. CT sections were obtained through the upper, middle and lower lungs. Attenuation was measured in the dependent and the nondependent portions of the lungs. Four of the 10 subjects showed regions of inhomogeneity in lung attenuation during rapid exhalation. In supine position, the average increase in lung attenuation during exhalation was 219 HU in the dependent lung regions and 171 HU in the nondependent regions. Nearly identical densitometric results were obtained in supine and prone positions.

Vock et al (12) analyzed the quantitative features of the lungs in a population of children with radiographically normal lungs. Five-mm collimated CT scans using moderate inspiration were evaluated. The mean lung density of three levels was averaged. The CT density of the lung in children ranged between -750 HU at the age of 10

years to -880 HU at the age of 18 years. The mean lung density of 32 children over 7 years was -792 HU (95% range, -702 to -882 HU). From maximal inspiration to expiration mean lung density increased by 158 HU. Anteroposterior gradient averaged 56 HU at the subcarinal level and increased with maximal expiration.

Density gradients between the dependent and the nondependent lung regions are strongly influenced by lung volume. Verschakelen et al (17) studied the effect of changes in lung volume on lung density in dependent and nondependent parts of the lung. Their study group consisted of 6 healthy subjects. Spirometrically controlled CT scans were obtained at 90%, 50%, and 10% vital capacity. Changes in lung volume caused different changes in lung density in the dependent and the nondependent parts of the lungs. The effect of lung volume was greater on the dependent than on the non-dependent regions of the lungs in the upper as well as the lower zones of the lungs. The anteroposterior density gradient is less pronounced at inspiration than at expiration.

### 3.4 Reproducibility of quantitative CT

Breath hold at full inspiration is generally considered as the condition giving the best results (18). Reproducibility of mean lung density measurements under tight spirometric conditions - 50% vital capacity - in ten healthy volunteers was on the order of 5% (14). Kohz et al (19) examined the reproducibility of densitometry in patients with pulmonary disease. One-mm collimated spirometric triggered CT scans were obtained twice, using a 5 minute break, at 50% vital capacity, and reconstructed with a high-frequency algorithm. With tight spirometric control, the average deviation in mean attenuation values between the first and the second examination was 10 HU.

### 3.5 CT lung densitometry - pathologic correlation in emphysema

Hayhurst et al (20) calculated lung densities in CT scans of eleven patients with peripheral lung carcinoma and compared this with pathological examination of lung specimens and found that patients with emphysema had significantly more pixels in the EMI range -450 to -500 than did patients without emphysema ( $p < 0.001$ ; 1 EMI unit = 2 HU).

Gould et al (21) compared the lowest 5th percentile of the lung frequency distribution of EMI numbers of two 13-mm thick CT sections of 28 lungs of patients who proceeded to lobe or lung resection for lung tumor with the mean value of the surface area of the walls of the distal airspaces per unit lung volume (AWUV) in the pathologic specimens. They found a significant negative correlation between the lowest 5th percentile and this AWUV ( $r = -0.77$ ,  $p < 0.001$ ). The authors concluded that quantitative

CT scans can noninvasively diagnose, quantitate and locate mild to moderate emphysema in humans in life.

Müller et al (22) used a CT software program to highlight pixels within a desired density range to calculate the overall percentage of lung area of low density and analyzed with this program the lungs or lobes of 28 patients prior to thoracotomy for lung tumor. Ten-mm CT scans were obtained at 10-mm intervals and all patients received intravenous contrast material. The CT scans were also visually assessed for the presence and extent of emphysema. Results of both methods were compared with the results of pathological examination of the corresponding surgical specimen. The percentage CT area with attenuation less than -910 HU showed the highest correlation with the pathologic grade of emphysema ( $r = 0.94$ ,  $p < 0.001$ ). This correlation was slightly better than the correlation between results of visual assessment and the pathological grade of emphysema ( $r = 0.90$ ,  $p < 0.001$ ). The authors defined -910 HU as the optimal threshold value to differentiate between normal and emphysematous lung. However, because the threshold value may vary with different scanners and techniques, users were advised first to determine the optimal threshold value for their scanner.

Gevenois et al (23) analyzed CT scans of the lungs from 63 subjects undergoing surgical resection of a lung cancer or lung transplantation because of emphysema. One-mm collimated scans were obtained at 10-mm intervals. They calculated the percentage of lung tissue with X-ray attenuation values lower than various threshold values and compared the results with a corresponding set of morphometric data. At inspiration, the relative area of lung parenchyma with attenuation coefficient of less than -950 HU correlated very well with the macroscopic severity of pulmonary emphysema ( $r = 0.926$ ,  $p < 0.001$ ). The authors concluded that the relative area of lung parenchyma with attenuation coefficients of less than -950 HU is a valid index of macroscopic pulmonary emphysema. In a follow-up study they compared CT data at expiration and inspiration with microscopic and macroscopic morphometric methods to quantify emphysema (24) and demonstrated that -910 HU was a valid threshold for macroscopic and -820 HU for microscopic emphysema if the CT scan was made during expiration. Minus 950 HU proved to be the best threshold value for both macroscopically and microscopically quantified emphysema if the CT scan was made during inspiration.

### 3.6 CT lung densitometry-physiologic correlation in emphysema and interstitial lung disease

Kinsella et al (25) analyzed pulmonary CT scans by calculating the percentage area of lung tissue with a density below various density thresholds and demonstrated a significant correlation between this area and pulmonary function indices of emphysema.

They concluded that determination of the percentage of lung areas of low X-ray attenuation provides a useful method for quantitating the overall extent of emphysema in life.

Gould et al (26) correlated the mean density as well as lowest 5th percentile of the lung frequency distribution of EMI numbers with measurements of airflow limitation and the diffusing capacity of the lung for carbon monoxide in 80 cigarette smokers ranging from normal subjects to patients with chronic obstructive pulmonary disease. In agreement with Kinsella inverse correlations ranging from 0.54 to 0.77 were observed. The authors concluded that decrease of CT numbers, which reflects loss of surface area of the distal airspaces, is a major index of pulmonary function in patients with smoking related chronic obstructive pulmonary disease.

Knudson et al (27) calculated the percentage of pixels in the range -900 to -1024 HU in 64 patients with some form of airflow obstruction. CT scans were obtained at full inspiration and expiration. The best correlation of low attenuation pixels and physiologic parameters consistent with a diagnosis of emphysema was observed on CT scans obtained at expiration. They concluded that CT scans taken at full expiration effectively revealed abnormal permanent enlargement of airspaces characteristic of emphysema. In their opinion, CT taken at full inspiration may reveal hyperaeration, which is not the same as emphysema.

Hartley et al (28) studied the value of CT densitometry in a population with interstitial lung disease. The study population consisted of 60 asbestos-exposed subjects and 24 subjects with interstitial pulmonary fibrosis. Various densitometric parameters were derived from the frequency distribution of Hounsfield numbers and correlated with accepted methods of assessing interstitial lung disease, i.e. the chest radiograph, pulmonary function testing, bronchoalveolar lavage, and dyspnea assessment. The authors concluded that computer derived density analysis is a valid objective measure of interstitial lung disease and that it may yield information beyond that available in the diagnostic tools traditionally used.

### 3.7 Overview of experimental methods

#### *CT technique used in this thesis*

CT scans were performed with a Somatom Plus scanner (Siemens, Erlangen, Germany). The method of spirometrically controlled CT densitometry of the lung we applied has been developed by Kalender and coworkers (14). The CT scanner was triggered by a respiratory gating device in order to achieve precise control of the level of inspiration. A hand-held, open spirometer system was connected to the CT scanner and to a microcomputer. In this open spirometer system, air flow causes rotation of a

set of turbines. Body temperature pressure saturated corrections are applied. Accuracy is specified to be 2 percent (14). Flow and volume are derived by counting rotations. A spirometric curve can be followed on the display monitor of the CT scanner. Patients are placed supine on the CT couch and asked to breathe through the mouth piece. The procedure starts with a measurement of the inspiratory vital capacity. Subsequently, a user-selected level of inspiration expressed in terms of a percentage of the inspiratory vital capacity, has to be selected. When the patient inhales again to this selected level of inspiration, the microcomputer generates the trigger signals which is simultaneously sent to the spirometer and to the CT scanner. The valve in the spirometer is closed and the airflow is stopped for the duration of the CT scan and the CT scan sequence is initiated.

In each person four spirometrically gated CT scans were obtained. Two anatomical levels were chosen by means of a topogram: 5 cm above and 5 cm below the level of the carina, thereby providing representative scans of the upper and the lower parts of the lungs. At each level two scans, at 90 and 10 percent of the inspiratory vital capacity respectively, were obtained using spirometric control. The following scanning parameters were employed: 1.0-mm collimation, 137 kVp, 220 mAs, 1.0 second scanning time. We applied a 360 degree scan, a matrix size of 512x512, and a field of view of approximately 350 mm. Scans were reconstructed in the standard or in the soft detail resolution mode. The full width at half maximum of the point spread function of the soft detail reconstruction filter is 1.86 mm and the sample volume 3.92 mm<sup>3</sup> (29). No contrast medium was injected.

### *Image evaluation*

The CT data were transmitted to a graphical workstation (SPARCstation 1+, Sun Microsystems, Mountain View, Calif) and analyzed semiautomatically with software developed in our hospital. First, the boundaries of each lung were determined by using a fast contour following algorithm at a CT level of -200 HU using pixel tracing, to isolate the left and the right lung parenchyma (30). Subsequently the contour was eroded by 2 pixels to remove the circumference that partially corresponded to the thoracic wall. A manual correction for excluding the trachea or separating the lungs was incidentally necessary. A frequency distribution of CT numbers was subsequently generated of the right and the left lung, and of both lungs. The area under the curve was normalized so that histograms from subjects with different lung volumes could be compared. The mean, modal, and median lung density, and the histogram's full width at half-maximum were determined automatically as well as the cut-off points of the frequency distribution of Hounsfield numbers defining the lowest and the highest 10th percentile, and the pixel index, also called density mask, which is the percentage of the histogram area below the CT number of -910 HU.

### *Dosimetry*

We determined the effective dose ( $E$ ) received by the patient during the CT densitometric examination. For a scan consisting of one single section of 1 mm (tomogram) we determined the dose free in air using both TLD-100 chips (LiF; Solon Technologic Instruments, Wemelskirchen, Germany) and a pencil ionization chamber (Capintec PC-4P, Capintec Inc., Pittsburg) connected to a Capintec 192 A electrometer. Dose conversion factors published by GSF (31) were used to convert the central axis dose to organ doses. From these results the effective dose due to a single CT section scan was estimated as  $E = 33 \mu\text{Sv}$  according to IRCP-60 (32). The entrance dose due to the AP projection (topogram, for tomogram planning; technique: 120 kV, 450 mAs, 2-mm collimation, 500 mm scan length) was measured using TLD's on a humanoid thorax phantom (33). The effective dose due to the AP-topogram was estimated at about  $67 \mu\text{Sv}$ , using dose conversion factors as calculated by the NRPD (34). A complete densitometric investigation consisting of 1 topogram and 4 tomograms, then caused an effective dose of  $E = 0.20 \text{ mSv}$ , with an estimated uncertainty of about 30 percent.

### 3.8 Conclusions

Densitometry has the potential to become an important addition to standard lung tests in determining and following the extent of emphysema and interstitial lung disease. Unfortunately the CT number histogram of the lung is very dependent on the scan parameters used. Consequently, there is an obvious need for standardization of section thickness, reconstruction filter, segmentation level, the number of erosions, not using intravenous contrast administration and the inspiratory level at which CT images are obtained.

### REFERENCES

1. Rosenblum LJ, Mauceri RA, Wellenstein DE, et al. Density patterns in the normal lung as determined by computed tomography. *Radiology* 1980; 137:409-416.
2. Zerhouni EA, Spivey JF, Morgan RH, et al. Factors influencing quantitative CT measurements of solitary pulmonary nodules. *J Comput Assist Tomogr* 1982; 6:1075-1087.
3. Levi C, Gray JE, McCullough EC, Hattery RR. The unreliability of CT numbers as absolute values. *AJR* 1982; 139:443-447.
4. McCullough EC, Morin RL. CT-number variability in thoracic geometry. *AJR* 1983; 141:135-140.
5. Kemerink GJ, Lamers RJS, Thelissen GRP, van Engelshoven JMA. CT densitometry of the lungs: scanner performance. *J Comput Assist Tomogr* 1996; 20:24-33.
6. Kemerink GJ, Lamers RJS, Thelissen GRP, van Engelshoven JMA. Scanner conformity in CT densitometry of the lungs. *Radiology* 1995; 197:749-752.

7. Adams H, Bernard MS, McConnochie. An appraisal of CT pulmonary density mapping in normal subjects. *Clin Radiol* 1991; 43:238-242.
8. Kemerink GJ, Kruize HH, Lamers RJS, van Engelshoven JMA. CT lung densitometry: dependence of CT number histograms on sample volume and consequences for scan protocol comparability. *J Comput Assist Tomogr* 1997; 21:948-954.
9. Kalender WA, Fichte H, Bautz W, Skalej M. Semiautomatic evaluation procedures for quantitative CT of the lung. *J Comput Assist Tomogr* 1991; 15:248-255.
10. Kemerink GJ, Lamers RJS, Thelissen GRP, van Engelshoven JMA. The nonlinear partial volume effect and computed tomography densitometry of foam and lung. *Med Phys* 1995; 22:1445-1450.
11. Zerhouni EA, Naidich DP, Stitik FP, Khouri NF, Siegelman SS. Computed tomography of the pulmonary parenchyma. II. Interstitial disease. *J Thorac Imaging* 1985; 1:54-64.
12. Vock P, Malanowski D, Tschaepeler H, Kirks DR, Hedlund LW, Effmann EL. Computed tomographic lung density in children. *Invest Radiol* 1987; 22:627-632.
13. Webb RW, Stern EJ, Kanth N, Gamsu G. Dynamic pulmonary CT: findings in healthy adult men. *Radiology* 1993; 186:117-124.
14. Kalender WA, Rienmüller R, Seissler W, Behr J, Welke M, Fichte H. Measurement of pulmonary parenchymal attenuation: use of spirometric gating with quantitative CT. *Radiology* 1990; 175:265-268.
15. Rhodes CG, Wollmer P, Fazio F, Jones T. Quantitative measurement of extravascular lung density using positron emission and transmission tomography. *J Comput Assist Tomogr* 1981; 5:783-791.
16. Kalender WA, Fichte H, Bautz W, et al. Reference values for lung density and structure measured by quantitative CT. *Somatom Plus Conference*. Vienna 1994.
17. Verschakelen JA, Van Fraeyenhoven L, Laureys G, Demedts M, Baert AL. Differences in CT density between dependent and nondependent portions of the lung. *AJR* 1993; 161:713-717.
18. Wegener OH, Koeppe P, Oeser H. Measurement of lung density by computed tomography. *J Comput Assist Tomogr* 1978; 2:263-273.
19. Kohz P, Stäbler A, Beinert T, et al. Reproducibility of quantitative, spirometrically controlled CT. *Radiology* 1995; 197:539-542.
20. Hayhurst MD, Flenley DC, McLean A, et al. Diagnosis of pulmonary emphysema by computerised tomography. *Lancet* 1984; ii:320-322.
21. Gould GA, Macnee W, McLean A, et al. CT measurements of lung density in life can quantitate distal airspace enlargement: an essential defining feature of human emphysema. *Am Rev Respir Dis* 1988; 137:380-392.
22. Müller NL, Staples CA, Miller RR, Abboud RT. "Density mask": an objective method to quantitate emphysema using computed tomography. *Chest* 1988; 94:782-787.
23. Gevenois PA, de Maertelaer V, De Vuyst P, Zanen J, Yernault JC. Comparison of computed density and macroscopic morphometry in pulmonary emphysema. *Am J Respir Crit Care Med* 1995; 152:653-657.
24. Gevenois PA, De Vuyst P, Sy M, et al. Pulmonary emphysema: quantitative CT during expiration. *Radiology* 1996; 199:825-829.
25. Kinsella M, Müller NL, Abboud RT, Morrison NJ, DyBuncio A. Quantification of emphysema by computed tomography using a density mask program and correlation with pulmonary function tests. *Chest* 1990; 97:315-321.
26. Gould GA, Redpath AT, Ryan M, et al. Lung CT density correlates with measurements of airflow limitation and the diffusing capacity. *Eur Respir J* 1991; 4:141-146.
27. Knudson RJ, Standen JR, Kaltenborn WT, et al. Expiratory computed tomography for assessment of suspected pulmonary emphysema. *Chest* 1991; 99:1357-1366.
28. Hartley PG, Galvin JR, Hunninghake GW, et al. High-resolution CT-derived measures of lung density are valid indexes of interstitial lung disease. *J Appl Physiol* 1994; 76:271-277.
29. Kemerink GJ, Kruize HH, Lamers RJS. The CT's sample volume as a approximate, instrumental measure for density resolution in densitometry of the lung. *Med Phys* 1997; 24:1615-1620.



30. Pavlidis T. Algorithms for graphics and image evaluation. Berlin: Springer Verlag, 1982.
31. Drexler G, Panzer W, Widenmann L, Williams G, Zankl M. The calculation of dose from external photon exposures using reference human phantoms and Monte Carlo Methods. Part III: Organ doses in X-ray diagnosis, GSF-B Bericht S-1026, 1985.
32. ICRP Publication 60. Recommendations of the International Commission on Radiological Protection. Oxford: Pergamon Press, 1990.
33. Pearce JG, Milne ENC, Gillan GD, Roeck WW. Development of a radiographic chest phantom with disease simulation. *Invest Radiol* 1979; 14:181-184.
34. Hart D, Jones DG, Wall BF. Estimation of effective dose in diagnostic radiology from entrance surface dose and dose-area product measurements. Chilton NRPB-R262, 1994 influence of lung volume. *AJR* 1993; 161:713-717.

## CHAPTER 4

---

# Scanner conformity in CT densitometry of the lungs

Gerrit J. Kemerink

Rob J.S. Lamers

Guillaume R.P. Thelissen

Jos M.A. van Engelshoven

## ABSTRACT

**Purpose:** To quantify inter- and intrascanner conformity in computed tomography (CT) densitometry of the lungs.

**Materials and methods:** With six scanners from four manufacturers a lung densitometry protocol with several variations was applied for performance comparison. Phantoms included water, air, and a humanoid thorax phantom equipped with a dog lung and exchangeable pseudolungs of polyethylene foam.

**Results:** All scanners produced acceptable CT numbers (Hounsfield units) for water, but some not for air. An incorrect calibration of air density affected all CT numbers at lung densities, but the error was easily corrected. Some systems were more sensitive to object size than others were. Sensitivity of CT numbers to section thickness, reconstruction filter, zoom factor, and table height was small, except for two scanners in relation to section thickness.

**Conclusion:** After correction for poor air calibration, scanner conformity was acceptable when the reproducibility of lung densitometry in clinical practice was set as a reference.

## INTRODUCTION

Computed tomographic (CT) densitometry of the lungs is extensively used in research and is of growing clinical interest (see, eg, references 1-4 and references therein). A relevant issue for the present applications, and certainly for a more general introduction, is conformity among the various scanners on the market. In other fields of densitometry relatively poor interscanner, and even intrascanner, conformity of CT numbers (Hounsfield units), has been reported (5-7). Moreover, CT scanners were traditionally not optimized for the low-attenuation studies that are relevant to investigations of lung disease. To our knowledge, no systematic scanner comparison in lung densitometry has been published so far, although the scale of activities seems to warrant such an investigation. The present study reports the results from a few widespread scanners, and it addresses the problem of correcting CT-determined densities obtained with a scanner having a poor calibration at air density.

## MATERIALS AND METHODS

### CT-scanners

Six CT scanners were included in the study (Table 1). All systems are third-generation scanners, except the Picker system, which is fourth-generation. With all systems scans were obtained that might be chosen for a combined densitometric and high-resolution CT study. The scanning parameters chosen according to this approach are given in Table 1. Only densitometric results were evaluated. A specialist of the manufacturing or sales company of each scanner collaborated in the measurements, except in the case of the two Siemens scanners of our own hospital.

**Table 1.** Scanners and Scanning Protocol.

Manufacturer*	Scanner	HV <sup>†</sup> (kV)	Section Thickness (mm)	mAs	Scanning Duration (sec)	Reconstruction Filter <sup>‡</sup>
GE	Highlight	140	1.5	250	2	STD
Philips	SR 7000	140	1.5	250	2	4
Philips	LX	120	1.5	175	1.9	4
Picker	PQ-2000	130	1.5	200	1	STD
Siemens	Somatom Plus	137	1.0	220	1	AB 7055
Siemens	Somatom Plus	137	1.0	220	1	AB 7055

Note. \*GE Medical Systems, Milwaukee, Wis; Philips Medical Systems, Best, the Netherlands; Picker International Inc, Cleveland, Ohio; Siemens Aktiengesellschaft, Erlangen, Germany; <sup>†</sup>HV = high voltage; <sup>‡</sup>All reconstruction filters are the standard type. Shown are manufacturer's code number or acronym.

### Phantoms

The following phantoms were used:

1. A circular, water-filled phantom of 20-cm diameter.
2. A humanoid thorax phantom (8) containing lungs of a dog and having an empty lower thorax section that could be equipped with foam to simulate lungs. A ring of 3-cm-thick pig fat was placed around the "lean" phantom to simulate an "obese" thorax. This ring of lard was frozen to stabilize its form.
3. Various pieces of polyethylene foam (PSG, Wellen, Belgium) with a relatively uniform and accurately determined density (9) were used as pseudolungs in the thorax phantom.

## Measurements

The CT numbers for water and air, yielding the two calibration points of the Hounsfield scale were measured. The CT number of air was measured within the empty lean and obese thorax, as well as in the empty gantry. The CT number of water was determined with the 20-cm-diameter phantom in the middle of the gantry, by using a large circular region of interest covering about 80 % of the phantom cross section.

The dog lungs in the humanoid phantom were measured at a position that had been marked on the outside of the phantom. The CT number was calculated as an average over a hand-drawn region completely including the left lung.

The CT numbers of the various pieces of polyethylene foam were determined with the foam in the lean and in the obese phantom. The results, consisting of CT numbers versus foam density, were fitted with the linear function  $\text{CT number} = \text{offset} + \text{slope} \times \text{density}$ . The CT number for air (empty phantom) was included in the fit.  $\chi^2$  analysis was used as a measure of the quality of the fit; for a proper fit and realistic error estimates  $\chi^2$  should be of the order of 1.

The correlation of CT number with some variations in the standard protocol was also investigated. We determined the influence of section thickness, reconstruction filter, zoom factor, and table height. In principle these parameters should not affect the average CT number, at least not for homogeneous materials. We used the water phantom, air, and the obese thorax phantom with polyethylene foam at density of 109 kg/m<sup>3</sup> (for short: foam-109). We also looked for the possible occurrence of data truncation: Some scanners do not use CT numbers below -1023 or -1024 HU, whereas owing to noise such values may well occur for lungs of extreme low density (eg, in patients with emphysema) (9).

Assuming a well-calibrated scanner, the density of water-equivalent tissue, as lung is (10), can simply be calculated from the measured CT number by adding 1000 (strictly, the correcting at air density should be 1001.3, changing to about 998.0 at water density). The density so obtained is in kilograms per cubic meter. In the remainder of this article we use CT numbers because they are the numbers given by the scanner.

## RESULTS

The CT numbers found for water, air, dog lung and foam 109 are shown in Table 2. The results for water were similar for all scanners. For air, dog lung and foam 109, the CT number with the Philips scanners deviated from the results of the other scanners. Table 3 presents the results of the measurements of foam in the lean and obese thorax phantom. The latter results are presented in the form of the offset and the slope of the linear function fitted to the data. The figure shows, as an example, the foam data

**Table 2.** CT Numbers (Hounsfield units) for Water, Air, Dog Lung and Foam 109.

Scanner Type	water	Air	Air in Lean Thorax	Air in Obese Thorax	Dog Lung*	Corrected Dog Lung*	Corrected Lean Thorax Foam 109 <sup>†</sup>	Corrected Obese Thorax Foam 109 <sup>†</sup>
Highlight	+1.2	-1008	-1005	-1000	-912	-907	-890	-893
SR 7000	+1.0	- 984	- 985	- 985	-887	-902	-896	-896
LX	-2.4	- 984	- 983	- 983	-888	-905	-896	-894
PQ-2000	-0.3	- 999	- 997	-1001	-912	-915	-897	-896
Somatom 1	+2.6	- 999	-1001	-1000	-910	-910	-893	-894
Somatom 2	-1.5	-1000	- 999	-1000	-911	-911	-894	-894

Note. Scanning parameters are in Table 1; \* Lean thorax; <sup>†</sup>Corrected for error in CT number for air (see text).

**Table 3.** Measurements of Foam in the Lean and Obese Thorax.

Scanner type	Lean Thorax			Obese Thorax		
	Offset* (HU)	Slope* (HU/[kg/m <sup>3</sup> ])	$\chi^2$	Offset* (HU)	Slope* (HU/[kg/m <sup>3</sup> ])	$\chi^2$
Highlight	-1005	0.999	0.64	-1000	0.985	0.24
SR 7000	- 985	0.953	0.37	- 985	0.961	0.33
LX	- 983	0.949	0.1	- 983	0.961	0.26
PQ-2000	- 997	0.950	0.71	-1001	0.951	1.15
Somatom 1	-1001	0.973	1.58	- 999	0.959	1.23
Somatom 2	-1000	0.978	1.32	- 999	0.967	3.30

Note. Scanning parameters are in Table 1; \* Results from a fit with the linear function CT number = offset + slope polyethylene density.

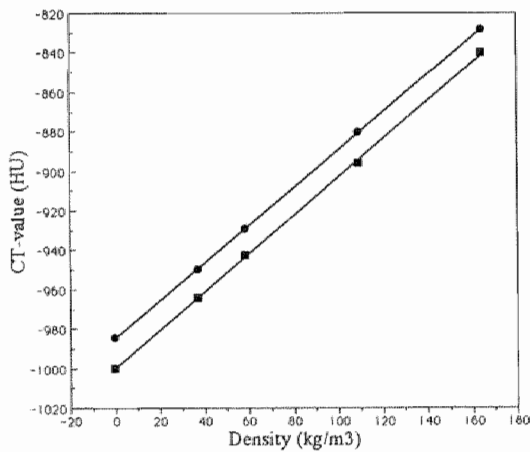


**Figure.** CT numbers of polyethylene foam in the lean and obese thorax phantom versus polyethylene density. Experimental data, together with a fitted linear function, are shown for the Philips SR 7000 scanner (●) and the Siemens Somatom Plus scanner (■) (Somatom 2 in Tables 2 and 3).

points, together with the line fitted to them, for the Philips SR 7000 (top) and the Siemens Somatom Plus scanner (bottom). The quality of the fit was usually good, as was also evidenced with  $\chi^2$  value.

With all scanners, the CT numbers of air, water, and foam 109 were also measured at section thicknesses of 3, 5, and 10-mm. The Philips scanners, in contrast to the other scanners, showed considerable section thickness-dependent differences in CT numbers for air and foam. Averaging for each scanner of the non-Philips scanners the results for the four different section thicknesses, where the averaging is performed separately for air, water, and foam 109, produced standard deviations of these intrascanner averages between 0.1 and 1.2 HU. For air, the Philips SR 7000 produced -984 HU (1.5-mm section thickness), -992 HU (3 mm), -994 HU (5 mm), and -996 HU (10 mm); and the LX produced -984 HU (1.5 mm), -991 HU (3 mm), -994 HU (5 mm), and -992 HU (10 mm). Especially for sections of 1.5-mm thickness, large deviations from the ideal value of -1000 HU were observed. The CT numbers for foam 109 showed similar shifts.

The influence of the type of reconstruction filter was normally very small: Intrascanner changes were almost always less than 1 HU, the maximum change being 2.0 HU. Greater deviations might be found in those cases in which data truncation occurs. The filters tested were, for the GE Highlight scanner, STD (standard), bone, detail, soft, and smooth; for the Picker PQ-2000 scanner: STD, sharp, and smooth; for the Philips SR 7000 and LX scanner: 4, 5, 8, and 9; and for the Somatom Plus scanners: standard, high-resolution, ultra-high-resolution, and soft.

Zoom factor variation between 1.0 and 3.0 never modified CT numbers by more than 1 HU.

Changes in table height over a 5-cm range never affected CT numbers by more than 1.5 HU. Some systems (Picker, Philips) allow scanning with the table in such a low position that it is partly outside the scan field, which leads to falsification of CT numbers (often in the form of streak artifacts). Another system (Siemens) allows only a 5-cm vertical positioning range.

The Highlight and the Somatom Plus scanners are prone to data truncation: Data are truncated at -1024 and -1023 HU, respectively.

## DISCUSSION

The CT numbers for water indicate that all scanners tested are reasonably well adjusted at this major calibration point. For air the situation is dependent on the scanner. The Siemens Somatom Plus scanners produced values that are under all tested circumstances within 1 or 2 HU from the ideal value of -1000 HU. In contrast, both Philips scanners showed a deviation of slightly more than 15 HU when a section thick-

ness of 1.5 mm was used. Without correction, such a deviation induces a large error in the estimated lung density (eg, at a density of  $100 \text{ kg/m}^3$  the error would be 15 %).

The GE system produces CT numbers for free air that are approximately -1008 HU, 8 HU too low. For air within the thorax phantom, the Picker and GE systems show differences on the order of 4-5 HU between data from the lean and obese thorax.

All foam data could be fitted well with a linear function, indicating that within the experimental accuracy of about 2 %, all tested scanners appear to be linear in the low-density range for a given phantom. Between the lean and obese thorax data obtained with the GE and Picker systems however, a systematic difference of 3-4 HU existed in all data points, similar to the difference observed for air. For one scanner the difference is positive; for the other, however, it is negative. In these experiments each piece of foam was measured in the lean thorax; then the ring of lard was placed in position, and with the foam lung in place, the obese thorax data were acquired. The shift in CT number must therefore be related to phantom size or phantom composition. Phantom size will affect the relative amount of scattered radiation, and phantom composition, since fat is not equivalent to water, affects beam hardening. The resulting effects in the various scanners are dependent on a number of instrumental details and calculational corrections. Factors that at least in principle are beneficial for quantitative CT are (a) relatively heavy X-ray beam filtration, (b) a detector diaphragm that limits section thickness, (c) a flat beam filter, and (d) good detector collimation, which is more difficult to achieve in a fourth- than in a third-generation scanner. The presence of a detector diaphragm is especially important for thin sections, but only the Somatom Plus scanners have it as a standard feature. Not only these systems, however, but also the two Philips systems showed no systematic shift in data between the lean and obese thoraxes. It is probably that these subtle effects are dependent not only on the hardware but also on the exact implementation of several corrections with the software.

The slope of the foam curves for the different scanners varies between 0.949 and  $0.999 \text{ HU}/(\text{kg/m}^3)$ . No substantial difference exists between the slopes for the lean and obese thorax data for any scanner. When the X-ray spectrum, filtration, and detector response of the scanner are known, the polyethylene slope can be used to obtain an estimate of the calibration curve for low-density water-equivalent tissue. In essence, under the present circumstances the ratio of the effective mass attenuation coefficients of water and polyethylene is needed for this conversion. Complications due to scanners using a water-based beam-hardening correction are negligible, since the thickness of polyethylene is small: For all foam lungs it is less than  $2.5 \text{ g/cm}^2$ . For the Somatom Plus scanner the required simulations were performed (9), resulting in slopes for water-equivalent tissue that are close to the ideal value of 1.00. The calculations were not performed for the other scanners.

It is found, without exception, that the foam curves shift with the corresponding air point, as exemplified in the Figure. This finding suggests a simple method for the



correction of CT numbers obtained by using a scanner with poor air calibration. It necessitates the measurement of the CT number of air, preferentially within a phantom that resembles a thorax as closely as possible, and it simply entails a correction of every measured CT number with the error in the air value. For example, when the air value equals -1008 HU, +8 HU is added to all measured CT numbers. In Table 2 the corrected CT numbers for the dog lung and foam 109 were calculated according to this method. Averaged over all scanners, the CT number for foam 109 in the lean thorax is  $-894.3 \pm 2.4$  HU, in the obese thorax,  $-894.4 \pm 1.2$  HU. The largest difference between the results of any two scanners was 7 HU. These results indicate a fair inter- and intrascanner conformity in densitometric estimates in the low-density range. For the dog lung, a larger spread in CT numbers was observed: The average corrected CT number was  $-908.2 \pm 4.7$  HU. A considerable part of the variation is due to the inhomogeneous density of the lung, and the resulting sensitivity to phantom positioning, slice thickness, and region definition. Homogeneous foam is clearly preferred for studies of this type.

A theoretically better approach to correcting poor air calibration consists in effectively making a calibration curve with an air and a water point and calculating the density according to the equation  $\text{lung density} = (1000/[\text{CT number water} - \text{CT number air}])(\text{measured lung CT number} - \text{CT number air})$ . This method should be more accurate, especially at higher densities.

Concerning the tested acquisition and reconstruction parameters that in principle should not affect CT numbers, it can be concluded that all scanners appear to be well designed. The only serious exception is the section thickness dependence of CT numbers of air for the two Philips scanners. Philips stated that they have largely solved this problem and that they started installing modifications. Substantial CT number falsification by truncation at -1023 or -1024 HU (9), as is possible with the Somatom Plus and the Highlight scanners, is likely to occur at extreme low densities or low mAs values, especially in combination with a high-resolution filter. When it occurs, it leads to an erroneous upward shift of the average CT number. The phenomenon is easily recognized in a histogram: At the low end, tail truncation is seen, with a peak containing the truncated pixels at the most negative CT number the system can handle. Reconstruction with a smoother filter often will remedy the problem as far as the average CT number is concerned.

The present results compare favorably with those reported in the past (5-7). Several explanations exist for this observation. First of all, the equipment has been greatly improved in the decade since the previous measurements were performed. Second, the older work concentrated on densitometry of small, nearly water-equivalent objects, sometimes within a medium of greatly different density, where partial volume effects and reconstruction filter-related effects are of importance. In the present work,

in which CT numbers averaged over large areas are considered, these problems do not play a role.

In summary, all scanners tested have an acceptable calibration at water density. At low densities the scanners differ in their behavior. CT numbers from the GE Highlight and Picker PQ-2000 scanners show some sensitivity to phantom size or composition. The Philips scanners SR 7000 and LX have a poor, section-thickness-dependent calibration, but the systems are not very sensitive to phantom size or composition. The Siemens Somatom Plus systems are well calibrated and not very sensitive to phantom size or composition.

A simple correction for the scanners with a poor calibration at air density has been proposed. After this correction is applied, the conformity of all scanners in the low-density range was fair: At a density of about  $100 \text{ kg/m}^3$  the standard deviation of the average over all scanners is less than 3 HU, and the maximum observed interscanner difference is 7 HU. The observed interscanner variability will generally still be smaller than the reproducibility of CT-densitometry in clinical practice (9,11).

All scanners are well designed with respect to CT number sensitivity to reconstruction filter, zoom factor, table height, and section thickness, with the exception of the two Philips systems in relation to sensitivity to section thickness.

In conclusion, when correction for poor air calibration is applied, all systems tested can be used for densitometry of the lungs, and meaningful comparison of results from the various scanners tested is possible.

## REFERENCES

1. Stern EJ, Frank MS. CT of the lung in patients with pulmonary emphysema: Diagnosis, quantification, and correlation with pathologic and physiologic findings. *AJR* 1994; 162:791-798.
2. Rienmüller RK, Behr J, Kalender WA, et al. Standardized quantitative high resolution CT in lung diseases. *J Comput Assist Tomogr* 1991; 15:742-749.
3. Lamers RJS, Thelissen GRP, Kessels AG, Wouters EFM, van Engelshoven JMA. Chronic obstructive pulmonary disease: Evaluation with spirometrically controlled CT lung densitometry. *Radiology* 1994; 193:109-113.
4. Adams H, Bernard MS, McConnochie K. An appraisal of CT pulmonary density mapping in normal subjects. *Clin Radiol* 1991; 43:238-242.
5. Levi C, Gray JE, McCullough EC, Hattery RR. The unreliability of CT numbers as absolute values. *AJR* 1982; 139:443-447.
6. McCullough EC, Morin RL. CT-number variability in thoracic geometry. *AJR* 1983; 141:135-140.
7. Zerhouni EA, Spivey JF, Morgan RH, Leo FP, Stitik FP, Siegelman SS. Factors influencing quantitative CT measurements of solitary pulmonary nodules. *J Comput Assist Tomogr* 1982; 6:1075-1087.
8. Pearce JG, Milne ENC, Gillan GD, Roeck WW. Development of a radiographic chest phantom with disease simulation. *Invest Radiol* 1979; 14:181-184.
9. Kemerink GJ, Lamers RJS, Thelissen GRP, van Engelshoven JMA. CT densitometry of the lungs: scanner performance. *J Comput Assist Tomogr* 1996; 20:24-33.

10. ICRU-report 44: Photon, electron, proton and neutron interaction data for body tissues. Bethesda, Md: International Commission on Radiation Units and Measurements, 1989.
11. Kalender WA, Rienmüller R, Seissler W, Behr J, Welke M, Fichte H. Measurement of pulmonary parenchymal attenuation: Use of spirometric gating with quantitative CT. *Radiology* 1990; 175:265-268.

## CHAPTER 5

---

# On segmentation of lung parenchyma in quantitative computed tomography of the lung

Gerrit J. Kemerink

Rob J.S. Lamers

Bas J. Pellis

Han H. Kruize

Jos M.A. van Engelshoven

## ABSTRACT

**Purpose:** To investigate the influence of segmentation threshold and number of erosions on parameters used in quantitative computed tomography (CT) of the lung (erosions are shrink-operations on the segmented area).

**Materials and methods:** Parameters assessed were mean lung density, area of the segmented lung, two percentiles and the pixel index which is the relative area of the histogram below -905 Hounsfield units (HU). We analyzed images of 10 emphysematous and 10 non-emphysematous patients, that had been scanned at carina level in inspiration and expiration, using sections of 1, 2, 3, 5 and 10 mm in combination with a standard, a smooth and an ultra-smooth reconstruction kernel. The lungs were segmented using pixel tracing at thresholds of -200, -400 and -600 HU with 0 - 4 erosions, followed by histogram analysis.

**Results:** The area of the segmented lungs decreased with 0.9 to 3.2 % per 100 HU decrease in threshold and with 2.2 to 3.1 % per erosion, dependent on patient group and level of inspiration. Estimated mean lung density changed up to 30 % by changing threshold and number of erosions. The pixel index and the 10th percentile depended only slightly on threshold and number of erosions, but the 90th percentile showed a strong dependence of up to 40 %.

**Conclusion:** The segmentation protocol can have a large impact on densitometric parameters and standardization is mandatory for obtaining comparable results. Ideally a threshold equal to the average of the densities of lung and soft tissue should be used, but -400 HU will do in a limited but common density range (-910 to -790 HU). For densitometry two erosions are recommended, for volumetry zero erosions should be used.

## INTRODUCTION

Densitometry of the lung has found application without sufficient attention to methodological aspects. For instance, CT number calibration was seldomly addressed, while for several scanners considerable errors at low densities can exist (1). Although the scan protocol may affect densitometric parameters, not all relevant properties of the scan technique were usually specified. Suboptimal protocols have also been applied. It was recently shown that density resolution is an important parameter (2-4) and that it is quite bad for the so called thin-section densitometry protocol, which was widely used, also by ourselves (5). Estimation of parameters that depend on the shape of the lung histogram, like the pixel index and percentiles, should not be done with this protocol (3,4). Also different segmentation protocols have been applied, without assessment of the effect on densitometric results. The consequences

of this lack of attention to methodology are suboptimal work and incomparability of most studies.

In an effort to contribute to the required methodological knowledge, this study addresses segmentation of the lung. According to the literature a few different methods have been applied for the semi-automatic segmentation of the lungs (6-10). Hedlund et al used gradients in CT numbers together with CT number ranges, both in an edge tracking method and a method that was based on the selection of contiguous pixels within the lung (6). Kalender et al introduced pixel tracing, whereby contiguous pixels in a certain CT number range were traced along the border of the lung (7). Other investigators applied methods that binarize the CT image using a threshold that discriminates lung from soft tissue (9,10). When segmentation errors occur, they can be corrected manually, or, as shown by Kalender et al (7) and Zagers et al (8), by software that still may need some manual help.

A serious problem of segmentation is the inadvertent inclusion of pixels partially corresponding to soft tissue surrounding the lung. Such pixels can have a large impact on densitometric parameters of the parenchyma, especially in patients with lungs of low density as in emphysema. Although it is clear that the magnitude of the effect will depend on segmentation threshold and number of erosions, this dependence has not yet been studied. According to the literature a few segmentation thresholds have been used: -200 HU (7), -380 HU (8) and -400 HU (10). In several studies the segmentation procedure was poorly described and it was often not reported whether subsequent erosions had been applied. Even the manual of the widely used software package Pulmo CT does not specify threshold and number of erosions (7).

Unexamined so far is also the influence of segmentation threshold and spatial resolution on the area of the segmented lung regions. The area is relevant because it is the basis for the calculation of the lung volume, which may have important applications in checking and correcting spirometry in longitudinal CT studies, and in quantifying the effect of reduction surgery. Note that spatial resolution can be varied over a wide range with section thickness and reconstruction kernel. Most studies published so far reported section thickness, but none the in-plane spatial resolution, although this latter parameter can have a significant effect on densitometric quantities (3).

In this study we investigate, for different patients and scan protocols, the effects of segmentation threshold and number of erosions on several frequently used densitometric parameters, including the area of the segmented lung. We applied a pixel tracing algorithm for automatic segmentation (11).

## MATERIALS AND METHODS

The following acquisition parameters were used on our CT scanner (Somatom Plus, Siemens, Erlangen, Germany): a non-spiral scan of  $360^\circ$ , a scan time of 1 s, a high voltage of 137 kV, a tube load of 220 mAs, the large focal spot ( $1.3 \times 1.2 \text{ mm}^2$ ), a  $512 \times 512$  matrix and a field of view of approximately 310 mm (zoom factor  $\sim 1.6$ ) corresponding to a pixel size of about 0.6 mm. Air calibrations were performed daily. The calibration of this scanner at low densities is adequate and stable over time (1).

Two groups of patients were analyzed: one group consisted of 10 persons with emphysema, the second group of 10 non-emphysematous persons with various forms of lung disease or normal lungs. The study was approved by the medical ethical committee of our institution and all patients gave informed consent. The two groups were scanned in inspiration and expiration, yielding 4 categories of data. The scans were made at the level of the carina with the patient in supine position, using section thicknesses (S) of 1, 2, 3, 5 and 10 mm. Carina level was chosen because segmentation at this position can have some problems. The complete scan protocol causes an effective dose to the patient of approximately 1 mSv. All scan data were reconstructed with 3 different reconstruction kernels: standard (STD, Siemens code AB7055), soft (SFT, AB7057) and soft detail (SD, AB7059). Consequently, each of the 4 categories consisted of 150 images. According to the CT-manufacturer the full width at half maximum (FWHM) of the point spread function (PSF) is 1.13 mm for the STD, 1.40 mm for the SFT and 1.86 mm for the SD kernel. For patient comfort we did not apply spirometry during the 10 scans, but we have excluded from analysis those patients whose mean density, averaged over all section thicknesses, had a large standard deviation (see below).

All images were transferred to an image processing station (ICON Power PC, Siemens Gammasonics, Hoffman Estate, IL). Using pixel tracing (7,11), the lungs were semi-automatically segmented using 3 different thresholds (T): -200 HU, -400 HU and -600 HU. A starting point for segmentation was automatically determined by software. Values of -200 and -400 HU have been used before according to the literature; we added -600 HU to see the effect of a low threshold. The tracing algorithm yields a lung contour consisting of contiguous pixels with CT numbers as close as possible to the threshold, but not exceeding this. When user interaction was required the action was logged to get an impression of the frequency of the problem in relation to segmentation threshold and scan parameters. Subsequently both lung regions were subjected to 0, 1, 2, 3 or 4 erosions (E). One erosion corresponds to the removal of all pixels lying along the circumference of the segmented area, having at least one of their eight neighbours outside the area. Histograms were created from the left lung, the right lung and the total lung, and the following histogram parameters were calculated: the area of the lung region, the mean CT number, the pixel index  $PI(-905)$ , the 10th percentile  $P(10)$

and the 90th percentile  $P(90)$ . The mean CT number is for the (water equivalent) lung directly related to the mean density ( $\rho$ ):  $\rho = (1000 + \text{CT number}) / 1000 \text{ g/cm}^3$ . Because of this simple relation we will also present density sometimes in terms of the CT number. The pixel index  $PI(-905)$  defines the relative area of the histogram below -905 HU, and  $P(10)$  and  $P(90)$  define the CT number below which 10 %, respectively 90 %, of the histogram area extends. The pixel index (or density mask) has been used as a quantitative measure for emphysema (9). We chose  $PI(-905)$  as the average of -900 and -910 HU which both have been used (ref's 9 and 12 and many subsequent studies).

A problem when trying to illustrate the systematic effects of segmentation threshold, number of erosions, section thickness and reconstruction kernel, is the variation in histogram parameters introduced by two other mechanisms. First, scans with different section thickness necessarily differ in the (heterogeneous) lung tissue that is sampled. Second, small differences in the degree of inspiration or expiration will exist. To reduce the impact of these two effects we included in our analysis only patients whose standard deviation of mean density, calculated from all sections in each single respiratory status, was less than 6 HU for emphysematous patients, and less than 12 HU for non-emphysematous patients ( $T = -400 \text{ HU}$ ,  $E = 2$ ). The density is thus taken as criterium to judge constancy of inspiration and the identicalness of the tissue looked at.

Further reduction was obtained by averaging values from all patients within each of the 4 categories. This was done after largely eliminating inter-patient differences in lung properties by subtracting from each histogram parameter a patient specific reference value. This reference value was the average over all 15 combinations of section thickness and reconstruction kernel of that same parameter for  $T = -400 \text{ HU}$  and 2 erosions of that patient. Thus each patient has for each respiratory status and each histogram parameter a reference value. Averaging over 15 combinations was performed to increase the robustness of the reference value. Note that the present approach assumes that a densitometric parameter changes for all patients in a similar way around his reference value when segmentation threshold, number of erosions or spatial resolution are changed. Lung areas of each patient were expressed as a percentage of his reference area, and changes in area are given in percent-point (i.e. as simple differences between these percentages).

The advantage of averaging a histogram parameter over all patients in a given category is that trends are much more clearly reflected than they do in the data from a single patient. Therefore, this average was further used in regression analysis. Another approach to examining the large set of data would have been to perform regression analysis on the scatterplots of individual patients, and to average the slopes of all patients belonging to the same category. With this latter method essentially identical results were obtained, but less suitable graphs for visual presentation.



According to simulations to be discussed, it is expected that for a given segmentation threshold the area is approximately linearly dependent on spatial resolution. As an effective measure for spatial resolution we used the geometric mean  $R = (FWHM^2 \times S)^{\frac{1}{3}}$ , with FWHM the width of the PSF and S the section thickness. This particular choice for R accounts for the fact that partial volume averaging occurs in all three orthogonal directions. This R resulted in an approximately linear relation with lung area, and thus in a meaningful presentation of the data of all 15 combinations of kernel and section thickness in a single graph. The same way of presentation was chosen for  $\rho$ , PI(-905), P(10) and P(90), because also rather good linearity was obtained for these parameters. For PI(-905) the quality of a linear fit, as judged from  $\chi^2$  and visual inspection, was considerably better when R was used instead of the previously used inverse square root of the sample volume(3), while for P(10) and P(90) the quality of the fit was very similar. For consistency, R was used here in all cases.

The dependence of the size of the segmented area on different reconstruction kernels and segmentation thresholds was also studied theoretically. We assumed a sharp density step between lung and the surrounding soft tissue, and convolved this step with the point spread function of the reconstruction kernels. For simplicity we assumed in most simulations that the thorax cavity locally has flat walls and that only the in-plane spatial resolution mattered. The results show the CT number dependent shift in apparent lung border with respect to the original (step) position.

We also measured the volume of a phantom that consisted of 2 polyethene bottles that had been cast into polymethylmethacrylate (PMMA or perspex). The volume of each compartment was determined by filling with water and weighing. The phantom was scanned with its long axis making angles of about 10 degrees with the axis of the scanner, both in the horizontal and in the vertical plane. The reason for this way of positioning was to get appropriate delineation of the flat bottom and top of the bottles in transversal images. Different section thicknesses, reconstruction kernels and inter-slice distances were applied. The zoom factor was 1.7. The volume was calculated by adding the areas of all scans and multiplying this sum with the inter-slice distance.

Due to the very large amount of lung histogram related data (we analyzed the right, the left and the total lung in 600 images) only a limited, more or less representative part will be presented. For instance, we only give results for the total lung and not for the two separate lungs. Since densitometry has been applied in particular for the quantification of emphysema during inspiration, we will generally present data for this category, but when relevant also data for the other categories will be given.

## RESULTS

### *Manual correction of automatically generated contour*

Table 1 shows the frequency of manual operations required to correct the automatic segmentation of CT images obtained at the level of the carina. These numbers are averages over 10 patients and 15 combinations of section thickness and reconstruction kernel (thus 150 images). Figure 1 illustrates the dependence on effective spatial resolution ( $R$ ): to improve statistics we added all data of the emphysematous and non-emphysematous groups, both in inspiration and expiration, resulting in 40 cases per point. At a threshold of -600 HU the automatic segmentation was in several cases poor for non-emphysematous patients in expiration. This was caused by the relatively high density of the lung in this category (mean density  $-795 \pm 73$  HU, maximum -652 HU), which made that parts of the lung were excluded.

### *Area of segmented lung regions*

Figure 2 shows, for the group of emphysematous patients in inspiration, the dependence of the area of the segmented lung on segmentation threshold, effective spatial resolution and number of erosions. Note that each point is the average of 10 patients, and that each patient's value was expressed as a percentage of his reference value minus 100 %. For the other 3 data categories (emphysema expiration, non-emphysema inspiration and expiration) the results were qualitatively similar, except for some differences in slopes and intercepts. Table 2 gives these slopes of the scatter plots of segmented area versus effective resolution  $R$  for each of the 4 data categories, all 3 thresholds and zero erosions.

The dependence of the area on segmentation threshold was calculated from the difference in areas obtained for the thresholds of -200 HU and -600 HU. For zero erosions one so finds:  $-0.9 \pm 0.2$  % of the reference area per 100 HU decrease in threshold for the emphysematous patients in inspiration,  $-1.2 \pm 0.2$  % per 100 HU for this group in expiration,  $-1.6 \pm 0.3$  % per 100 HU for the non-emphysematous patients in inspiration, and  $-3.2 \pm 0.6$  % per 100 HU in expiration. The change in segmented area per erosion, for 2-mm thick sections reconstructed with the SD kernel (an average  $R$ ) and averaged over the 3 different thresholds, is for the emphysematous patients in inspiration  $-2.2 \pm 0.1$  % and in expiration  $-2.5 \pm 0.1$  %, and for non-emphysematous patients respectively  $-2.4 \pm 0.1$  % and  $-3.1 \pm 0.5$  %. These results show that 1 erosion already has a large impact on estimated lung area, and consequently on lung volume if that would be derived.

**Table 1.** Frequency of Manual Operations Required to Correct Automatic Segmentation<sup>⋆</sup>.

Threshold (HU)	Inspiration			Expiration		
	-200	-400	-600	-200	-400	-600
<b>Emphysema</b>						
Separation R&L lungs	61	57	30	68	57	24
Exclusion R bronchus	85	53	15	97	69	14
Exclusion L bronchus	17	7	2	6	2	2
<b>Non-emphysema</b>						
Separation R&L lungs	37	27	13	28	18	10
Exclusion R bronchus	78	62	17	73	29	2
Exclusion L bronchus	2	1	0	29	20	0

Note. <sup>⋆</sup> Each percentage pertains to 150 images: 10 patients, 5 section thicknesses and 3 reconstruction kernels. Data are presented as percentages.

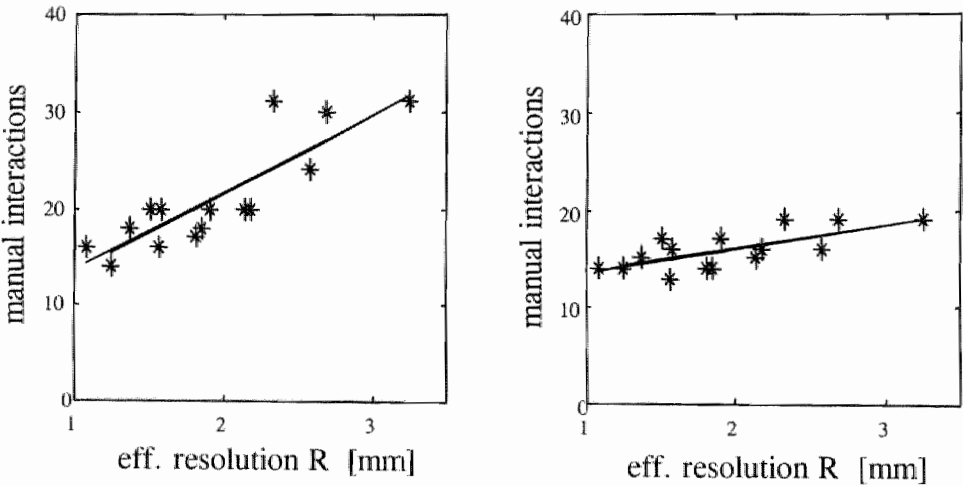


**Figure 1.** Manual corrections per 40 cases to improve automatic segmentation of the lungs, as a function of effective spatial resolution  $R$  ( $=|FWHM'_{PSF-S}|^{1/3}$ ). Data of emphysematous and non-emphysematous patients in inspiration and expiration were added. Segmentation threshold was -400 HU. Left: manual exclusion of trachea or right bronchus. Right: manual separation of left and right lung.

**Table 2.** Slope<sup>&</sup> of Scatter Plot of Segmented Lung Area versus Effective Spatial Resolution.

Threshold (HU)	-200	-400	-600
<b>Emphysema</b>			
inspiration	0.57 ± 0.15	0.29 ± 0.15	-0.50 ± 0.13
Expiration	1.82 ± 0.32	1.27 ± 0.30	0.47 ± 0.27
<b>Non-emphysema</b>			
inspiration	0.36 ± 0.37	-0.38 ± 0.34	-1.69 ± 0.37
Expiration	2.80 ± 0.54	1.78 ± 0.53	-0.39 ± 0.57

Note. <sup>&</sup> unit of slope is percent of reference area per unit change of effective spatial resolution (%/mm). No erosions have been applied.

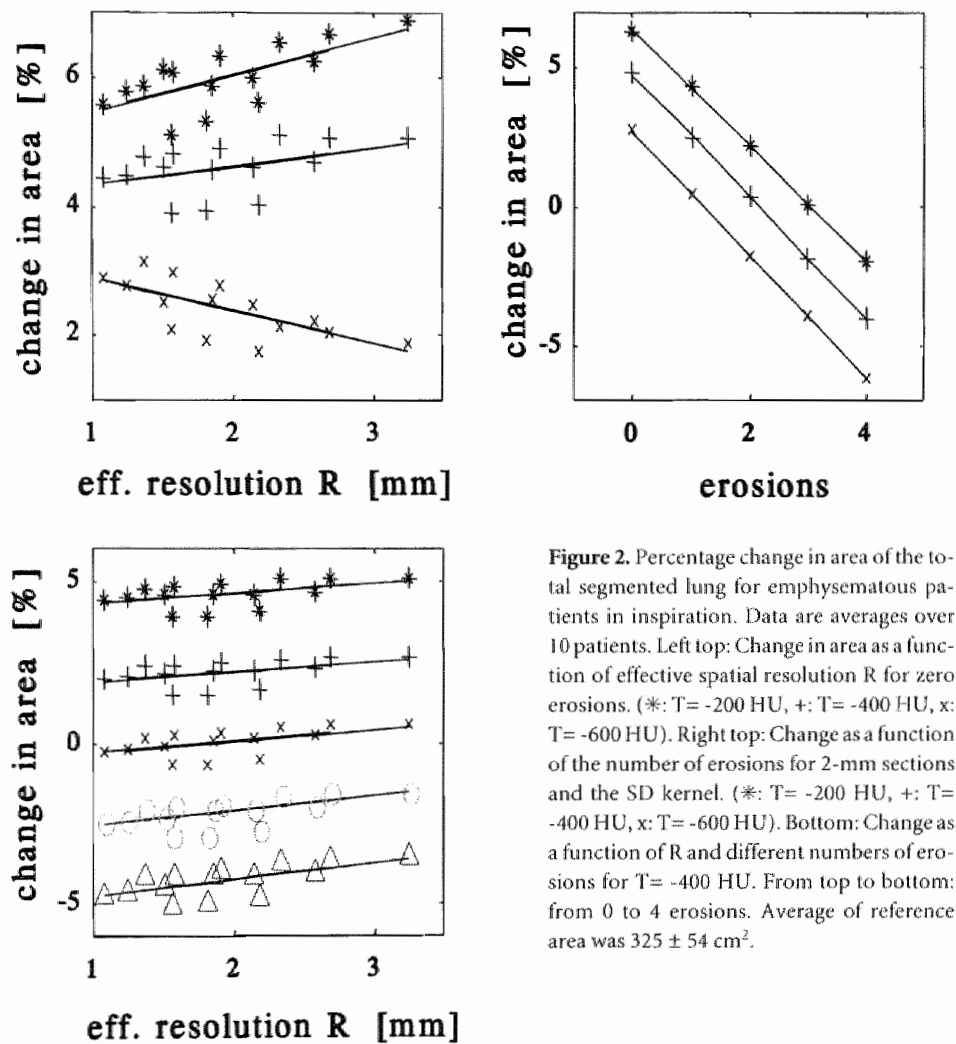


**Figure 2.** Percentage change in area of the total segmented lung for emphysematous patients in inspiration. Data are averages over 10 patients. Left top: Change in area as a function of effective spatial resolution R for zero erosions. (\*: T= -200 HU, +: T= -400 HU, x: T= -600 HU). Right top: Change as a function of the number of erosions for 2-mm sections and the SD kernel. (\*: T= -200 HU, +: T= -400 HU, x: T= -600 HU). Bottom: Change as a function of R and different numbers of erosions for T= -400 HU. From top to bottom: from 0 to 4 erosions. Average of reference area was  $325 \pm 54 \text{ cm}^2$ .

**Table 3.** Slope of Scatter Plot of mean CT Number of the Lung versus Effective Spatial Resolution

Erosions	0 (HU/mm)	2 (HU/mm)	4 (HU/mm)
<b>Emphysema</b>			
inspiration	6.7 ± 0.4	4.7 ± 0.4	3.1 ± 0.4
Expiration	4.0 ± 0.6	2.4 ± 0.5	0.6 ± 0.4
<b>Non-emphysema</b>			
inspiration	6.9 ± 0.8	4.9 ± 0.8	2.7 ± 0.8
Expiration	4.5 ± 0.9	2.9 ± 0.8	0.8 ± 0.7

Note. Segmentation threshold was -400 HU.

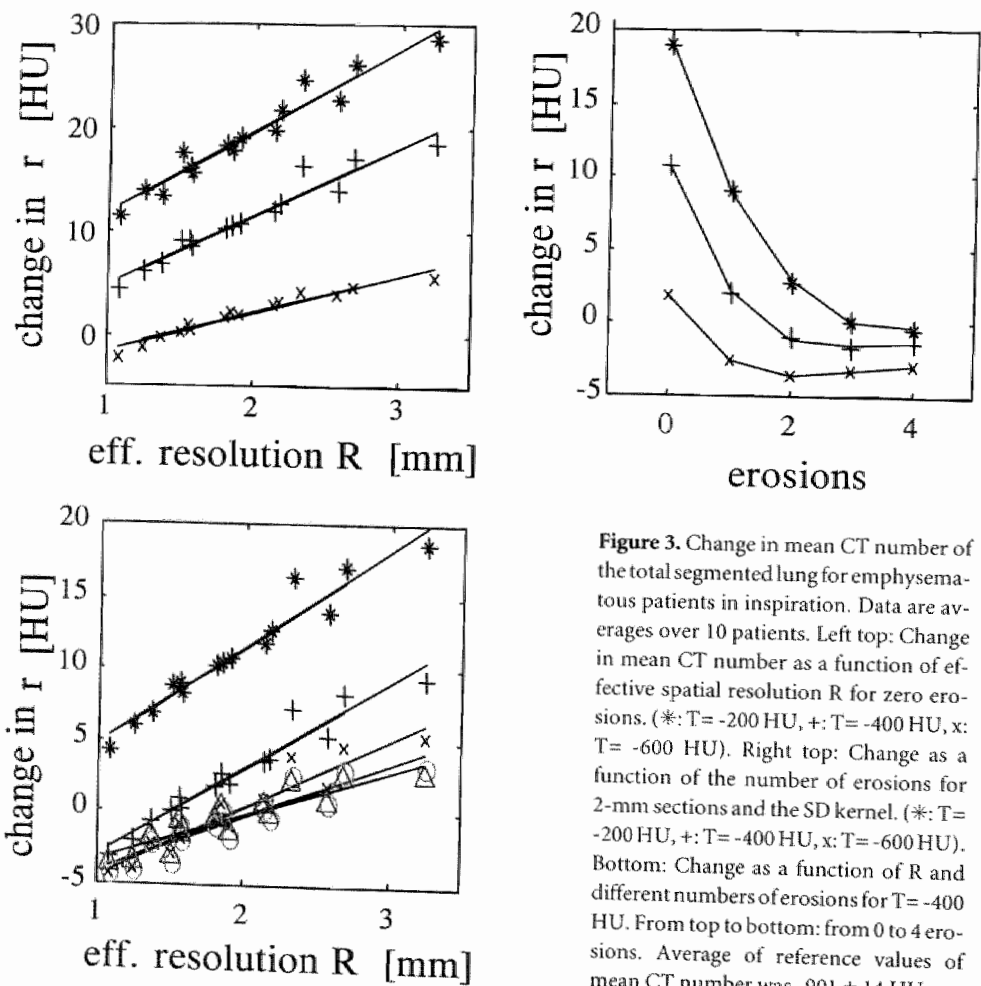


**Figure 3.** Change in mean CT number of the total segmented lung for emphysematous patients in inspiration. Data are averages over 10 patients. Left top: Change in mean CT number as a function of effective spatial resolution R for zero erosions. (\*: T = -200 HU, +: T = -400 HU, x: T = -600 HU). Right top: Change as a function of the number of erosions for 2-mm sections and the SD kernel. (\*: T = -200 HU, +: T = -400 HU, x: T = -600 HU). Bottom: Change as a function of R and different numbers of erosions for T = -400 HU. From top to bottom: from 0 to 4 erosions. Average of reference values of mean CT number was -901 ± 14 HU.

## Mean lung density

Figure 3 shows, for the emphysematous patients in inspiration, the dependence of the mean CT number on segmentation threshold, effective spatial resolution and number of erosions. Large differences in mean density up to 30% can be obtained (the mean CT number for this category of data was -901 HU, corresponding to  $\rho = 0.099 \text{ g/cm}^3$ ). Results for the other 3 data categories were similar. The slopes of the scatter plots of the mean CT number versus effective spatial resolution, for  $T = -400 \text{ HU}$  and 0, 2 and 4 erosions, are given in Table 3. The decrease of the mean density with segmentation threshold was calculated from the differences between the mean densities obtained for the thresholds of -200 HU and -600 HU. For two erosions one obtains:  $-1.8 \pm 0.7 \text{ HU}$  per 100 HU threshold decrease for the emphysematous patients in inspiration,  $-2.6 \pm 0.9 \text{ HU}$  per 100 HU for this group in expiration,  $-3.2 \pm 1.2 \text{ HU}$  per 100 HU for the non-emphysematous patients in inspiration, and  $-7.0 \pm 1.2 \text{ HU}$  per 100 HU in expiration.

## PI(-905), P(10) and P(90)

Figures 4 and 5 illustrate the dependence of the pixel index PI(-905) and the percentile P(10) on segmentation threshold, spatial resolution and number of erosions, again for the emphysema group in inspiration. Both parameters are only slightly dependent on threshold and number of erosions. The dependence on spatial resolution is much more pronounced. The same observations hold for the other 3 data categories.

Figure 6 presents the results for the percentile P(90), also for the emphysema group in inspiration. Changes of more than 40% of the density corresponding to P(90) are possible due to changing segmentation threshold and number of erosions (average P(90) is -821 HU for this group, corresponding to a density of  $0.179 \text{ g/cm}^3$ ). The slope of the scatterplot of P(90) versus R decreases from (on average) positive to negative when the number of erosions is sufficiently increased: for zero erosions and a threshold of -400 HU, the slopes for each of the 4 categories are 11 HU/mm (emph., insp.), 0 HU/mm (emph., exp.), 8 HU/mm (non-emph., insp.) and -4 HU/mm (non-emph., exp.), while for 4 erosions the corresponding values are -1, -9, -2 and -12 HU/mm.

## Simulations and phantom study

The results of the measurements on the two-bottle phantom are shown in Table 4. We used a segmentation threshold of -430 HU, a value which was the average CT number for air in the bottles and the surrounding PMMA. The error in the estimated volume is small for this theoretically optimal threshold and independent of spatial resolution.

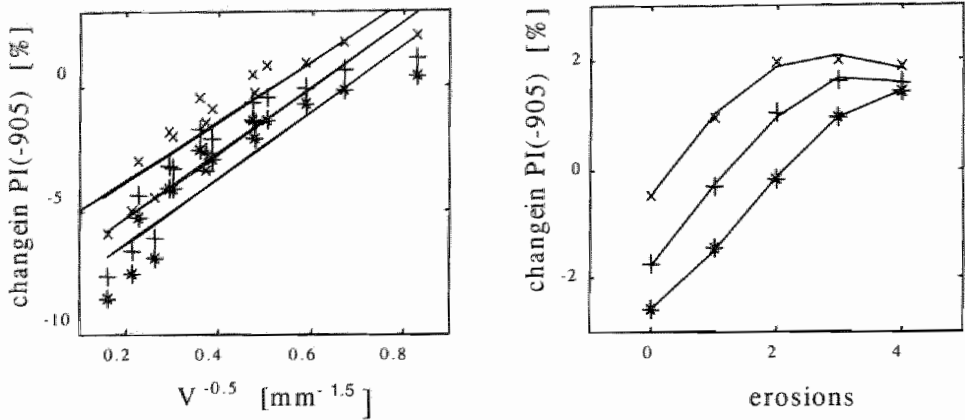


**Figure 4.** Change in pixel index  $PI(-905)$  of the total segmented lung for emphysematous patients in inspiration. Data are averages over 10 patients. Left: Change in  $PI(-905)$  as a function of the inverse square root of the sample volume for zero erosions. Right: Change in  $PI(-905)$  as a function of the number of erosions for 2-mm sections and the SD kernel. (\*:  $T = -200$  HU, +:  $T = -400$  HU, x:  $T = -600$  HU). Average of reference  $PI(-905)$  values was  $64 \pm 8$  %.

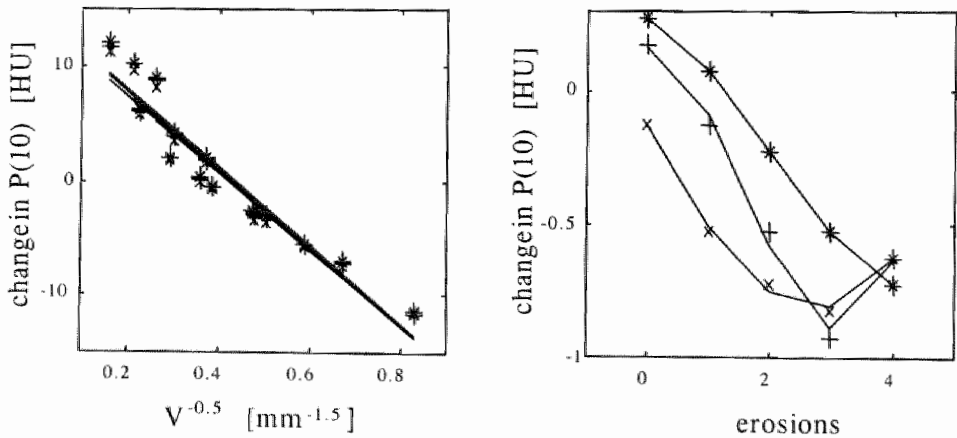


**Figure 5.** Change in percentile  $P(10)$  of the total segmented lung for emphysematous patients in inspiration. Data are averages over 10 patients. Left: Change in  $P(10)$  as a function of inverse square root of the sample volume for zero erosions. Right: Change in  $P(10)$  as a function of the number of erosions for 2-mm sections and the SD kernel. (\*:  $T = -200$  HU, +:  $T = -400$  HU, x:  $T = -600$  HU). Average of reference  $P(10)$  values was  $-974 \pm 17$  HU.

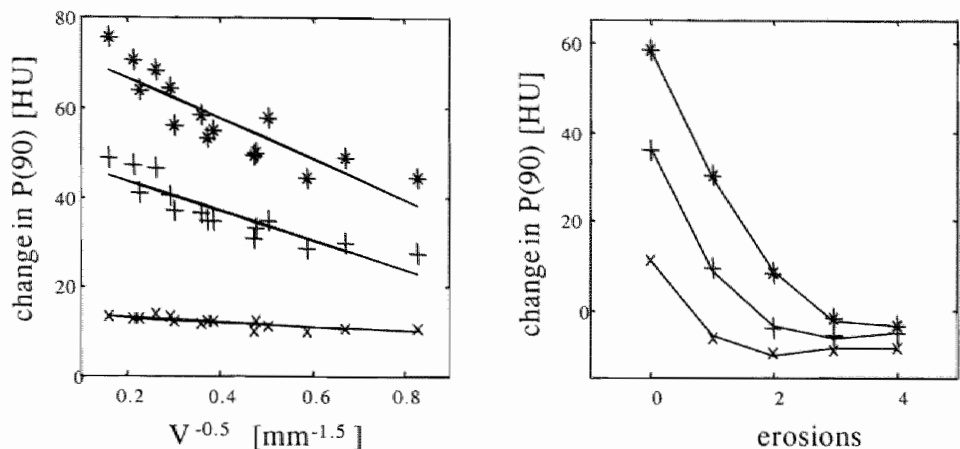


**Figure 6.** Change in percentile P(90) of the total segmented lung for emphysematous patients in inspiration. Data are averages over 10 patients. Left: Change in P(90) as a function of the inverse square root of the sample volume for zero erosions. Right: Change in P(90) as a function of the number of erosions for 2-mm sections and the SD kernel. (\*: T= -200 HU, +: T= -400 HU, x: T= -600 HU). Average of reference P(90) values was  $-821 \pm 15$  HU.

**Table 4.** Error in Volume estimate of Two-Bottle Phantom<sup>&</sup>

Section thickness (mm)	slice distance (mm)	recon. kernel	error in CT estimate		
			left (%)	right (%)	total (%)
1	10	STD	-0.72	-0.32	-0.52
1	10	SD	-0.69	-0.26	-0.47
5	5	STD	-0.33	-0.35	-0.34
5	5	SD	-0.33	-0.40	-0.37
10	10	STD	-0.01	-0.14	-0.06
10	10	SD	-0.11	-0.05	-0.03

Note. <sup>&</sup> volumes: left bottle 2.670 L, right 2.686 L and total  $5.355 \pm 0.005$  L.

Figure 7 shows the results of the convolution of the point spread function of the STD and the SD reconstruction kernels with a step function representing the border between lung and soft tissue. In these simulations we assumed a CT number of lung of -900 HU, the average for our group of emphysematous patients in inspiration, and of 50 HU for soft tissue. The shift for a given threshold is in first approximation linearly dependent on the spatial resolution, and so is the area for shifts small compared to the linear size of the region as is here the case. Simulations with cylindrically and spherically shaped borders gave nearly identical results as long as the radii were larger than about one centimeter.



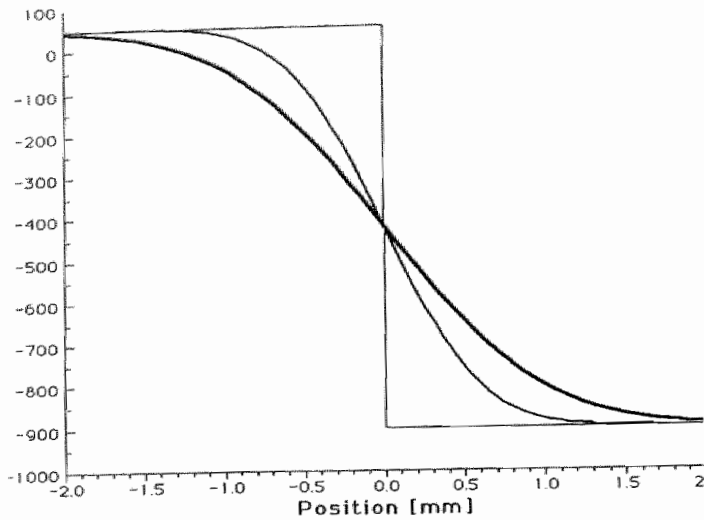


**Figure 7.** Simulation of lung border in a CT image by the convolution of the point spread function of the reconstruction kernel with a step border between lung (mean CT number -900 HU) and soft tissue (mean CT number 50 HU). Thin line: border assumed in case of infinitely good spatial resolution. Medium: border obtained when using the STD kernel ( $\text{FWHM}_{\text{FST}}=1.13$  mm). Fat: border obtained when using the SD kernel ( $\text{FWHM}_{\text{FST}}=1.86$  mm).

## DISCUSSION

### *Manual correction of automatically generated contours*

At carina level the number of manual corrections that is required is high, and this number increases with worsening of the spatial resolution, but decreases with decreasing threshold. These findings are in agreement with the assumption that thin septa and the finite spatial resolution, possibly in combination with some motion, are causing the failure during automatic segmentation. Note that poorer spatial resolution enhances the smearing out of small structures, thus lowering the CT values of thin septa. A low threshold is thus better suited for segmentation along thin septa, but a too low value, as our threshold of -600 HU for non-emphysematous patients in expiration, can lead to the exclusion of parts of the lung. At a threshold of -400 HU manual corrections were on average 30 % less frequently required than at the more commonly used threshold of -200 HU (7). We did not yet implement automatic correction algorithms, as for instance was done by Kalender et al (7) and Zagers et al (8). Note that

Zagers et al reported that even with automatic correction between 29 and 48 % of the images required user interaction.

### *Area of segmented lung regions*

A good starting point for the discussion of the segmented lung area is Figure 7. It shows that for a threshold that is equal to the average CT number of lung and soft tissue the position of the border of the lung is independent of spatial resolution. When a threshold is higher than this average CT number, the border will be found too far outward and the area will be overestimated. If spatial resolution is made worse in this situation, the overestimation will increase. For low thresholds the opposite occurs. Our experimental findings are largely, but not fully, in agreement with the simulations: 1. the segmented area decreases with decreasing threshold, as expected. 2. For all 4 categories the slope of the area versus spatial resolution curve decreases with decreasing segmentation threshold, and the slopes are positive for a threshold of -200 HU, as one would expect. However, for -600 HU the slope is negative only for 3 out of the 4 categories, and at -400 HU the difference in slopes between inspiration and expiration is opposite to what one would expect. One obvious flaw of our model is that it neglects medium sized vasculature that is depicted in the CT images with a broad range of CT numbers, as a consequence of the finite resolution. These vessels can drop below the segmentation threshold when section thickness is increased or in-plane resolution is lowered. This phenomenon leads to an increase in area with poorer spatial resolution that counteracts the decrease at low thresholds that is associated with a (full) step border in other places.

From a theoretical point of view, and neglecting the complications just discussed, it is best to use a threshold that is close to the average CT number of lung and soft tissue. Our phantom study corroborates this: the volumes derived for the two bottles were nearly identical for the STD and SD kernel, and they matched the true values quite well. At least for this phantom section thickness and reconstruction kernel are not critical for volume estimation. When the threshold deviates from the optimal value, an estimate of the systematic error can be made: a difference of 100 HU between threshold and mean CT number of lung and soft tissue will result in an error between 0.9 and 3.2 % in the area estimation, depending on patient and respiratory status. Therefore, if one would decide to use in general practice a threshold of -400 HU, this threshold would for instance for lungs with a mean CT number between -910 HU and -790 HU never be off by more than 30 HU from the optimal value. The systematic error in the area would then generally be less than 1 %. In this study no mean density below -910 HU was observed, and only in the group of non-emphysematous patients 4 persons exceeded -790 HU in expiration (highest was -652 HU). However, for volumetry it seems also possible to make a quick estimate of the mean density and to

choose an optimal threshold accordingly. Note that in longitudinal studies random errors are probably more important than threshold related effects, at least as long the threshold is kept fixed and the same scan protocol is used. Random errors depend among others on the degree of control of inspiration and on patient positioning.

For volumetry no erosions should be applied, because 1 erosion already reduced the area with about 2 - 3 %. Note that these percentages are approximately proportional to the linear dimension of a pixel.

### *Mean lung density*

Large differences of up to 30 % in estimated density could be introduced by changing segmentation threshold and number of erosions. Note that this number is for the average of 10 patients, in individual cases the effect can still be larger. These variations are caused by the inclusion or exclusion of relatively high density pixels at the circumference of the lung region. Such pixels are the result of spill over of soft tissue into the lung region by the finite resolution. They can be removed by lowering the segmentation threshold and/or applying erosions. For a given threshold, the density decreased only very slowly when more than 2 erosions were applied. Small differences for different thresholds remained, however, probably due to structures that are above the lower threshold, but below the higher. In case of the higher threshold many erosions may be required in some locations to remove these structures to the degree that they were excluded at the lower threshold. As discussed in the section on area estimation, vasculature may be involved, but also other small structures of high density (e.g. septa), as well as transitions between lung and soft tissue that appear smooth in the CT image (6).

The present results show that the estimated mean density in patient studies is dependent on spatial resolution, i.e. on section thickness and reconstruction kernel, through its effect on segmentation. The dependence is not very strong, but in previous publications we suggested (incorrectly) that there was no relation, which was based on consideration of bulk materials (2,3). This dependence is strongest when no erosions are applied, and it is reduced by eroding. For instance, for a threshold of -400 HU and averaging over all 4 categories of patients, the slope reduced from 5.5 HU/mm to 1.8 HU/mm after 4 erosions. The slopes are positive because with increasing R, i.e. poorer resolution, the border profile becomes flatter so that for a given threshold more high density pixels will be included in the segmented region.

For many purposes a threshold of -400 HU and 2 erosions may be adequate. For lungs with very low or high density the threshold should be adapted, e.g. to the average CT number of lung and soft tissue as discussed above. An advantage of using -400 HU as a threshold, as compared to the more frequently used -200 HU, is that the chance for successful automatic segmentation is somewhat higher. The rather widely used

program Pulmo CT applies values that generally will be non-optimal: a threshold of -200 HU and 1 erosion (7).

When comparability between different investigations is mandatory, one should use the same segmentation parameters, and preferably also the same scan protocol.

### *PI(-905), P(10) and P(90)*

The pixel index PI(-905) and the percentile P(10) are only slightly dependent on segmentation threshold and number of erosions. Changing segmentation threshold and number of erosions affects initially only a limited number of pixels that belong to the high density part of the CT number histogram of the lung (well above -905 HU). Consequently, the relative change in PI(-905) is roughly equal to the relative change in histogram area. For P(10), when properly expressed in density, the relative change is still smaller. However, both parameters are rather strongly dependent on section thickness and reconstruction kernel (i.e. on R or sample volume) (3).

P(90) depends heavily on segmentation threshold and number of erosions, and to a lesser degree on spatial resolution. Changes of up to 40% in the density corresponding to P(90) are possible because high density pixels are involved.

The effect of decreasing resolution for uniform cellular materials is a smoother image, a narrower histogram and thus a lower P(90) (3). For segmented lung this effect (a negative slope of P(90) versus R) becomes only manifest after removal of high density pixels at the circumference of the lung region by a sufficiently low threshold and enough erosions.

The dependence of PI(-905), P(10), P(90) on resolution was studied before. For the quantification of these parameters it was recommended to use a section thickness and reconstruction kernel with  $Sx(1.064x\text{FWHM})^2 \geq 8 \text{ mm}^3$ , and for comparability, to adhere to a standard scan protocol (2,3).

## Conclusions

Most clinical densitometric studies published so far paid little attention to methodological aspects. This has led to work that was not always optimal, and to incomparability of different studies. Only with due attention to scan and analysis protocols quantitative CT of the lung has a chance of a more general and useful application.

In this study we investigated, for emphysematous and non-emphysematous patients and for different scan protocols, the influence of segmentation threshold and number of erosions on the following densitometric parameters: area of the segmented lung, mean lung density, the pixel index PI(-905) and the percentiles P(10) and P(90). The results indicate that different scan and segmentation protocols in principle can

lead to unacceptably large differences in densitometric parameters. Ideally a segmentation threshold equal to the average of the densities of lung and soft tissue should be used. However, for much of the work a threshold of -400 HU will be adequate. For densitometry two erosions can be recommended, while for volumetry zero erosions should be applied. For comparability of data the same scan and analysis protocols should be applied.

## REFERENCES

1. Kemerink GJ, Lamers RJS, Thelissen GRP, van Engelshoven JMA. Scanner conformity in CT densitometry of the lungs. *Radiology* 1995; 197:749-752.
2. Kemerink GJ, Kruize HH, Lamers RJS, van Engelshoven JMA. Density resolution in quantitative computed tomography of foam and lung. *Med Phys* 1996; 23:1697-1708.
3. Kemerink GJ, Kruize HH, Lamers RJS, van Engelshoven JMA. CT lung densitometry: dependence of CT numbers histograms on sample volume and consequences for scan protocol comparability. *J Comput Assist Tomogr* 1997; 21:948-954.
4. Kemerink GJ, Kruize HH, Lamers RJS. The CT's sample volume as an approximate, instrumental measure for density resolution in densitometry of the lung. *Med Phys* 1997; 24:1615-1620.
5. Lamers RJS, Thelissen GRP, Kessels AG, Wouters EFM, van Engelshoven JMA. Chronic obstructive pulmonary disease: evaluation with spirometrically controlled CT lung densitometry. *Radiology* 1994; 193:109-113.
6. Hedlund LW, Anderson RF, Goulding PL, Beck JW, Effmann EL, Putman CE. Two methods for isolating the lung area of a CT scan for density information. *Radiology* 1982; 144:353-357.
7. Kalender WA, Fichte H, Bautz W, Skalej M. Semiautomatic evaluation procedures for quantitative CT of the lung. *J Comput Assist Tomogr* 1991; 15:248-255.
8. Zagers R, Vrooman HA, Aarts NJM, et al. Quantitative analysis of computed tomography scans of the lungs for the diagnosis of pulmonary emphysema. *Invest Radiol* 1995; 30:552-562.
9. Müller NL, Staples CA, Miller RR, Abboud RT. "Density Mask": an objective method to quantitate emphysema using computed tomography. *Chest* 1988; 94:782-787.
10. Bae KT, Slone RM, Gierada DS, Yusem RD, Cooper JD. Patients with emphysema: quantitative CT analysis before and after lung volume reduction surgery. *Radiology* 1997; 203:705-714.
11. Pavlidis T. Algorithms for graphics and image processing Berlin: Springer Verlag, 1982.
12. Hayhurst MD, Flenley DC, McLean A, et al. Diagnosis of pulmonary emphysema by computerised tomography. *Lancet* 1984; 2:320-322.

## CHAPTER 6

---

# Reproducibility of spirometrically controlled CT lung densitometry in a clinical setting

Rob J.S. Lamers  
Gerrit J. Kemerink  
Marjolein Drent  
Jos M.A. van Engelshoven

## ABSTRACT

**Purpose:** The aim of this study was to assess the reproducibility of spirometrically gated computed tomographic (CT) lung densitometry at defined levels of inspiration in hospitalized patients.

**Materials and methods:** On two consecutive days, spirometric gated CT sections were obtained from twenty hospitalized patients at 5 cm above and 5 cm below the carina, and at 90% and 10% of the vital capacity (VC). The mean, modal, and median lung densities were calculated, the cut-off points of the frequency distribution of Hounsfield units (HU) defining the lowest and the highest 10th percentile, as well as the histogram full width at half maximum. The lung density parameters of corresponding CT sections of both studies were compared. Reproducibility was expressed as the standard deviation of the signed difference between the results of day 1 and day 2 divided by  $\sqrt{2}$ . Reproducibility data were correlated with results of airflow limitation.

**Results:** At 90% VC, reproducibility in both lung zones was on the order of 3-14 HU. At 10% VC, reproducibility was worse by approximately a factor of three. No relationship was found between reproducibility and results of airflow limitation.

**Conclusion:** Objective measurement of lung density at spirometrically controlled levels of inspiration is a reproducible method in assessing pulmonary density. Reproducibility of lung density measurements is not influenced by very severe respiratory insufficiency. The most reproducible computed tomographic lung density measurements can be obtained at 90% vital capacity.

## INTRODUCTION

Densitometry of the lung is extensively used in pulmonary research. It has the potential to become an important addition to standard lung function tests in diagnosing and following the extent of pulmonary emphysema and interstitial lung disease. For recent reviews of this extensive work we refer to the literature (1-2). The value of the technique is clearly proven in pulmonary emphysema. During inspiration computed tomography (CT) correlates well with the pathologic score of emphysema (3). Expiratory CT reflects airway obstruction and air-trapping more than it does emphysema (4,5). Densitometric data may contribute to improved patient selection and to better evaluation of the response to volume reduction surgery (6,7). Densitometry may provide an additional measure in selecting the side of greatest severity for unilateral lung reduction surgery (7).

The methodology of CT densitometry has been established as well as factors affecting parameters derived from a histogram of Hounsfield numbers (HU). The accuracy and scanner conformity of modern CT scanners have proved to be adequate after cor-

rection for poor air calibration (8,9). CT number histograms of the lung are strongly dependent on section thickness and reconstruction filter (10-12). To optimize CT evaluation procedures, semi-automatic algorithms isolating lung parenchyma by fast contour tracking have been developed, as well as automatic evaluation algorithms calculating various densitometric parameters automatically. Usually, mean lung density is determined as an average over a relatively large area. Unfortunately, it can be spuriously misleading especially at localized disease onset (13). Mean lung density, however, is not the only available densitometric parameter which can be extracted from the CT data. Pixel index analysis (3,4,14) and the lowest 10th percentile of the frequency distribution of densities (15) have shown promising results in the assessment of emphysema.

If densitometry of the lung is used for diagnosis and follow-up of pulmonary emphysema or interstitial lung disease, the overall precision of the procedure has to be established. Reproducibility errors due to instrumental and technical factors have generally been considered to be smaller than patient-related factors. The CT density of the lung is considerably influenced by the level of inspiration at which the CT images are obtained. Control and monitoring of this level of inspiration during scanning is of major importance to obtain reproducible CT lung density measurements. A spirometrically controlled CT technique has been developed, offering the opportunity to obtain CT scans at defined levels of inspiration (16).

The purpose of this study was to assess the reproducibility of a number of histogram-related parameters of single CT slices through the upper and the lower zones of the lungs at 90% and 10% of the vital capacity (VC) in a hospitalized patient population.

## MATERIALS AND METHODS

Twenty hospitalized patients without the presence of pneumonia or lung tumor on the plain chest radiograph participated in this study. There were 11 men and 9 women, aged 18-63 yrs (median, 44 years). Ten patients had never smoked and ten were smokers or former smokers (mean consumption, 52 pack-years). Causes of hospitalization were: exacerbation chronic obstructive pulmonary disease (COPD) ( $n = 14$ ); pulmonary embolism ( $n = 2$ ); hemoptysis ( $n = 2$ ); and chest wall pain ( $n = 2$ ). The mean VC as measured at the pulmonary function laboratory was  $3830 \pm 1116$  ml (85% pred; range 63 - 147 % pred) and the mean forced expiratory volume in one second ( $FEV_1$ ) was  $2404 \pm 1166$  ml (82% pred; range 30 - 148 % pred). The study was approved by the local medical ethics committee.



### *Quantitative Assessment of CT scans*

Two CT studies for quantitative assessment of lung density were conducted on two separate days and were performed by two different operators. The topogram was obtained at full inspiration. Two anatomical levels were selected from the topogram: 5 cm above and 5 cm below the level of the carina. To control the level of inspiration during scanning, the patient was asked to breathe through a small hand held spirometer (Micro Medical Instruments, Rochester, UK), which was connected to the CT scanner (16). Patients were instructed and allowed 1 min to accustom to the spirometer. Subsequently the patient performed a breathing VC manoeuvre to determine the VC. At each anatomical level two scans were obtained at 90% and 10 % of the inspiratory VC, respectively. The air-flow through the spirometer was interrupted mechanically by a closing valve, at which time a trigger signal started the scanner. The level of inspiration was kept constant for the duration of the CT scan. The CT scans of the lungs were obtained in supine position with the same CT scanner (Somatom Plus; Siemens, Erlangen, Germany) with 1.0-mm collimation, 137 kVp, 220 mA, and 1 s scanning time. Scans were reconstructed in the soft-detail resolution mode. The full width at half maximum of the point spread function of this reconstruction filter was 1.86 mm and the sample volume 3.92 mm<sup>3</sup> (12). No intravenous contrast material was employed. All patients completed the CT study within 10 minutes.

### *Data Analysis*

CT data were digitally transferred for analysis to a Sun SPARCstation (SUN Microsystems, Mountain View, Calif). The parenchyma of both lungs was delineated automatically by a density-discriminating computer program, which contoured at a density discriminating level of -200 HU. Subsequently, the contour of the lung was eroded by 3 pixels. Software determined histogram shape-related parameters automatically: the mean, modal, and median lung density; the cut-off points of the frequency distribution of HU numbers defining the lowest 10th and the highest 10th percentile, and the histogram full width at half maximum. Densitometric parameters of the two studies were compared. Reproducibility was expressed in Hounsfield units as the standard deviation of the signed difference between results of day 1 and day 2 divided by  $\sqrt{2}$  (17). This standard deviation may serve as an estimate of the variability of many repeated measurements.

### *Statistical Analysis*

A one-sample *t* test was used to determine whether the differences between day 1 and day 2 were statistically significant. The Shapiro-Wilk test was used to test if the differ-

ence between the data on day 1 and day 2 could be considered as normally distributed. Relationships between reproducibility data and  $FEV_1$  % pred were evaluated by Spearman's rank correlation test. A probability value less than 0.05 was considered statistically significant.

## RESULTS

The data derived from quantitative analysis of the CT scans are summarized in Table 1 and on reproducibility of CT densitometry measurements expressed in HU in Table 2. Similar differences between the various parameters derived from distributions of HU numbers of consecutive CT examinations were observed in the upper and the lower zones of the lungs at 90% VC. These differences were worse by a factor of three at 10% VC. At 90% VC, the relative difference of the mean lung density expressed as a percentage between the first and the second examination was 3% in the upper as well as the lower zones of the lungs, and 6% and 5%, respectively, at 10% VC. The highest 10th percentile of the frequency distribution appeared the most prone to variation at both levels of inspiration.

According to the Shapiro-Wilk test, the difference data could be considered as normally distributed. No significant difference ( $p < 0.05$ ) existed between results from any parameter on day 1 and day 2, except for the full width at half maximum for the data from 5 cm below the carina at 10% VC.

No statistically significant relation was found between reproducibility of CT densitometry and  $FEV_1$  % pred.

## DISCUSSION

The reproducibility of spirometrically controlled CT densitometry of the lung was surprisingly good. The most reproducible CT lung density measurements were obtained at 90% VC. Reproducibility was worse by a factor of three at 10% vital capacity. In the upper and the lower zones of the lungs comparable differences in measurements between two successive scans were observed. The highest 10th percentile of the frequency distribution appeared to be more prone to variation. From 90% VC to 10% VC, the mean lung density increased 80 HU in the upper zones of the lungs and 86 HU in the lower zones. This is much less than reported by Webb et al (18) who found an increase in attenuation of 200 HU in healthy volunteers. Our numbers are more consistent with air-trapping and are a reflection of the study population, in which patients with COPD are well represented.

**Table 1.** Average Densitometric Results at 90% and 10% Vital Capacity (VC) expressed in Hounsfield Units.

	90 % VC		10 % VC	
<b>Upper zones</b>				
Mean lung density	-877	(23)	-797	(53)
Modal	-911	(23)	-845	(54)
Median	-900	(22)	-825	(54)
Lowest 10th percentile	-935	(23)	-845	(54)
Highest 10th percentile	-809	(30)	-691	(57)
Full width at half-max.	59	(15)	76	(13)
<b>Lower zones</b>				
Mean lung density	-865	(28)	-779	(70)
Modal	-914	(23)	-847	(60)
Median	-900	(24)	-820	(67)
Lowest 10th percentile	-940	(23)	-889	(57)
Highest 10th percentile	-776	(42)	-631	(97)
Full width at half-max.	64	(14)	106	(26)

Note. Data are presented as mean, and SD in parenthesis

**Table 2.** Reproducibility of Quantitative Computed Tomographic Studies of the Lung at 90% and 10% Vital Capacity (VC) expressed in Hounsfield Units.

	90 % VC	10 % VC
<b>Upper zones</b>		
Mean lung density	3	10
Modal	6	13
Median	4	13
Lowest 10th percentile	5	17
Highest 10th percentile	9	31
Full width at half-max.	6	9
<b>Lower zones</b>		
Mean lung density	3	11
Modal	6	20
Median	5	15
Lowest 10th percentile	7	18
Highest 10th percentile	14	38
Full width at half-max.	7	12

Lung density is determined by the relative proportions of gas, blood, extracellular fluid, and pulmonary tissue. Computerized methods using standard techniques calculate the density characteristics automatically from the frequency distribution of HU. The highest 10th percentile, the full width at half maximum, the modal lung density, and the median lung density have at present no proven clinical relevance in the quan-

tification of pulmonary emphysema or interstitial lung disease. However, lung density parameters were chosen because they reflect different aspects of the shape of the histogram of CT numbers. The highest 10th percentile of the frequency distribution was the densitometric parameter that showed the greatest variability between successive scans. This difference is probably caused by the contour tracing algorithm used for isolating the lung. This algorithm is inspiration dependent which possibly results in a different cut-off point of central vessels.

The degree of lung inflation as measured by direct spirometry has been shown to vary markedly with identical breath holding instruction on a series of consecutive CT scans (19). In cooperative patients, breath holding at full inspiration is considered the most reproducible lung volume resulting in the lowest variation in lung density between consecutive scans (19). Submaximal efforts have major effects on lung density measurements as density values vary inversely with lung volume. Monitoring of the patient's effort will minimize patient-related errors and can be accomplished by spirometric gating of the CT scanner (16). The flow-volume curve appears on the display monitor of the CT scanner. Feedback control of the spirometric curve makes it easier to coach patients for a truly maximal effort, especially in those who suffer from severe airflow limitation, and is of indispensable help to assess patient discomfort. Submaximal effort is easily detected and the scan can be canceled. Partly for that reason reproducibility was not influenced by very severe respiratory insufficiency. Moreover, the range of mean attenuation values from inspiration to expiration is narrower in patients with COPD than in patients with normal  $FEV_1$  % pred values (20).

The aim of the study was to address the question of respiration control on the reproducibility of standardized CT density measurements. Since maximal efforts with spirometrically controlled CT in supine position may be particularly fatiguing for dyspnoeic patients, we decided to scan at 90% and 10% of the VC. If reproducibility of histogram related-parameters is satisfactory at both levels of inspiration, a free choice on grounds of clinical interest can be made. Incidentally, the densitometric procedure had to be aborted because a patient was unable to reach the 90% VC or the 10% VC trigger level at the end of the procedure. After a timely interruption of the spirometric procedure, density measurements could always be completed successfully after 1 minute of rest. We finished the complete spirometric procedure including the VC manoeuvre within about 10 minutes.

Noninvasive measurements of lung density by quantitative CT have a great potential for diagnostic purposes and follow-up after therapy. Reproducibility aspects have to be taken into account before application of this technique in practice. At 50% VC the standard deviation of the estimated mean attenuation values was after a 5 min pause 10 HU (13). This level of inspiration is suitable to differentiate between patients suffering from idiopathic lung fibrosis and patients with COPD. However, this level is of limited value in the differentiation between chronic bronchitis, pulmonary emphy-

sema, and healthy parenchyma. CT scans obtained at full expiration have shown to correlate well with physiologic phenomena consistent with airflow limitation (4,5). Small airways disease may remain completely undetected on routine suspended full inspiration scans and become conspicuous only at suspended full expiration. Paired inspiratory-expiratory CT scans are useful for distinguishing small airways disease from healthy lungs and pulmonary emphysema (20).

There are a few potential sources of variation in the level of inspiration which could influence the reproducibility of CT density measurements. Differences between the two operators in patient coaching may have an important impact on the VC manoeuvre, the result of which is subsequently used for gating the CT scanner. Patients are more familiar with the spirometer on the second day. Although VC shows variation over the day within individuals (21), examinations were arbitrarily scheduled without taking the point of the day into account, to reflect the clinical situation as closely as possible. In patients with COPD, bronchodilator therapy was continued between CT scans. No differences in the clinical state of the patients were reported. Differences between the data on day 1 and day 2 were normally distributed and no statistically significant difference was noted between the data from day 1 and 2, which makes a systematic source of variation in VC measurements unlikely.

In conclusion, results of spirometrically controlled CT densitometry are highly repeatable estimates of lung density. Reproducibility of lung density measurements was not influenced by severe respiratory insufficiency. In expiration, reproducibility was worse by a factor of three. If computer tomographic scans obtained at residual volume are used for diagnosis and follow-up, respiratory control is mandatory.

## REFERENCES

1. Morgan MDL. Detection and quantification of pulmonary emphysema by computed tomography: a window of opportunity. *Thorax* 1992; 47:1001-1004.
2. Gevenois PA, Yernault JC. Can computed tomography quantify pulmonary emphysema? *Eur Respir J* 1995; 5:843-848.
3. Gevenois PA, de Maertelaer V, De Vuyst P, Zanen J, Yernault JC. Comparison of computed density and macroscopic morphometry in pulmonary emphysema. *Am Rev Respir Dis* 1995; 152:653-657.
4. Gevenois PA, De Vuyst P, Sy M, et al. Pulmonary emphysema: quantitative CT during expiration. *Radiology* 1996; 199:825-829.
5. Gould GA, Redpath AT, Ryan M, et al. Lung CT density correlates with measurements of airflow limitation and the diffusing capacity. *Eur Respir J* 1991; 4:141-146.
6. Bae KT, Slone RM, Gierada DS, Yusem RD, Cooper JD. Patients with emphysema: quantitative CT analysis before and after lung volume reduction surgery. *Radiology* 1997; 203:705-714.
7. Holbert JM, Brown ML, Scierba FC, et al. Changes in lung volume and volume of emphysema after unilateral lung reduction surgery: analysis with CT densitometry. *Radiology* 1996; 201:793-797.
8. Kemerink GJ, Lamers RJS, Thelissen GRP, van Engelshoven JMA. Scanner conformity in CT densitometry of the lungs. *Radiology* 1995; 197:749-752.

9. Kemerink GJ, Lamers RJS, Thelissen GRP, van Engelshoven JMA. CT densitometry of the lungs: scanner performance. *J Comput Assist Tomogr* 1996; 20:24-33.
10. Kemerink GJ, Kruize HH, Lamers RJS. Density resolution in quantitative computed tomography of foam and lung. *Med Phys* 1996; 23:1697-1708.
11. Kemerink GJ, Kruize HH, Lamers RJS, van Engelshoven JMA. CT lung densitometry: dependence of CT number histograms on sample volume and consequences for scan protocol comparability. *J Comput Assist Tomogr* 1997; 21:948-954.
12. Kemerink GJ, Kruize HH, Lamers RJS. The CT's sample volume as an approximate, instrumental measure for density resolution in densitometry of the lungs. *Med Phys* 1997; 24:1615-1620.
13. Kohz P, Stäbler A, Beinert T, et al. Reproducibility of quantitative, spirometrically controlled CT. *Radiology* 1995; 197:539-542.
14. Müller NL, Staples CA, Miller RR, Abboud RT. "Density Mask": an objective method to quantitate emphysema using computed tomography. *Chest* 1988; 94:782-787.
15. Gould GA, MacNee W, McLean A, et al. CT measurements of lung density in life can quantitate distal airspace enlargement: an essential defining feature of human emphysema. *Am Rev Respir Dis* 1988; 137:380-392.
16. Kalender WA, Rienmüller R, Seissler W, Behr J, Welke M, Fichte H. Measurement of pulmonary parenchymal attenuation: use of spirometric gating with quantitative CT. *Radiology* 1990; 175:265-268.
17. van Hastenberg RPJM, Kemerink GJ, Hasman A. On the generation of short-axis and radial long-axis slices in thallium-201 myocardial perfusion single-photon emission tomography. *Eur J Nucl Med* 1996; 23: 924-931.
18. Webb RW, Stern EJ, Kanth N, Gamsu G. Dynamic pulmonary CT: findings in healthy adult man. *Radiology* 1993; 186:117-124.
19. Robinson P, Kreel L. Pulmonary tissue attenuation with computed tomography: comparison of inspiratory and expiratory scans. *J Comput Assist Tomogr* 1979; 3:740-748.
20. Lamers RJS, Thelissen GRP, Kessels AG, Wouters EFM, van Engelshoven JMA. Chronic obstructive pulmonary disease: evaluation with spirometrically controlled CT lung densitometry. *Radiology* 1994; 193:109-113.
21. American Thoracic Society. Lung function testing: selection of reference values and interpretative strategies. *Am Rev Respir Dis* 1991; 144:1202-1218.



## CHAPTER 7

---

# Chronic obstructive pulmonary disease: Evaluation with spirometrically controlled CT lung densitometry

Rob J.S. Lamers

Guillaume R.P. Thelissen

Alfons G.H. Kessels

Emiel F.M. Wouters

Jos M.A. van Engelshoven



## ABSTRACT

**Purpose:** To compare the computed tomographic (CT) lung densitometry results in patients with chronic obstructive pulmonary disease (COPD) and in control subjects (healthy persons).

**Materials and methods:** Spirometrically gated CT sections at 5 cm above and 5 cm below the carina at 90% and 10% vital capacity (VC) were imaged in patients and controls. Various densitometric parameters were derived from the CT data, and results were compared between the two levels of inspiration.

**Results:** Densitometric results in patients with emphysema were substantially different from those in patients with chronic bronchitis and in controls at 90% and 10% VC. Differences in patients with chronic bronchitis and in controls were not significant at 90% VC but were significant at 10% VC ( $p < 0.001$ ). The mean changes in densitometric parameters between 90% and 10% VC were substantially greater in controls than in patients with COPD.

**Conclusion:** It may be possible to classify lung disease with only two CT sections obtained at the same anatomic level, one at 90% and one at 10% VC, irrespective of the densitometric parameter used.

## INTRODUCTION

Computed tomography (CT) is a sensitive technique for evaluation of the presence and severity of emphysema. Visual assessment of emphysema by means of thin-section CT correlates well with the pathologic grade of this disease, and thin-section CT may be an accurate noninvasive examination for use in the diagnosis of emphysema in vivo, although the mildest forms of emphysema may be missed (1). Because visual assessment of thin-section CT scans of the lungs is subject to interobserver and intraobserver variability, methods have been developed to calculate automatically the relevant density characteristics from the CT sections for the diagnosis of emphysema (2-4). Because the status of inspiration affects the lung density characteristics, control of the level of respiration during scanning (spirometrically controlled CT) is mandatory to improve the reproducibility and accuracy of density measurements (5).

The aims of this study were (a) to compare the results of spirometrically controlled CT lung densitometry in patients with emphysema or chronic bronchitis and healthy persons at different levels of inspiration, (b) to compare results of spirometrically controlled CT densitometry of the upper and the lower zones of the lungs, (c) to compare the results of spirometrically controlled CT lung densitometry and of visual assessment of thin-section CT scans of the lungs with those of pulmonary function tests, and

(d) to correlate the results of spirometrically controlled CT lung densitometry with those of visual assessment of thin-section CT scans of the lungs.

## MATERIALS AND METHODS

Three groups of individuals participated in the study. Patients with chronic obstructive pulmonary disease were prospectively selected by one pulmonologist (E.F.M.W.). Twenty consecutive patients fulfilled the pulmonary functional criteria for emphysema (6): diffusing constant for carbon monoxide ( $K_{CO}$ ) less than 60% of that predicted and forced expiratory volume within 1 second ( $FEV_1$ ) less than 70% of that predicted (group 1). Twenty consecutive patients fulfilled the clinical criteria for chronic bronchitis as formulated by the American Thoracic Society (7): history of productive cough on most days for at least 3 months of the year for at least 2 successive years and, accordingly, a normal  $K_{CO}$  ( $> 80\%$  of that predicted) and an obstructive lung function impairment ( $FEV_1 < 70\%$  of that predicted) that does not change markedly over several months of observation (group 2). Results in both groups were compared with those of a group of healthy persons who had no pulmonary symptoms or history of pulmonary disease and who had normal results of lung function tests ( $K_{CO} > 80\%$  of that predicted;  $FEV_1 > 80\%$  of that predicted). Detailed smoking history and informed consent were obtained from each participant. The study was approved by the local medical ethics committee.

### *Pulmonary Function Studies*

Pulmonary function tests were performed within 3 months before CT densitometry. Spirometric measurements were obtained by means of a wet spirometer (Gould Pulmonet III, Sensor Medics, Bithoven, The Netherlands);  $FEV_1$  was expressed as a percentage of the reference values (8). Lung volumes were measured with whole-body plethysmography and were expressed as a percentage of the reference values (8). The diffusing capacity was measured by the single-breath method (Masterlab; Jaeger, Würzburg, Germany).  $K_{CO}$  was calculated as diffusing capacity divided by the alveolar volume.

### *Quantitative Assessment*

CT scans of the lungs for quantitative assessment of lung density patterns were obtained with the patients supine and with use of a commercially available scanner (Somatom Plus; Siemens, Erlangen, Germany). Scanning parameters were 1.0-mm collimation, 137 kVp, 220 mA, and 1.0-second scanning time. Scans were recon-

structed in the standard-resolution mode. No contrast medium was injected. To control the level of inspiration during scanning, the patient was asked to breathe through a small handheld spirometer (Micro Medical Instruments, Rochester, England), which was connected to the CT scanner. The spirometric curve could be followed on the display monitor of the CT scanner, and measurement of the vital capacity was made and displayed on the monitor before the CT scans were obtained. At user-selected levels of inspiration, the air flow through the spirometer could be inhibited by a closing valve, which triggered scanning to start. The level of inspiration was constant for the duration of CT scanning. This technique was described comprehensively by Kalender et al (5). Two anatomical levels were chosen by means of a scout view: 5 cm above and 5 cm below the level of the carina. At each level, two scans, at 10% and 90% inspiratory vital capacity, respectively, were obtained. The CT data were transferred to a graphical workstation (SUN SPARCstation 1+; SUN Microsystems, Mountain View, Calif) and were analyzed. First, the boundaries of each lung were determined by a density-discriminating computer program, and both lungs were automatically focussed on. A frequency histogram of Hounsfield units (HU) was subsequently generated (Figure). The area under the curve was normalized. From the data of each scan, three spirometrically controlled CT densitometric parameters were derived: mean lung density, percentage of pixels in the -910 to -1024 HU range (pixel index), and cut-off point in the histogram (Hounsfield unit number) that defines the lowest 10th percentile of the histogram (Figure).

### *Visual Assessment*

In each person, five thin-section CT scans (1.0-mm collimation, 137 kVp, 220 mA, 1.0-second scanning time, high-frequency reconstruction algorithm) were obtained during breath hold at end-inspiration: two scans of the upper zones at 3 cm and 6 cm above the carina, two scans of the lower zones at 3 cm and 6 cm below the carina, and one scan at the level of the carina. Each scan was scored independently by two observers (R.J.S.L., J.M.A.v.E.) who were not aware of clinical findings for the overall severity of emphysema according to the direct observational method of Sakai et al (9). Images were made at a level (-800 HU) and window width (1600 HU) appropriate for lung detail. Each section was scored for the severity of emphysema according to a four-point scale, as follows: 0, no emphysema; 1, low-attenuation areas smaller than 5 mm in diameter; 2, circumscribed low-attenuation areas larger than 5 mm in diameter in addition to those smaller than 5 mm in diameter; and 3, diffuse low-attenuation areas without intervening normal lung or large, confluent low-attenuation areas. The extent of emphysema was scored for each section also according to a four-point scale: 1, less than 25% cross-sectional area involvement; 2, 25%-50% cross-sectional involvement; 3, 50%-75% cross-sectional area involvement; and 4, more than 75% cross-sectional

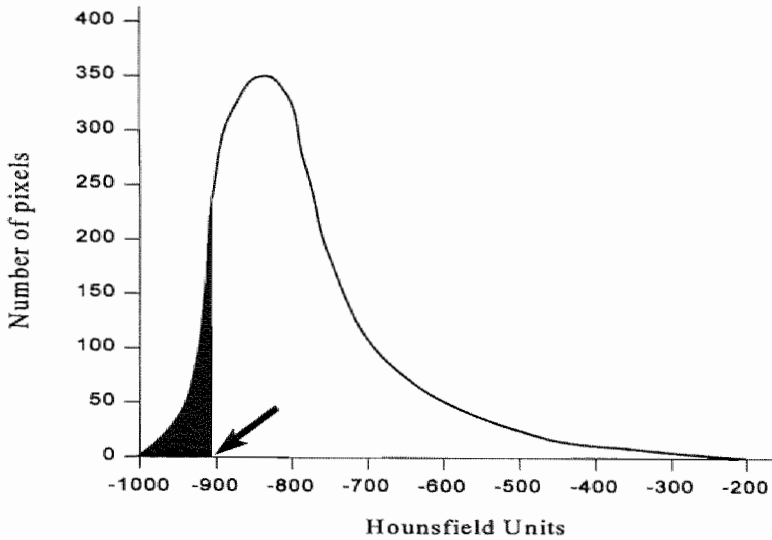


**Figure.** Frequency distribution of CT numbers in the lung. Arrow marks the Hounsfield number that defines the lowest 10th percentile; shaded area indicates the percentage of pixels that form the lowest 10th of the frequency distribution.

area involvement. For each of the 10 lung sections, the score for severity of emphysema was multiplied by the score for the extent, and the resultant scores were subsequently summed, which resulted in a definite emphysema score. Visual emphysema scores could range from zero to 120. The mean visual emphysema score of both observers was calculated for the purpose of this study.

### *Statistical Analysis*

A student *t* test was used to determine whether differences in spirometrically controlled CT lung density parameters between the three groups at the two levels of inspiration in the upper and lower zones and between the upper and the lower zones were statistically significant. A two-tailed probability value of less than 0.05 was considered statistically significant. Correlation coefficients were calculated between the various spirometrically controlled CT lung density parameters, the mean visual emphysema score, and the results of pulmonary function tests. To determine two-tailed *p* values for the differences of correlation coefficients in the upper zones, a bootstrap technique was used as proposed by Efron (10), because these correlation coefficients are statistically dependent.

## RESULTS

The characteristics of the three groups are summarized in Table 1. Healthy persons were significantly younger ( $p < 0.001$ ) and their cigarette consumption was significantly lower ( $p < 0.001$ ) compared with patients with emphysema or chronic bronchitis. Weight of patients with emphysema was significantly lower ( $p < 0.001$ ) than was weight of patients with chronic bronchitis and of healthy persons. Height did not differ in the three groups. No statistically significant difference in airway obstruction was found between the patients with emphysema and those with chronic bronchitis ( $FEV_1$ , 46% and 51% of that predicted, respectively). Total lung capacity in patients who had emphysema was statistically significantly higher than that of patients who had chronic bronchitis and that of healthy persons ( $p < 0.001$ ).

**Table 1.** Subject Characteristics.

Parameter	Patients with Emphysema (n=20)			Patients with Chronic Bronchitis (n=20)		Healthy Persons (n=20)	
	Mean ± SD		p*	Mean ± SD	p†	Mean ± SD	p‡
Age (y)	60 ± 8			70 ± 7		53 ± 12	
Height (cm)	171 ± 8			171 ± 8		175 ± 10	
Weight (kg)	61 ± 11	<.001		76 ± 11		78 ± 10	
Cig. cons. (pack-years)	49 ± 26			40 ± 31		17 ± 12	<.001
Male gender	14			19		20	
FEV <sub>1</sub> (% predicted)	46 ± 12			51 ± 14		110 ± 18	<.001
IVC (% predicted)	100 ± 26			87 ± 18	<.001	111 ± 14	
TLC (% predicted)	111 ± 8	<.001		99 ± 9		100 ± 11	
DL <sub>CO</sub> (% predicted)	61 ± 14	<.001		100 ± 19		111 ± 19	
K <sub>CO</sub> (% predicted)	47 ± 8	<.001		95 ± 12		90 ± 9	

Note. SD = standard deviation; \* Patients with emphysema versus those with chronic bronchitis; † Patients with chronic bronchitis versus healthy persons; ‡ Patients with emphysema versus healthy persons.

The mean visual emphysema score in patients with emphysema was significantly higher ( $50 \pm 26$ ) than that of patients with chronic bronchitis ( $5 \pm 13$ ,  $p < 0.001$ ) and that of healthy persons ( $1 \pm 2$ ,  $p < 0.001$ ), but there was no significant difference in the mean visual emphysema scores of patients with chronic bronchitis and healthy persons. All patients with emphysema had emphysematous changes that were visually assessed at thin-section CT (range, 16-116), whereas only two patients with chronic bronchitis had a mean visual emphysema score greater than 15 (19 and 57, respectively).

**Table 2.** Densitometric Results at 10% and 90% Vital Capacity with the Patient Supine.

Vital Capacity (%)	Patients with Emphysema (n=20)		Patients with Chronic Bronchitis (n=20)		Healthy Persons (n=20)	
	Mean $\pm$ SD	p*	Mean $\pm$ SD	p†	Mean $\pm$ SD	p‡
<b>Upper zones</b>						
Mean lung density						
- 10	-862 $\pm$ 27	<.001	-827 $\pm$ 38	<.001	-786 $\pm$ 39	<.001
- 90	-886 $\pm$ 23	<.001	-852 $\pm$ 32		-858 $\pm$ 29	<.001
Pixel index						
- 10	42 $\pm$ 14	<.001	27 $\pm$ 16	<.001	9 $\pm$ 11	<.001
- 90	56 $\pm$ 12	<.001	38 $\pm$ 17		41 $\pm$ 20	<.001
Lowest 10th perc.(HU)						
- 10	-967 $\pm$ 20	<.001	-941 $\pm$ 26		-893 $\pm$ 38	<.001
- 90	-977 $\pm$ 17	<.001	-951 $\pm$ 25		-948 $\pm$ 23	<.001
<b>Lower zones</b>						
Mean lung density						
- 10	-849 $\pm$ 31	<.001	-809 $\pm$ 55	<.001	-767 $\pm$ 56	<.001
- 90	-873 $\pm$ 24	<.001	-843 $\pm$ 22		-847 $\pm$ 34	<.001
Pixel index						
- 10	41 $\pm$ 16	<.001	28 $\pm$ 14	<.001	13 $\pm$ 13	<.001
- 90	54 $\pm$ 12	<.001	39 $\pm$ 12		42 $\pm$ 20	<.001
Lowest 10th perc.(HU)						
- 10	-961 $\pm$ 16	<.001	-941 $\pm$ 21	<.001	-906 $\pm$ 37	<.001
- 90	-972 $\pm$ 14	<.001	-953 $\pm$ 14		-950 $\pm$ 23	<.001

Note. SD = standard deviation; \* Patients with emphysema versus those with chronic bronchitis; † Patients with chronic bronchitis versus healthy persons; ‡ Patients with emphysema versus healthy persons.

The densitometric results in the three study groups are summarized in Table 2. At both levels of inspiration the mean lung density, pixel index, and lowest 10th percentile of the frequency distribution in patients with emphysema were statistically significantly different from those of patients with chronic bronchitis and from those of healthy persons ( $p < 0.001$ ). There was also a statistically significant difference between these parameters in patients with chronic bronchitis and in healthy persons at 10% vital capacity ( $p < 0.001$ ) but not at 90% vital capacity. The corresponding densitometric results for the upper and lower zones of the lungs in the three groups did not differ significantly.

The mean changes in densitometric parameters between 10% and 90% vital capacity for each study group are summarized in Table 3. The mean changes in these densitometric parameters in the upper and the lower zones of the lungs were significantly greater in healthy persons than in patients who had emphysema or chronic bronchitis ( $p < 0.001$ ), whereas the mean changes in patients who had emphysema and in those

**Table 3.** Changes in Densitometric Parameters between 10% and 90% Vital Capacity.

	Patients with Emphysema (n=20)	Patients with Chronic Bronchitis (n=20)	Healthy Persons (n=20)	
	Mean ± SD	Mean ± SD	Mean ± SD	p*
<b>Upper zones</b>				
Mean lung density	23 ± 14	25 ± 28	73 ± 40	<.001
Pixel index	-14 ± 7	-10 ± 9	-32 ± 21	<.001
Lowest 10th percentile	10 ± 6	10 ± 11	52 ± 32	<.001
<b>Lower zones</b>				
Mean lung density	23 ± 15	24 ± 19	85 ± 50	<.001
Pixel index	-13 ± 8	-11 ± 10	-30 ± 20	<.001
Lowest 10th percentile	11 ± 8	12 ± 15	46 ± 29	<.001

Note. All values are expressed in Hounsfield units. SD = standard deviation; \* Statistically significant difference in comparison with patients with emphysema and patients with chronic bronchitis.

who had chronic bronchitis did not differ significantly ( $p > 0.05$ ). In no group were changes in densitometric parameters in the upper zones of the lungs significantly different from the corresponding densitometric parameters in the lower zones of the lungs.

Table 4 summarizes the results of the comparison between pulmonary function tests, densitometric parameters, and mean visual emphysema score. The best correlations were found for FEV<sub>1</sub> and K<sub>CO</sub> and the three densitometric parameters at 10% vital capacity in the upper zones of the lungs. The correlations between FEV<sub>1</sub> and the densitometric parameters were poor if the CT scan was made at 90% vital capacity, whereas the correlations between K<sub>CO</sub> and the densitometric parameters were similar at 10% and at 90% vital capacity. K<sub>CO</sub> had the highest correlation with the mean visual emphysema score.

The correlations between the mean visual emphysema score and the various densitometric parameters in upper and lower zones of the lungs are shown in Table 5. The best correlation was between the percentage of pixels with attenuation of less than -910 HU and the mean visual emphysema score in the upper zones of the lungs at 10% vital capacity ( $r = 0.69$ ,  $p < 0.001$ ). Comparison of the correlation coefficients of the three densitometric parameters and the mean visual emphysema score revealed no statistically significant differences. In a comparison of correlation coefficients at 10% vital capacity and the corresponding correlation coefficients at 90% vital capacity, only the correlation coefficient between the pixel index and the mean visual emphysema score differed statistically significantly ( $p < 0.05$ ); A correlation coefficient was greatest at 10% vital capacity.

**Table 4.** Correlation of Densitometric Parameters and Mean Visual Emphysema Score with Pulmonary Function Tests in Whole Population.

Pulmonary Function Test (% predicted)	Mean Lung Density	p	Pixel Index	p	Lowest 10th Percentile (HU)	p	Mean Visual Emphysema score	p
<b>Upper zones</b>								
10% vital capacity								
- FEV <sub>1</sub>	.56	<.001	-.66	<.001	.62	<.001	-.51	<.001
- Total lung capacity	.18		-.15		.13		-.28	
- K <sub>co</sub>	.52	<.001	-.50	<.001	.47	<.001	-.69	<.001
90% vital capacity								
- FEV <sub>1</sub>	.15		-.15		.29	<.05	-.51	<.001
- Total lung capacity	.22	<.01	.19		.11		-.28	
- K <sub>co</sub>	.41	<.001	-.40	<.001	.43	<.01	-.69	<.001
<b>Lower zones</b>								
10% vital capacity								
- FEV <sub>1</sub>	.49	<.001	-.59	<.001	.61	<.001	-.51	<.001
- Total lung capacity	.08		-.12		.02		-.28	
- K <sub>co</sub>	.41	<.001	-.47	<.001	.43	<.001	-.69	<.001
90% vital capacity								
- FEV <sub>1</sub>	.1		-.17		.36	<.001	-.51	<.001
- Total lung capacity	.22		.12		.11		.28	
- K <sub>co</sub>	.39	<.001	-.34	<.01	.44	<.001	-.69	<.001

**Table 5.** Correlation between Mean Visual Emphysema Score and Densitometric Parameters.

	Mean Lung Density (r)	Pixel Index (r)	Lowest 10th Percentile (r)
<b>Upper zones</b>			
10% vital capacity	-.60	.69 } p < .05	-.60
90% vital capacity	-.57	.54 }	-.62
<b>Lower zones</b>			
10% vital capacity	-.40	.47 } p < .05	-.47
90% vital capacity	-.37	.32 }	-.50

Note. All correlation coefficients are statistically significant: p < .001.



## DISCUSSION

The present study confirms the value of spirometrically controlled CT densitometry in the quantitative assessment of lung density at selected levels of inspiration (5). In patients who had emphysema, regardless of the level of inspiration, all three densitometric parameters differed substantially from the corresponding values in patients who had chronic bronchitis and in healthy persons, whereas those in patients who had chronic bronchitis and in healthy persons were statistically significantly different only at 10% vital capacity. The densitometric results in the upper and lower zones of the lungs were more or less identical.

CT densitometry gives objective and observer-independent information about diseases such as pulmonary emphysema and pulmonary fibrosis that affect lung density. Until now, three densitometric parameters have commonly been used: mean lung density (2); pixel index, which indicates overall percentage of lung involved with emphysema (2,4,11); and the CT EMI number that defined the lowest 5th percentile of the frequency distribution (3). These parameters are related to the physical density (in grams per cubic centimeter) of the scanned volume and are dependent not only on the structure of the lung tissue but also on the level of inflation and perfusion (12). Control of the level of inspiration during scanning, therefore, is important, especially when absolute lung density values will be used for diagnosis and follow-up. A spirometer connected to the CT scanner provides spirometrically triggered CT images. Reproducibility on the order of 5% can be achieved (5). This technique was used during our study and proved to be an easy applicable method that could be performed in all patients within 10 minutes. The computer program for CT data analysis, which includes contour tracking of both lungs, background deletion, and histogram analysis, permitted an instant quantitative evaluation of the CT information.

In patients with emphysema, all the densitometric parameters that we used at 10% and 90% vital capacity differed statistically significantly from the corresponding values in healthy persons and in patients with chronic bronchitis, presumably due to alveolar destruction. In patients with chronic bronchitis and in healthy persons, these parameters differed at 10% vital capacity but not at 90% vital capacity, which may indicate that there was air trapping in patients with chronic bronchitis. This, combined with the differences in the changes in the densitometric parameters between 90% and 10% vital capacity in healthy persons and patients with chronic obstructive pulmonary disease, suggests that it may be possible to differentiate emphysema, chronic bronchitis, and healthy persons with the acquisition of two CT sections only: one section obtained at 90% vital capacity to distinguish emphysema from chronic bronchitis and healthy persons and a second, complementary section obtained at 10% vital capacity to distinguish chronic bronchitis from healthy persons.

A reduction in  $K_{CO}$ , especially when coupled with hyperinflation and airway obstruction, is the best functional indication of emphysema. Diminished  $K_{CO}$ , however, is nonspecific and can be found in a wide variety of pulmonary disorders that affect the alveolocapillary membrane including interstitial lung disease and pulmonary vascular disorders (13). Furthermore, the level of  $K_{CO}$  may vary widely even in patients with little or no emphysema (14). As much as 30% of the lung may be involved with emphysema without any evidence of functional impairment (15). Airway obstruction is not invariably present in patients with mild emphysema (16). To examine the capabilities of quantitative CT in more pronounced emphysema, a more extreme cutoff for the diagnosis of emphysema was chosen in the present study than is generally recommended (6). The marked emphysematous changes in the selected patients who had emphysema were confirmed by quantitative CT and visual assessment of the thin-section CT scans.

Macroscopic emphysema is rarely evenly distributed throughout the lungs and predominates mostly in the upper zones of the lungs (11). We did not find, however, expected differences between densitometric parameters in the upper and the lower zones of the lungs in our patients who had emphysema. This may have been caused by our relatively extreme inclusion criteria and by the selection of only patients with severe emphysema. The high mean visual emphysema score ( $50 \pm 26$ ) in this patient group, which is an assessment of the extent of emphysema in both lungs together, confirms this assumption. Our densitometric parameters were calculated from one section only, which may cause sampling error. The correlations between the mean visual emphysema score and the densitometric parameters in the upper zones of the lungs, however, were not statistically significantly different from the corresponding correlations in the lower zones of the lungs.

In the present study, three densitometric parameters - mean lung density, pixel index, and lowest 10th percentile of the frequency distribution - were compared with the mean visual emphysema score, which revealed no important differences. Gould et al (3) compared the extent of emphysema as scored pathologically in a lung section and the lowest 5th percentile of the frequency distribution of EMI numbers in a corresponding CT section of 28 lung or lobe specimens after resection for a solitary tumor and found a statistically significant correlation between morphometric changes and the densitometric parameter. Our correlation between the lowest 10th percentile and the mean visual emphysema score was somewhat lower, but we calculated the mean visual emphysema score of both lungs together instead of the pathological score of one corresponding lung section. Müller et al (2) reported excellent correlation between the pathologic emphysema score and the percentage of lung with emphysema but a weak correlation with the mean lung density, which was, in their opinion, of limited value because it did not detect regional localized areas of emphysema. They, however, obtained relatively thick (1 cm) CT sections at maximal inspiration after the infusion of a

contrast medium without controlling the level of inspiration during scanning. Gurney et al (11) found a good correlation in 59 smokers between the pixel index of the whole lungs obtained at inspiration with the mean visual emphysema score. Their correlation is higher than ours, presumably because we correlated the pixel index of only one CT section, which may have caused sampling errors.

The correlation of morphologic information such as CT data with the results of pulmonary function tests is done by many authors, and some of them claim high correlation (4,17). We found a fair and statistically significant correlation between  $K_{CO}$  and the mean visual emphysema score and moderate correlation between  $FEV_1$  and the mean visual emphysema score. The correlation between  $K_{CO}$  and the densitometric parameters at 90% and 10% vital capacity were lower than the correlation between  $K_{CO}$  and the mean visual emphysema score, which may reflect the sampling error. The correlation between  $FEV_1$  and the densitometric parameters were more or less similar to the correlation between  $FEV_1$  and the mean visual emphysema score when the CT section was obtained at 10% vital capacity and was significantly lower than the correlation between  $FEV_1$  and the mean visual emphysema score when the CT sections were taken at 90% vital capacity.

In conclusion, spirometrically controlled CT lung densitometry is a well-tolerated examination that provides objective information about the density of the lung. There was a statistically significant correlation between objective and subjective parameters. Densitometric parameters were statistically significantly different in patients with emphysema compared with patients with chronic bronchitis and healthy persons, irrespective of the level of inspiration, but differed only at 10% vital capacity in patients with chronic bronchitis compared with healthy persons. The mean change in densitometric parameters between 90% vital capacity and 10% vital capacity was large in healthy persons and was much less in patients with emphysema or chronic bronchitis. On the basis of these results, we presume that two sections obtained at the same level - one at 90% vital capacity and one at 10% vital capacity - are suitable for the classification of persons into one of the three groups. Because of our relatively extreme selection criteria, however, we selected mainly patients with severe emphysema; our results, therefore, may be applicable only in this patient group. Further prospective studies are needed to evaluate the sensitivity and specificity of CT lung densitometry in the differential diagnosis of emphysema or chronic bronchitis.

## REFERENCES

1. Miller RR, Müller NL, Vedral S, Morrison NJ, Staples CA. Limitations of computed tomography in the assessment of emphysema. *Am Rev Respir Dis* 1989; 139:980-983.
2. Müller NL, Staples CA, Miller RR, Abboud RT. "Density Mask": an objective method to quantitate emphysema using computed tomography. *Chest* 1988; 94:782-787.

3. Gould GA, MacNee W, McLean A, et al. CT measurements of lung density in life can quantitate distal airspace enlargement: an essential defining feature of human emphysema: *Am Rev Respir Dis* 1988; 137:380-392.
4. Kinsella M, Müller NL, Abboud RT, Morrison NJ, DyBuncio A. Quantitation of emphysema by computed tomography using a "density mask" program and correlation with pulmonary function tests. *Chest* 1990; 97:315-321.
5. Kalender WA, Rienmüller R, Seissler W, Behr J, Welke M, Fichte H. Measurement of pulmonary parenchymal attenuation: use of spirometric gating with quantitative CT. *Radiology* 1990; 175:265-268.
6. Openbrier DR, Irwin MM, Rogers RM, et al. Nutritional status and lung function in patients with emphysema and chronic bronchitis. *Chest* 1983; 83:17-22.
7. American Thoracic Society. Chronic bronchitis, asthma and pulmonary emphysema: a statement by the Committee on Diagnostic Standards for Nontuberculous Respiratory Diseases. *Am Rev Respir Dis* 1962; 85:762-767.
8. Quanjer PH. Standardized lung function testing. *Bull Eur Physiopathol Respir* 1983; 19:7-44.
9. Sakai F, Gamsu G, Im JG, Ray CS. Pulmonary function abnormalities in patients with CT-determined emphysema. *J Comput Assist Tomogr* 1987; 11:963-968.
10. Efron B. The Jackknife, the bootstrap and other resampling plans: regional conference series in applied mathematics. 1982; 38:27-36.
11. Gurney JW, Jones KK, Robbins RA, et al. Regional distribution of emphysema: correlation of high-resolution CT with pulmonary function tests in unselected smokers. *Radiology* 1992; 183:457-463.
12. Rosenblum LJ, Mauceri RA, Wellenstein DE, et al. Density patterns in the normal lung as determined by computed tomography. *Radiology* 1980; 137:409-416.
13. Klein JS, Gamsu G, Webb WR, Golden JA, Müller NL. High-resolution CT diagnosis of emphysema in symptomatic patients with normal chest radiographs and isolated low diffusing capacity. *Radiology* 1992; 182:817-821.
14. Thurlbeck WM, Henderson JA, Fraser RG, Bates DV. Chronic obstructive lung disease: a comparison between clinical, roentgenologic, functional criteria in chronic bronchitis, asthma and bronchiectasis. *Medicine* 1970; 49:81-145.
15. Pratt PC. Role of conventional chest radiography in diagnosis and exclusion of emphysema. *Am J Med* 1987; 82:998-1006.
16. Gelb AF, Gold WM, Wright RR, Bruch HR, Nadel JA. Physiologic diagnosis of subclinical emphysema. *Am Rev Respir Dis* 1973; 107:50-63.
17. Biernacki W, Gould GA, Whyte KF, Flenley DC. Pulmonary hemodynamics, gas exchange, and the severity of emphysema as assessed by quantitative CT scan in chronic bronchitis and emphysema. *Am Rev Respir Dis* 1989; 139:1509-1515.



## CHAPTER 8

---

# Emphysema and airflow limitation in patients with advanced chronic obstructive pulmonary disease: a CT study

Rob J.S. Lamers  
Emiel F.M. Wouters  
Gerrit J. Kemerink  
Jos M.A. van Engelshoven

## ABSTRACT

**Purpose:** To assess prospectively the association of emphysema with airflow limitation in patients with chronic obstructive pulmonary disease (COPD), and to study whether the diffusing capacity for carbon monoxide ( $DL_{CO}$ ) can be used as an indicator for emphysema.

**Materials and methods:** One hundred patients with COPD participated in this study. The population was primarily subdivided into three groups based on forced expiratory volume in one second ( $FEV_1$ ) % predicted results: stage I COPD is  $FEV_1 \geq 50\%$  predicted ( $n = 27$ ); stage II COPD is  $FEV_1$  35 to 49% predicted ( $n = 32$ ); and stage III COPD is  $FEV_1 < 35\%$  predicted ( $n = 41$ ). Secondly the population was subdivided based on  $FEV_1$  L results: advanced COPD is  $FEV_1 < 1L$  ( $n = 50$ ), and  $FEV_1 \geq 1L$  ( $n = 50$ ). Five high-resolution CT (HRCT) scans of the lungs were obtained for visual assessment of emphysema, and subsequently 2 spirometrically controlled CT scans at 90% and 10% of the inspiratory vital capacity for objective assessment of lung density. HRCT scores and CT lung densitometry results were correlated with  $DL_{CO}$  results.

**Results:** A low prevalence (15%) of CT-scored emphysema was observed in patients who had stage I COPD and a high prevalence (68%) of CT-scored emphysema in patients having stage III COPD. Lung density parameters increased at both levels of inspiration with increasing  $FEV_1$  % predicted values. Attenuation values were significantly higher in patients with stage I COPD than in patients with stage III COPD ( $p < 0.0001$ ). A high prevalence (93%) of CT-scored emphysema was observed in patients with  $DL_{CO} < 50\%$  predicted and a low prevalence (19%) in patients with  $DL_{CO} \geq 50\%$  predicted. There was significant correlation between  $DL_{CO}$  % predicted and the CT emphysema score ( $r = -0.70$ ,  $p < 0.0001$ ) and the mean lung density at 90 % vital capacity ( $r = 0.72$ ,  $p < 0.0001$ ). Also in patients with  $FEV_1$  values  $< 1L$ , the correlation between  $DL_{CO}$  % predicted and the CT emphysema score was  $-0.73$  ( $p < 0.0001$ ), and lung densitometry  $0.72$  ( $p < 0.0001$ ). However, in patients with  $DL_{CO} < 50\%$  predicted corresponding correlations were considerably lower ( $r = -0.47$ ,  $p < 0.05$ ;  $r = 0.26$ ,  $p < 0.005$  respectively).

**Conclusion:** Results suggest a distinct presence and degree of emphysema in patients with advanced COPD.  $DL_{CO}$  is a useful test to separate patients with COPD with emphysema from patients with COPD without emphysema. However,  $DL_{CO}$  measurements cannot be relied on for quantitative assessment of severity and extent of emphysema.  $DL_{CO}$  measurements are therefore valuable to select patients for radiologic emphysema assessment.

## INTRODUCTION

Chronic obstructive pulmonary disease (COPD) is defined as a disease state characterized by the presence of airflow limitation due to emphysema or chronic bronchitis (1). Emphysema is defined as the abnormal permanent enlargement of airspaces distal to the terminal bronchioles, accompanied by destruction of their walls without obvious fibrosis (1). Functional hallmarks of emphysema are decreased airflow at spirometry and decreased carbon monoxide single-breath diffusing capacity ( $DL_{CO}$ ) due to parenchymal destruction. The separate contribution of emphysema and chronic bronchitis in causing airflow limitation in COPD is difficult to assess because the mechanical principles underlying airflow obstruction are interrelated in a complex way. Some researchers ascribe a major role for emphysema in causing airflow limitation due to a loss of lung elastic recoil (2,3). Others suggest that emphysema is only a relatively minor determinant of pulmonary function in advanced COPD (4,5), and that the decrease in expiratory flow in patients with COPD is due to an inflammatory process in the small conducting airways (5-10). The  $DL_{CO}$  is supposed to be decreased in proportion to the severity of emphysema (11-13), but is also considered to be a non-specific indicator of impaired gas transfer, in particular, not suitable to detect mild emphysema (14).

To date, computed tomography (CT) is considered the most accurate imaging method for diagnosing emphysema *in vivo* (15-17) and CT findings in pulmonary emphysema correlate closely to pathologic findings. The overall extent of emphysema can be assessed subjectively by visual inspection of CT images, or objectively, by use of a computer program analyzing attenuation values. Drawback of visual scoring techniques is that they depend on the experience of the observer and an 10% intraobserver and interobserver variability has been reported (18). Lung density, however, is considerably influenced by the level of inspiration at which the CT images are obtained and control and monitoring of the degree of inspiration during scanning is important to obtain reproducible results. We reported a reproducibility of mean lung density measurements within 3 HU at 90% vital capacity and within 11 HU at 10% vital capacity using this respiratory triggered technique (19). Reproducibility of lung density measurements was not influenced by the presence of respiratory insufficiency (19).

Gelb et al throw doubt upon the value of the  $DL_{CO}$  to detect significant emphysema in patients with advanced COPD (4,5). They compared lung function and CT grading concerning pulmonary emphysema in patients with COPD and could not demonstrate a relation between airflow limitation ( $FEV_1$ ) and emphysema (CT emphysema score) and even between  $DL_{CO}$  % predicted and radiologically assessment of emphysema in patients with advanced COPD.

The purpose of our study was to assess the contribution of emphysema in causing airflow limitation in patients with advanced COPD, and to study the debated point



whether  $DL_{CO}$  can be used as an indicator for emphysema in advanced COPD. We used high resolution CT of the lungs, in combination with CT lung densitometry, as the gold standard for the diagnosis of emphysema and for assessment of its severity.

## MATERIALS AND METHODS

A group of 100 patients (71 men, 29 women; mean age 63 years; age range, 39–83 years) with COPD as defined by the criteria of the American Thoracic Society (20) was entered into this prospective study. All patients had respiratory symptoms (chronic productive cough and/or shortness of breath during exertion or at rest) as well as a forced expiratory volume in one second ( $FEV_1$ ) of less than 70% of the reference value and a difference between prebronchodilator and postbronchodilator values of  $FEV_1$  not exceeding 10% of predicted. CT scans were performed in a clinically stable period, free from exacerbation. Informed consent was obtained from all the patients. The study protocol was approved by the ethics committee of the hospital.

### *Pulmonary function studies*

Lung function measurements were obtained by means of a wet spirometer (Gould Pulmonet III; Sensor Medics, Bithoven, the Netherlands).  $FEV_1$  was expressed as a percentage of the reference values (21). Lung volumes were measured with whole-body plethysmography and expressed as a percentage of the reference values (21). The diffusing capacity for carbon monoxide ( $DL_{CO}$ ) was measured using the single-breath technique (MasterLab; Jaeger, Würzburg, Germany). Transfer factor for carbon monoxide ( $K_{CO}$ ) was calculated from the ratio of  $DL_{CO}$  to alveolar volume. Lung function tests were performed by trained technicians according to the ERS guidelines (22).

### *CT emphysema score*

From each person, five thin-section computed tomography (HRCT) scans of the lungs (Somatom Plus; Siemens, Erlangen, Germany) were obtained at full inspiration with the patient in supine position: two scans of the upper zones at 3 cm and 6 cm above the carina, two scans of the lower zones at 3 cm and 6 cm below the carina, and one at the level of the carina. Scanning parameters were 1.0-mm collimation, 137 kVp, 220 mA, 1.0 second scanning time, and a high-resolution reconstruction algorithm. Hardcopy images were photographed using a window setting appropriate for visualization of lung parenchyma (level: -800 HU; width: 1,600 HU). Each slice was scored by two radiologists (R.J.S.L., J.M.A. v. E.) separately, without awareness of clinical findings, to a visual CT emphysema score according to the method of Sakai, which is

based on the assessment of 2 aspects of emphysema: severity and extent (23). Severity was graded on a 4-point scale: 0, no emphysema; 1, low attenuation areas  $< 5$  mm in diameter; 2, circumscribed low attenuation areas  $> 5$  mm in addition to those  $< 5$  mm; 3, diffuse low attenuation areas without normal intervening lung. The extent of emphysema was determined using a 4-point scale: 1,  $< 25\%$  of the lung parenchyma involved; 2, 25 to 50% involvement; 3, 50 to 75% involvement; 4,  $> 75\%$  involvement. For each hemislice, the score for severity was multiplied by the score for the extent. The scores of the 5 CT slices were summed to yield a CT emphysema score that could range from zero (no emphysema) to 120 (severe emphysema). The mean CT emphysema score of both observers was calculated for the purpose of this study. Patients were considered to have no or trivial emphysema if the CT emphysema score was  $< 30$ , and to have significant emphysema if the CT emphysema score was  $\geq 60$ .

### *CT lung densitometry*

Additionally during the same session, CT scans of the lungs were obtained in supine position for quantitative assessment of lung density patterns. The following scanning parameters were employed: 1.0-mm collimation, 137 kVp, 220 mA, and 1.0 second scanning time. Scans were reconstructed in the soft-detailed resolution mode. The full width at half maximum of the point spread function of this reconstruction filter is 1.86 mm; the sample volume  $3.92 \text{ mm}^3$  (24). No intravenous contrast material was administered. In order to control the level of inspiration during scanning, the patient was asked to breath through a pocket spirometer connected with the CT scanner (25). At user-selected levels of inspiration airflow was interrupted mechanically by a closing valve in the spirometer at what time a trigger signal was generated to start the scanner. The level of inspiration was kept constant for the duration of the CT scan. CT scans were obtained at 5 cm above the level of the carina and at 90% and 10% of the inspiratory vital capacity. Evaluation of the CT images was done on a SUN Sparc 1+ graphical workstation (SUN Microsystems, Mountain View, Calif). Both lungs were segmented automatically at a CT level of -200 HU using pixel tracing (26). Subsequently, the segmented areas were slightly eroded (2 pixels) to remove the circumference that partially corresponded to the thoracic wall. The histograms of both lungs were analyzed together. The mean lung density and the cut-off point of the frequency distribution that defines the lowest 10th percentile were calculated. Both lung density parameters have been often used for tissue characterization (27-30). CT during 90% vital capacity is useful to assess the extent of emphysema, whereas CT during 10% vital capacity is helpful in assessing degrees of air trapping (31,32).

## Statistical analysis

Interobserver agreement of visual assessment of emphysema was tested using Spearman's rank correlation coefficient. Statistical comparison between groups of patients was performed with the Student's *t* test. The results of pulmonary function tests were correlated with the CT emphysema score using Spearman's rank correlation coefficient, and with CT lung densitometry results with the Pearson correlation coefficient. A probability of less than 0.05 was considered to indicate a statistically significant difference in all analyses.

## RESULTS

The results of pulmonary function tests, visual assessment of CT scan images, and CT densitometry of the lung are summarized in Table 1. Patients suffered from moderate to severe airflow limitation. In 50 patients the  $FEV_1$  was  $< 1L$ . Further there was a wide spectrum of  $DL_{CO}$  % predicted and  $K_{CO}$  % predicted values ranging from normal to greatly reduced. In 19 patients we were not able to perform a proper diffusing capacity measurement; of these, 17 patients with a  $FEV_1 < 1L$ , and 2 patients with a  $FEV_1 \geq 1L$ . There was good interobserver agreement for the CT emphysema score ( $r = 0.82$ ,  $p < 0.001$ ). The mean CT emphysema score in patients with a  $FEV_1 < 1L$  was 43 (range 0 - 117) and significantly higher ( $p < 0.05$ ) than the mean CT emphysema score of patients with a  $FEV_1 \geq 1L$  (27, range 0-102). In 18 patients (36%) with a  $FEV_1 < 1L$  and in 33 patients (66%) with a  $FEV_1 \geq 1L$ , the CT emphysema score was  $< 30$ , indicating no or trivial emphysema. In 17 patients (34 %) with a  $FEV_1 < 1L$  and in 9 patients (18%) with a  $FEV_1 \geq 1L$ , the CT emphysema was  $\geq 60$ , indicating significant emphysema. The mean CT emphysema score of the 19 patients in which we were not successful to obtain a reliable diffusing capacity measurement was 45 (range, 0-102).

According to the American Thoracic Society statement on interpretation of lung function tests, the population was subdivided into three groups (1): stage I COPD is  $50 \leq FEV_1 < 70$  % predicted; stage II COPD is  $35 \leq FEV_1 < 50$  % predicted; and stage III COPD is  $FEV_1 < 35\%$  predicted (Table 2). The mean CT emphysema score of patients with stage I COPD was 12 (range, 0-60) and significantly lower than the mean CT emphysema score (37; range 0-115) of patients with stage II COPD ( $p < 0.005$ ), and significantly lower than the mean CT emphysema score (48; range, 0-117) of patients with stage III COPD ( $p < 0.0001$ ). The relation between  $FEV_1$  % predicted and the CT emphysema score is described in Figure 1 ( $r = -0.46$ ,  $p < 0.0001$ ). In 23 of the 27 patients (85%) with stage I COPD the CT emphysema score was  $< 30$ . Furthermore, in 19 of the 41 patients (47%) with stage III COPD, the CT emphysema score was  $\geq 60$ .

**Table 1.** Pulmonary Function, CT Emphysema Score, and Lung Attenuation Data of 100 Patients with COPD.

Parameter	Mean	± SD	Range	
FEV <sub>1</sub> , % predicted	40	± 14	17	- 70
FEV <sub>1</sub> , L	1.09	± 0.41	0.41	- 2.36
FVC, % predicted	88	± 17	45	- 122
FEV <sub>1</sub> /FVC, %	46	± 15	23	- 111
TLC, % predicted	124	± 18	82	- 185
DL <sub>CO</sub> , % predicted	61	± 23	18	- 115
K <sub>CO</sub> , % predicted	64	± 27	17	- 136
CT emphysema score	35	± 32	0	- 117
MLD 90% VC, HU	-894	± 32	-785	- -957
MLD 10% VC, HU	-856	± 47	-733	- -940
LTP 90% VC, HU	-962	± 29	-870	- -1004
LTP 10% VC, HU	-942	± 42	-797	- -1005

Note. MLD = mean lung density and LTP = lowest 10th percentile are expressed in Hounsfield units. SD = standard deviation.

**Table 2.** Prevalence of Airflow Limitation Stratified for the CT Emphysema Score in 100 Patients with COPD.

		Patients (n)	CT Emphysema Score*			
			< 30	30-59	60-89	≥ 90
Stage I	COPD	27	23 (85)	3 (11)	1 (4)	0 (0)
Stage II	COPD	32	16 (50)	8 (25)	4 (13)	4 (13)
Stage III	COPD	41	13 (32)	9 (22)	15 (37)	4 (10)
			52	20	20	8

Note. \* CT emphysema score < 30 = no or trivial emphysema; 30 to 59 = mild emphysema; 60 to 89 = moderate emphysema; ≥ 90 = severe emphysema. Numbers in parenthesis are percentages. Percentages may not add to 100 because of rounding.

Lung density parameters increased at both levels of inspiration with increasing FEV<sub>1</sub> % predicted values (Table 3). Densitometric parameters in patients with stage I COPD were statistically significantly higher than those from patients with stage III COPD ( $p < 0.0001$ ), and also from those with stage II COPD at both levels of inspiration ( $p < 0.005$ ). Densitometric results between patients with stage II and stage III COPD did not differ significantly. The change between the densitometric data obtained at 90% vital capacity and at 10% vital capacity was significantly higher in patients with stage I COPD than the corresponding change between the densitometric data in patients with stage III COPD ( $p < 0.001$ ).

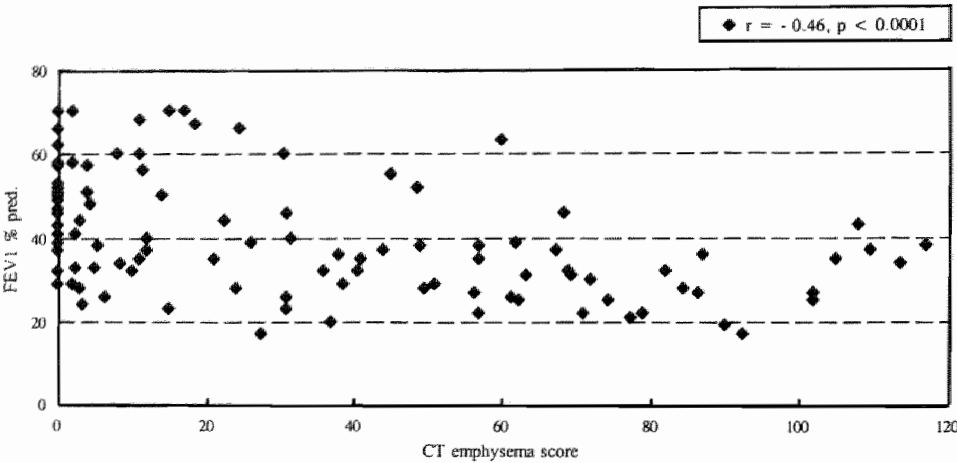


**Figure 1.** Relation between FEV1 % predicted and the CT emphysema score in 100 patients with irreversible air-flow limitation.

**Table 3.** Densitometric Results at 90% and 10% Vital Capacity of 100 Patients with COPD.

	Stage I COPD (n=27)	Stage II COPD (n=32)		Stage III COPD (n=41)	
Vital Capacity (%)	Mean ± SD	Mean ± SD	p*	Mean ± SD	p†
<b>Mean lung density (HU)</b>					
90	-873 ± 29	-897 ± 32	<.005	-905 ± 23	<.0001
10	-819 ± 34	-860 ± 47	<.0001	-877 ± 38	<.0001
<b>Lowest 10th perc. (HU)</b>					
90	-941 ± 21	-965 ± 29	<0.005	-974 ± 21	<.0001
10	-908 ± 37	-947 ± 45	<.0005	-963 ± 33	<.0001

Note. CT numbers are given as means ± SD, and expressed in Hounsfield Units (HU); \* Patients with stage II COPD versus those with stage III COPD; † Patients with stage III COPD versus those with stage I COPD.

**Table 4.** Densitometric Results at 90% and 10% Vital Capacity of 100 Patients with COPD Stratified for the CT Emphysema Score.

	CT Emphysema Score *			
Vital capacity (%)	< 30 (n=52)	30-59 (n=20)	60-89 (n=20)	≥ 90 (n=8)
<b>Mean lung density (HU)</b>				
90	-871 ± 23	-907 ± 13	-921 ± 20	-939 ± 10
10	-821 ± 38	-877 ± 21	-901 ± 25	-919 ± 12
<b>Lowest 10th perc.(HU)</b>				
90	-940 ± 22	-978 ± 11	-989 ± 8	-997 ± 5
10	-909 ± 37	-967 ± 16	-986 ± 12	-996 ± 7

Note. \* < 30 = no or trivial emphysema; 30 to 59 = mild emphysema; 60 to 89 = moderate emphysema; ≥ 90 = severe emphysema. CT numbers are given as means ± SD.

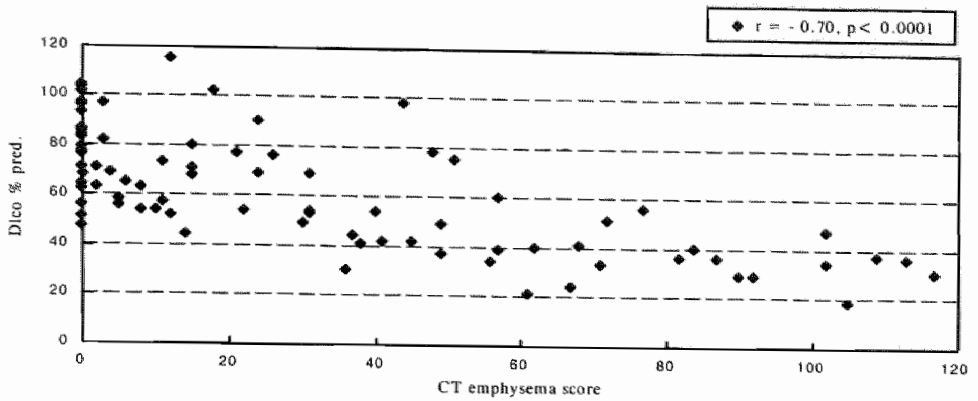


**Figure 2.** Relation between D1co % predicted and the CT emphysema score in 81 patients with irreversible airflow limitation.

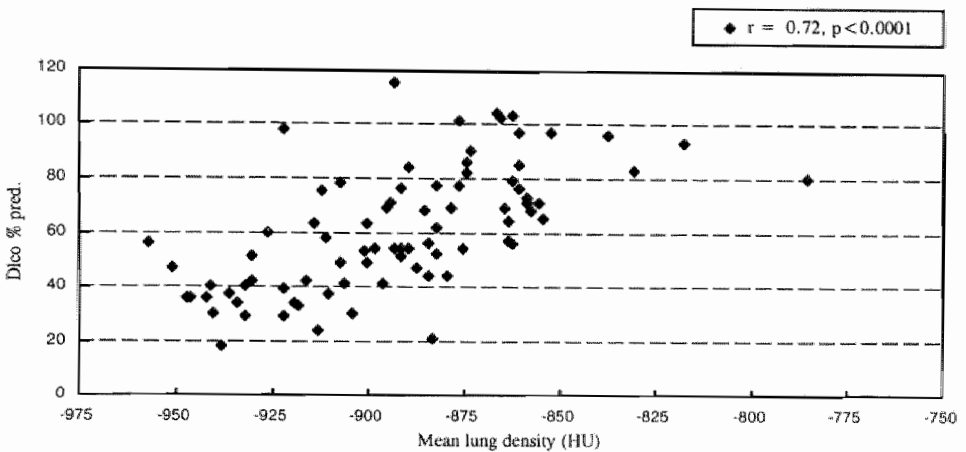


**Figure 3.** Relation between D1co % predicted and the mean lung density at 90% vital capacity in 81 patients with irreversible airflow limitation.

For further analysis the group of patients with COPD was subdivided on the basis of the CT emphysema score into four categories; no or trivial emphysema (CT grade < 30), mild emphysema (CT grade 30-59), moderate emphysema (CT grade 60-89), and severe emphysema (CT grade  $\geq 90$ ) (Table 4). With increasing extent of emphysema, as indicated by the CT emphysema score, attenuation values decreased at both levels of inspiration. Lung density parameters were significantly lower in the group with severe emphysema than in the group with no or trivial emphysema ( $p < 0.001$ ). The change between the mean lung density at 90% vital capacity and at 10% vital capacity in the group with severe emphysema was  $20 \pm 9$  HU, and for the lowest 10th percentile

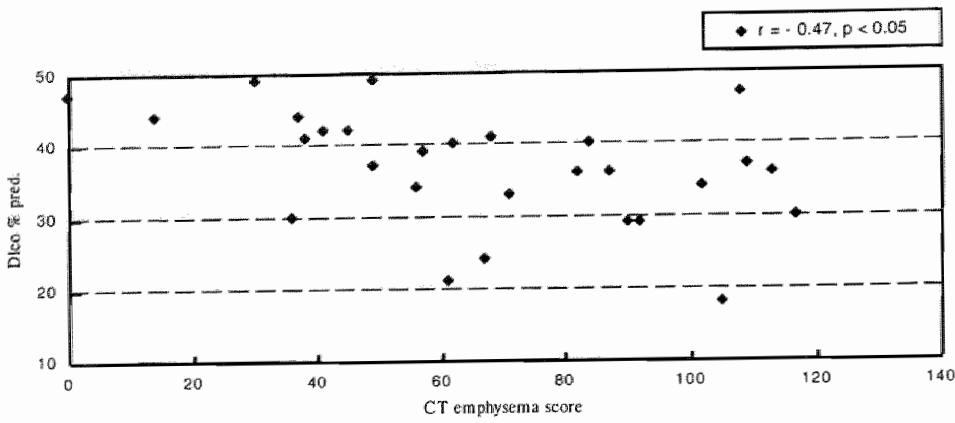


**Figure 4.** Relation between D1co % predicted and CT emphysema score in 28 patients with COPD and D1co % predicted less than 50.

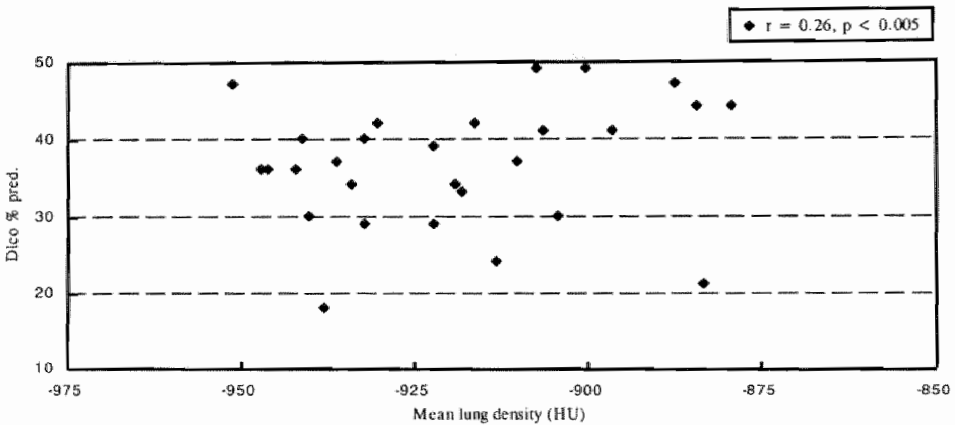


**Figure 5.** Relation between D1co % predicted and mean lung density at 90% vital capacity in 28 patients with COPD and D1co % predicted less than 50.

$1 \pm 3$  HU. In the group with no or trivial emphysema these changes between the densitometric data obtained at 90% vital capacity and 10% vital capacity were  $50 \pm 21$  HU and  $31 \pm 17$  HU respectively. Changes between the densitometric data were significantly smaller in the group with severe emphysema than in the group with no or trivial emphysema ( $p < 0.005$ ).

The relationship between  $DL_{CO}$  % predicted and the CT emphysema score in patients with COPD is shown in Figure 2 ( $r = -0.70, p < 0.0001$ ), and between  $DL_{CO}$  % predicted and the mean lung density at 90 % vital capacity in Figure 3 ( $r = 0.72, p < 0.0001$ ). In 28 patients (35%) the  $DL_{CO}$  was  $< 50$  % predicted, and in 53 patients (65%)

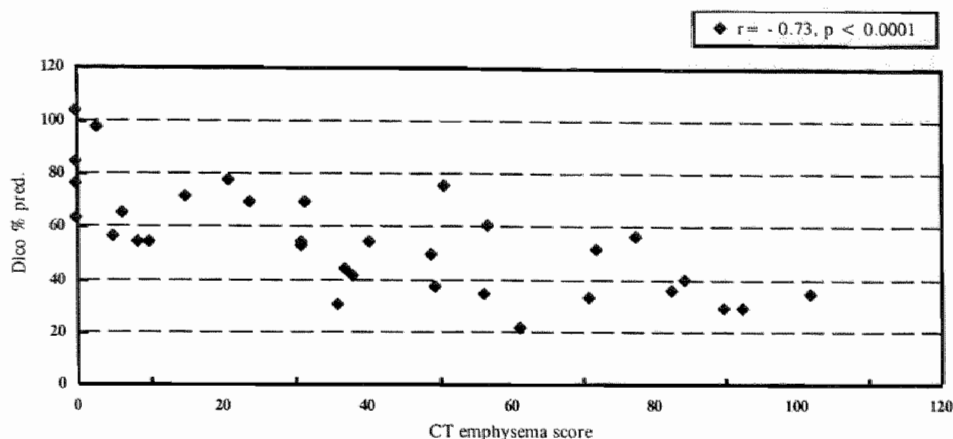


**Figure 6.** Relation between D1co % predicted and CT emphysema score in 33 patients with COPD and FEV1 less than 1L.

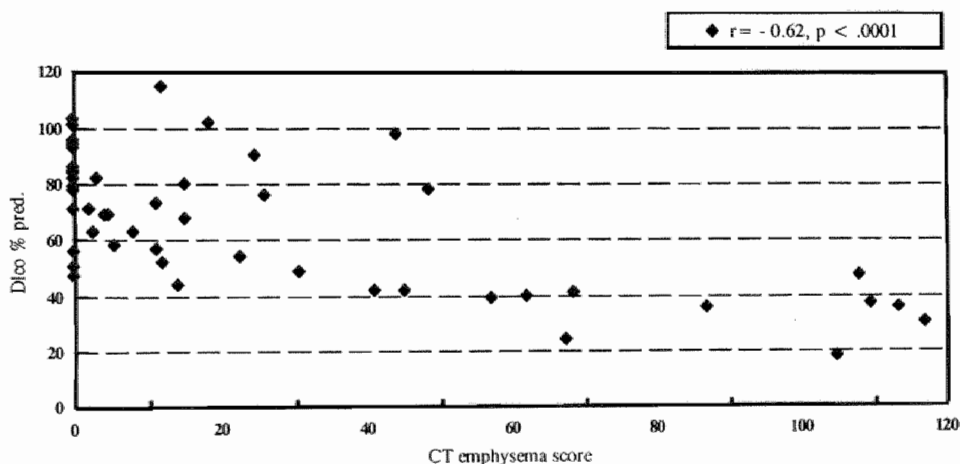


**Figure 7.** Relation between D1co % predicted and CT emphysema score in 48 patients with COPD and FEV1 equal to or more than 1L.

the  $DL_{CO}$  was  $\geq 50$  % predicted. In patients with  $DL_{CO} < 50$  % predicted, the relation between  $DL_{CO}$  % predicted and the CT emphysema score is described in Figure 4 ( $r = -0.47, p < 0.05$ ), and between  $DL_{CO}$  % predicted and the mean lung density at 90 % vital capacity in Figure 5 ( $r = 0.26, p < 0.005$ ). In patients with  $DL_{CO} \geq 50$  % predicted, a significant correlation was found between  $DL_{CO}$  % predicted and the CT emphysema score ( $r = -0.34, p < 0.05$ ), and between  $DL_{CO}$  % predicted and the mean lung density at 90 % vital capacity ( $r = 0.46, p < 0.001$ ). In 26 of 28 patients (93%) with  $DL_{CO} < 50$



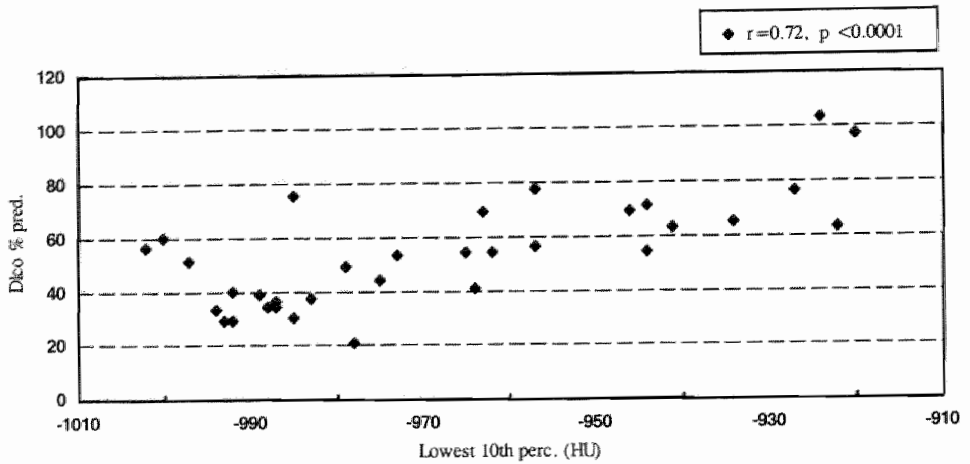


**Figure 8.** Relation between DLco % predicted and the lowest 10th percentile at 90% vital capacity in 33 patients with COPD and FEV1 less than 1L.

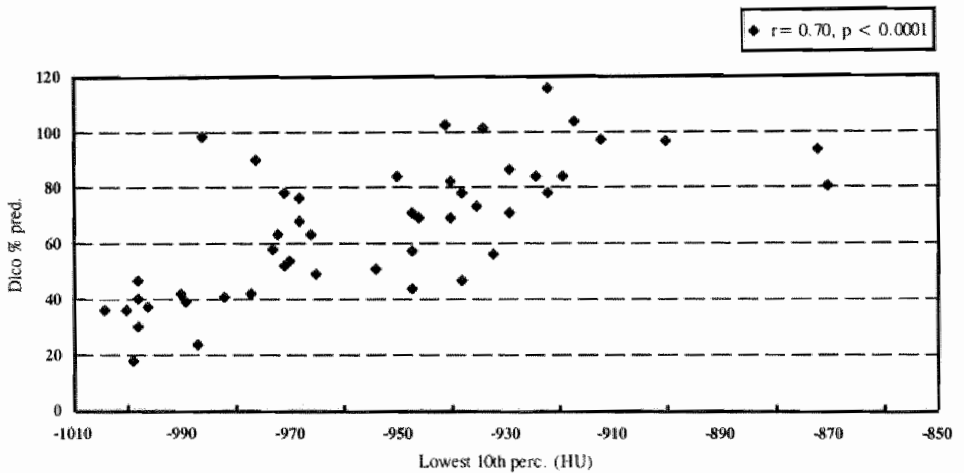


**Figure 9.** Relation between DLco % predicted and the lowest 10th percentile at 90% vital capacity in 48 patients with COPD and FEV1 equal to or more than 1L.

% predicted the CT emphysema score was  $\geq 30$ . In 43 of 53 patients (81%) with  $DL_{CO} \geq 50\%$  predicted the CT of the lung showed no abnormalities.

The relationship between  $DL_{CO}$  % predicted and the CT emphysema score in patients with  $FEV_1$  levels  $< 1L$  is shown in Figure 6 ( $r = -0.73, p < 0.0001$ ). All of the 13 patients with a  $FEV_1 < 1L$  and a  $DL_{CO} < 50\%$  predicted had emphysematous parenchymal changes (CT grade  $\geq 30$ ). Seven of these 13 patients (54%) had significant emphysema (CT grade  $\geq 60$ ). In 12 of 20 patients (60%) with a  $FEV_1 < 1L$  and a  $DL_{CO} \geq 50\%$  pre-

dicted, the CT of the lung was normal. The relationship between  $DL_{CO}$  % predicted and the CT emphysema score in patients with  $FEV_1$  levels  $\geq 1L$  is illustrated in Figure 7 ( $r = -0.62$ ,  $p < 0.0001$ ). In 31 of 33 patients (94%) with a  $FEV_1 \geq 1L$  and a  $DL_{CO} \geq 50\%$  predicted, the CT of the lung showed no abnormalities. In 9 of 15 patients (60%) with a  $FEV_1 \geq 1L$  and a  $DL_{CO} < 50\%$  predicted the CT scan of the lungs showed significant emphysematous changes. There was a significant correlation between  $DL_{CO}$  % predicted and the lowest 10th percentile of the frequency distribution at 90% vital capacity in patients with a  $FEV_1 < 1L$  ( $r = 0.72$ ,  $p < 0.0001$ ) (Figure 8), and also in patients with levels  $FEV_1 \geq 1L$  ( $r = 0.70$ ,  $p < 0.0001$ ) (Figure 9).

The correlation between  $DL_{CO}$  % predicted and the CT emphysema score in patients with  $FEV_1$  levels  $< 50\%$  predicted was  $-0.69$  ( $p < 0.001$ ). In 24 of 25 patients (96%) with a  $FEV_1 < 50\%$  predicted and a  $DL_{CO} < 50\%$  predicted, the CT emphysema score was  $> 30$ . In 16 of these 25 patients (64%) the CT emphysema score was  $\geq 60$ . In 23 of 32 patients (72%) with a  $FEV_1 < 50\%$  predicted and a  $DL_{CO} > 50\%$  predicted, the CT of the lung was  $< 30$ . The correlation between  $DL_{CO}$  % predicted and the CT emphysema score in patients with a  $FEV_1 \geq 50\%$  predicted was  $-0.32$  ( $p < 0.05$ ). In 19 of 22 patients (86%) with a  $FEV_1 \geq 50\%$  predicted and a  $DL_{CO} \geq 50\%$  predicted, the CT emphysema score was  $< 30$ . The CT emphysema score of all 4 patients with a  $FEV_1 \geq 50\%$  predicted and a  $DL_{CO} < 50\%$  predicted was  $\geq 60$ .

## DISCUSSION

In the studied population of patients with COPD, airflow limitation and emphysema were fairly correlated. Forty-six percent of patients with stage III COPD ( $FEV_1 < 35\%$  predicted) had significant emphysema (CT grade  $\geq 60$ ) as opposed to 4 percent of patients with stage I COPD ( $50 \leq FEV_1 < 70\%$  predicted). The same conclusion can be drawn from the correlation between  $FEV_1$  and CT densitometry of the lung. Airflow limitation and progression of emphysema was attended with lower attenuation values as measured on CT. Moreover, the carbon monoxide diffusing capacity ( $DL_{CO}$ ) was well related with the CT emphysema score and CT lung densitometry parameters in patients with COPD. In patients with advanced COPD ( $FEV_1 < 1L$ ), the CT emphysema score and lung densitometry correlated equally well with  $DL_{CO}$  % predicted. Results of the present study indicate a high prevalence of CT-scored significant emphysema in patients with COPD and  $DL_{CO}$  % predicted of less than 50, and a low prevalence of CT-scored significant emphysema in patients with COPD and  $DL_{CO}$  % predicted equal to or more than 50. However, in patients with COPD and  $DL_{CO}$  % predicted of less than 50, the CT emphysema score and CT lung densitometry showed a significant but low correlation with  $DL_{CO}$  % predicted. The  $DL_{CO}$  can not be relied on for quantitative assessment of severity and extent of emphysema.

Using a visual grading method, CT-scored significant emphysema was found mainly in patients with COPD with stage II or stage III COPD ( $FEV_1 < 50\%$  predicted). In contrast, in 85 % of patients with COPD with stage I COPD, the CT of the chest showed no abnormalities. The CT emphysema score in patients with advanced COPD was significantly higher than the CT emphysema score in patients with COPD and  $FEV_1$  equal or more than 1L. Our data confirm the conclusions reached by Miniati et al who found a high prevalence of emphysema as indicated by CT scores in patients with advanced COPD (33) but differ substantially from previous published data from Gelb et al who reported a limited presence of and role for emphysema in causing chronic expiratory airflow limitation in patients with advanced chronic obstructive lung disease (4). We have no unequivocal explanation for the difference in results between both studies. Both study populations showed a great resemblance with respect to age, indicators of airflow limitation, as well as  $DL_{CO}$  % predicted values. However, in our heterogeneous population of 100 patients with COPD the full range of CT emphysema scores was well-represented whereas in their study population, patients with severe emphysema as indicated by CT scores were probably under-represented.

In an effort to provide skill independent support to our visual observations we used CT densitometry to objectively quantify the extent of pulmonary emphysema. This is feasible since the performance of modern CT scanners is quite adequate for densitometry of the lungs (34). The stability of the CT system at air densities is within 1 HU, and reproducibility and accuracy for densities found for lung tissue were within 1-2 HU (35). Moreover, quantitative analysis of expiratory CT images has proved useful in assessing degrees of air-trapping in diseases affecting the airways. CT scans obtained during suspended full expiration in patients with small airways disease show focal air retention in lung parenchyma which can be densitometrically quantified (31,32,36). Air-trapping during exhalation in patients with COPD is reflected by a reduction in the change between the densitometric data obtained at inspiration and at expiration (37).

Lung density measurements obtained in the present study confirmed visual observations that patients with significant emphysematous destruction of lung parenchyma are found mainly in the patients with stage II and stage III COPD. Furthermore, with progression of airflow limitation, the lung density in patients with COPD obtained at 90% vital capacity and at 10% vital capacity decreased as expected. The change between the densitometric data obtained at both levels of inspiration in the group of patients with stage III COPD was significantly smaller than in patients with stage I COPD. Similar observations were obtained after stratification of the COPD population based on the degree of CT-scored emphysema. With increasing CT-scored emphysema, the mean lung density at 90% and 10% vital capacity CT numbers decreased progressively as expected. Besides, the change between the densitometric data obtained at 90% vital capacity and at 10% vital capacity was in the group of patients with

COPD and severe emphysema (CT grade  $\geq 90$ ) significantly smaller than in patients with COPD with no or trivial emphysema (CT grade  $< 30$ ). This smaller change between the densitometric data observed in patients with severe emphysema provides additional support to our hypothesis that emphysema is related to airflow limitation.

Quantitative techniques must be carefully controlled. Submaximal efforts have major effect on attenuation measurements as lung density values vary inversely with lung volume. We applied a spirometric gated CT technique which offers the opportunity to scan at defined levels of inspiration (25). A spirometric curve can be followed on the display monitor of the CT scanner. Feedback control makes it easier to coach patients for a truly maximal effort. CT densitometry of the lung is usually performed at full inspiration or at full expiration. However, maximal effort is particularly fatiguing for patients with advanced airflow limitation. Therefore, we scanned, for the convenience of our patients at 90% and 10% vital capacity trigger level.

The  $DL_{CO}$ , whether measured by single-breath or steady state method, expressed in absolute terms, as per cent predicted, or as function of alveolar volume, has constantly been considered as the best predictor of severity of emphysema. However, wide variations in correlation between  $DL_{CO}$  and the macroscopic extent of emphysema have been reported (27,38). We found a good correlation ( $r = -0.72$ ,  $p < 0.0001$ ) between  $DL_{CO}$  and the CT emphysema score in our population of patients with COPD. These results are in agreement with Gould et al (38) who found a similar inverse correlation between  $DL_{CO}$  and the lowest 10th percentile in a group of 80 subjects that ranged from normal subjects to patients with chronic respiratory failure. In another study, these authors reported a similar inverse correlation between the lowest 10th percentile of non-bullous lung and  $DL_{CO}$  in a group of 23 patients with varying degrees of emphysema and in addition bullous disease (39).

Gelb and coworkers question the usefulness of the  $DL_{CO}$  as indicator of significant emphysema (4). They found poor correlation between  $DL_{CO}$  and the CT emphysema grade in 23 patients with advanced airflow limitation defined as  $FEV_1$  levels less than 1L. Opposite to these results, we found a good correlation between  $DL_{CO}$  and the severity of emphysema independent of the degree of airflow limitation. Correlations were even higher in patients with advanced airflow limitation. Nevertheless, in our opinion, the  $DL_{CO}$  is a useful test to separate patients with COPD with emphysema from patients with COPD without emphysema. The vast majority of patients (93%) with COPD and a  $DL_{CO}$  % predicted of less than 50 % showed emphysematous changes at CT, and 56 % of these patients suffered from significant emphysema. Deviating from this, 23 % of patients with COPD and  $DL_{CO}$  % predicted of equal to or more than 50 showed emphysema on CT, and only a small minority of patients (4%) showed significant emphysematous parenchymal changes on CT.

In conclusion: Results suggest a distinct presence and degree of emphysema in patients with advanced COPD. The  $DL_{CO}$  is a reliable indicator of emphysema also in

patients with advanced chronic obstructive pulmonary disease. A high prevalence of CT-scored emphysema was observed in patients with COPD and  $DL_{CO}$  % predicted of less than 50. However,  $DL_{CO}$  measurements cannot be relied on for quantitative assessment of severity and extent of emphysema.  $DL_{CO}$  measurements are therefore useful measurements to select patients for radiologic emphysema assessment. Further prospective studies are needed to validate this stratification criterium.

## REFERENCES

1. ATS Statement. Standards for the diagnosis and care of patients with chronic obstructive pulmonary disease. *Am J Respir Crit Care Med* 1995; 152:S77-S120.
2. Mead JMM, Turner JM, Macklem PT, Little JB. Significance of the relationship between lung recoil and maximum expiratory flow. *J Appl Physiol* 1967; 22:95-108.
3. Kim WD, Eidelman DH, Izquierdo JL, Ghezzi H, Sietta MP, Cosio MG. Centrilobular and panlobular emphysema in smokers: two distinct morphologic and functional entities. *Am Rev Respir Dis* 1991; 144:1385-1390.
4. Gelb AF, Schein M, Kuei J, et al. Limited contribution of emphysema in advanced chronic obstructive pulmonary disease. *Am Rev Respir Dis* 1993; 147:1157-1161.
5. Gelb AF, Hogg JC, Müller NL, et al. Contribution of emphysema and small airways in COPD. *Chest* 1996; 109:353-359.
6. Hogg JC, Macklem PT, Thurlbeck WM. Site and nature of airway obstruction in chronic obstructive lung disease. *N Engl J Med* 1968; 278:1355-1360.
7. Cosio MG, Ghezzi H, Hogg JC, Corbin R, Loveland M, Dosman JJ, Macklem PT. The relations between structural changes in small airways and pulmonary function tests. *N Engl J Med* 1978; 298:1277-1281.
8. Wright JL, Lawson LM, Paré PD, Kennedy S, Wiggs B, Hogg JC. The detection of small airways disease. *Am Rev Respir Dis* 1984; 129:989-994.
9. Berend N, Wright JL, Thurlbeck WM, Marlin GE, Woolcock AJ. Small airways disease: reproducibility of measurements and correlation with lung function. *Chest* 1981; 79:263-268.
10. Hogg JC, JL Wright JL, Wiggs BR, Coxson HO, Opazo Saez A, Paré PD. Lung structure and function in cigarette smokers. *Thorax* 1994; 49:473-478.
11. Thurlbeck WM, Henderson JA, Fraser RG, Bates DV. Chronic obstructive lung disease: a comparison between clinical, roentgenologic, functional, and morphologic criteria in chronic bronchitis, emphysema, asthma, and bronchiectasis. *Medicine* 1970; 49:81-145.
12. Symonds G, Renzetti AD, Mitchell MM. The diffusing capacity in pulmonary emphysema. *Am Rev Respir Dis* 1974; 109:391-394.
13. West WW, Nagai A, Hodgkin JE, Thurlbeck WM. The National Institutes of Health intermittent positive pressure breathing trial. Pathological studies. *Am Rev Respir Dis* 1987; 135:123-129.
14. Pratt PC, Kilburn KH. A modern concept of the emphysemas based on correlations of structure and function. *Hum Pathol* 1970; 1:433-463.
15. Stern EJ, Frank MS. CT of the lung in patients with pulmonary emphysema: diagnosis, quantification, and correlation with pathologic and physiologic findings. *AJR* 1994; 162:791-798.
16. Thurlbeck WM, Müller NL. Emphysema: definition, imaging, and quantification. *AJR* 1994; 163:1017-1025.
17. Gevenois PA, Yernault JC. Can computed tomography quantify pulmonary emphysema. *Eur Respir J* 1995; 5:843-848.

18. Morgan MDL. Detection and quantification of pulmonary emphysema by computed tomography: a window of opportunity. *Thorax* 1992; 47:1001-1004.
19. Lamers RJS, Kemerink GJ, Drent M, van Engelshoven JMA. Reproducibility of spirometrically controlled CT lung densitometry in a clinical setting. *Eur Respir J* 1988; 11:942-945.
20. American Thoracic Society. Chronic bronchitis, asthma, and pulmonary emphysema: a statement by the Committee on Diagnostic Standards for Nontuberculous Respiratory Diseases. *Am Rev Respir Dis* 1962; 85:762-768.
21. Quanjer PH. Standardized lung function testing. *Bull Eur Physiopathol Respir* 1983; 19:7-44.
22. Quanjer P, Tammeling GJ, Cotes JE, Pedersen OF, Peslin R, Yernault JC. Lung volumes and forced ventilatory flows. Official statement of the European Respiratory Society. *Eur Respir J* 1993; 16 (Suppl 6):5-40.
23. Sakai F, Gamsu G, Im JG, Ray CS. Pulmonary function abnormalities in patients with CT-determined emphysema. *J Comput Assist Tomogr* 1987; 11:963-968.
24. Kemerink GJ, Kruize HH, Lamers RJS. The CT's sample volume as an approximate, instrumental measure for density resolution in densitometry of the lung. *Med Phys* 1997; 24:1615-1620.
25. Kalender WA, Rienmüller R, Seissler W, Behr J, Welke M, Fichte H. Measurement of pulmonary parenchymal attenuation: use of spirometric gating with quantitative CT. *Radiology* 1990; 175:265-268.
26. Pavlidis T. Algorithms for graphics and image processing. Springer Verlag, Berlin. 1982.
27. Gould GA, Macnee W, McLean A, et al. CT measurements of lung density in life can quantitate distal airspace enlargement: an essential defining feature of human emphysema. *Am Rev Respir Dis* 1988; 137:380-392.
28. Biernacki W, Gould GA, Whyte KF, Flenley DC. Pulmonary hemodynamics, gas exchange, and the severity of emphysema as assessed by quantitative CT scan in chronic bronchitis and emphysema. *Am Rev Respir Dis* 1989; 139:1509-1515.
29. Heremans A, Verschakelen JA, Van Fraeyenhoven L, Demedts M. Measurement of lung density by means of quantitative CT scanning. *Chest* 1992; 102:805-811.
30. Beinert T, Behr F, Mehnert F, et al. Spirometrically controlled quantitative CT for assessing diffuse parenchymal lung disease. *J Comput Assist Tomogr* 1995; 19:924-931.
31. Newman KB, Lynch DA, Newman LS, Ellegood D, Newell JD. Quantitative computed tomography detects air trapping due to asthma. *Chest* 1994; 106:105-109.
32. Gevenois PA, De Vuyst P, Sy M, et al. Pulmonary emphysema: quantitative CT during expiration. *Radiology* 1996; 199:825-829.
33. Miniati M, Filippi E, Falaschi F, et al. Radiologic evaluation of emphysema in patients with chronic obstructive pulmonary disease. *Am J Respir Crit Care Med* 1985; 151:1359-1367.
34. Kemerink GJ, Lamers RJS, Thelissen GRP, van Engelshoven JMA. Scanner conformity in CT densitometry of the lungs. *Radiology* 1995; 197:749-752.
35. Kemerink GJ, Lamers RJS, Thelissen GRP, van Engelshoven JMA. CT densitometry of the lungs: scanner performance. *J Comput Assist Tomogr* 1996; 20:24-33.
36. Eda S, Kubo K, Fujimoto K, Matsuzawa Y, Sekiguchi M, Sakai F. The relations between expiratory chest CT using helical CT and pulmonary function tests in emphysema. *Am J Respir Crit Care Med* 1997; 155:1290-1294.
37. Lamers RJS, Thelissen GRP, Kessels AG, Wouters EFM, van Engelshoven JMA. Chronic obstructive pulmonary disease: evaluation with spirometrically controlled CT lung densitometry. *Radiology* 1994; 193:109-113.
38. Gould GA, Redpath AT, Ryan M, et al. Lung CT density correlates with measurements of airflow limitation and the diffusing capacity. *Eur Respir J* 1991; 4:141-146.
39. Gould GA, Redpath AT, Ryan M, et al. Parenchymal emphysema measured by CT lung density correlates with lung function in patients with bullous disease. *Eur Respir J* 1993; 6:698-704.



## CHAPTER 9

---

# CT lung densitometry and visual assessment of thin-section CT in the diagnosis of coal worker's pneumoconiosis

Rob J.S. Lamers

Paul J.A. Borm

Alfons G.H. Kessels

Gerrit J. Kemerink

Emiel F.M. Wouters

Jos M.A. van Engelshoven



## ABSTRACT

**Purpose:** To assess the usefulness of computed tomographic (CT) lung densitometry in coal worker's pneumoconiosis (CWP).

**Materials and methods:** Spirometrically gated CT sections were obtained at 5 cm above and 5 cm below the carina at 90% and 10% vital capacity (VC) in a group of 66 persons consisting of 35 coal miners with a normal chest radiograph, 11 coal miners with a chest radiograph showing nodular opacities consistent with CWP, and 20 healthy volunteers. Various densitometric parameters were derived from the CT data. Additionally, thin-section CT scans were obtained in the upper and the lower zones of the lungs, and visually assessed for the presence and extent of CWP. Based on results of visual assessment, subjects were divided into three subsets. Densitometric parameters of CWP between the three groups were compared and correlated with results of visual assessment of CT scans at the same anatomical levels.

**Results:** With increasing extent of CWP higher densitometric values were observed at both levels of inspiration. Densitometric parameters between groups differed significantly in the upper zones only at 90% VC (all  $p > 0.01$ ). Good correlations between objective and subjective parameters of CWP were observed at 90% VC, being best in the upper zones. At 10% VC, correlations were always poor.

**Conclusion:** CT scans obtained at 90% VC in the upper zones of the lungs are the best candidates for lung densitometric measurements in CWP. Objective measurements of lung density correlate well with direct observational assessment of CWP provided that CT sections are obtained at 90% VC.

## INTRODUCTION

Coal worker's pneumoconiosis is usually diagnosed from a history of significant coal dust exposure and a combination of clinical, functional and radiographic findings. The chest radiograph appearance, coded according to the International Labor Organization (ILO 1980) criteria, is generally accepted as evidence of the presence of coal worker's pneumoconiosis without histological proof (1). However, the ILO classified chest radiograph may underestimate the presence of interstitial lung disease (2). Chest radiographs have a low sensitivity for detecting minimal to moderate grades of coal worker's pneumoconiosis (3). Visual assessment of thick-section computed tomography (CT) images has proven superior to the chest radiograph in the early detection of diffuse parenchymal lung diseases (4-6). Thin-section CT identifies even significantly more parenchymal opacities than thick-section CT (7-9). However, visual assessment of nodules at thin-section CT scans of the lungs was shown to be subject to interobserver variability (9).

Lung density measurements have the advantage of providing quantitative data automatically, thereby eliminating observer variability. Performance of modern generation CT scanners compare favorable with that reported in the past (10-12). Scanner conformity, reproducibility and accuracy of present CT scanners is adequate (13,14). The value of this technique is clearly proven in pulmonary emphysema where densitometric assessment correlates well with the pathologic score of emphysema (15-17). Assessment of parenchymal density on CT is a valid measure of the extent of interstitial lung disease (18,19). The physical density of the lung parenchyma increases proportionally to the amount of silicotic nodules present. As density changes rapidly and markedly with the level of inspiration, the necessity of reproducible levels of inspiration was a major limitation. This problem has been solved by applying spirometric control of the level of inspiration for gating the CT scanner (20).

Radiographic documentation of coal worker's pneumoconiosis is important for diagnosis, surveillance, compensation, and disease prevention (3). During a five year follow-up period in a group of 104 retired coal miners, a significant portion of this cohort showed progression of coal worker's pneumoconiosis on chest radiographs (21). Quantitative analysis of the frequency distribution of Hounsfield numbers defines the radiological extent and/or progression of coal worker's pneumoconiosis related to parenchymal changes by comparing results from base line to follow-up scans. Patients with other interstitial lung diseases, with diffuse fibrosing alveolitis and granulomatous lung disease, showing normal lung function tests, have been proven to differ significantly from healthy controls in the frequency distribution of CT numbers (22).

This study assesses coal worker's pneumoconiosis by (a) comparing the results of spirometrically controlled CT lung densitometry scans obtained from three groups of subjects: coal miners with a mild abnormal thin-section CT suggestive of coal worker's pneumoconiosis, coal miners with a more severe abnormal thin-section CT consistent with coal worker's pneumoconiosis, and persons with a normal thin-section CT and (b) relating results of spirometrically gated CT lung densitometry with those of visual assessment of thin-section CT scans. For this purpose, measurements in the upper and the lower zones of the lungs at two defined levels of inspiration were performed.

## MATERIALS AND METHODS

The initial study population consisted of 156 retired coal worker's who worked underground in the Belgian collieries for more than 20 years and who were involved in previous studies (23,24). Standard high-kilovoltage posteroanterior and lateral chest radiographs were obtained at maximal inspiration. Chest radiographs were read by a panel of three board medical officers, with a long term familiarity in reading and clas-

sifying pneumoconiosis according to ILO criteria for compensation purposes (1). Differences in opinion were resolved by consensus.

Based on these chest radiograph results, 35 coal miners aged 40 - 61 years (mean  $\pm$  standard deviation,  $47 \pm 8$  years) with a normal chest radiograph (ILO  $\leq 0/1$ ), and 11 coal miners aged 42 - 56 years ( $51 \pm 5$  years) with small rounded opacities (ILO  $> 0/1$ ) consistent with simple coal worker's pneumoconiosis, were randomly selected and invited to participate. A third group consisted of 20 non-exposed volunteers aged 31 - 78 years ( $53 \pm 12$  years), who had neither pulmonary symptoms nor any history of pulmonary diseases. Pulmonary function tests i.e. forced expiratory volume in 1 second (FEV<sub>1</sub>) and transfer coefficient (K<sub>CO</sub>) were both more than 80% of the predicted value in the latter group. Subject characteristics of our study groups (Table 1) showed that coal miners with a normal chest radiograph, coal miners with coal worker's pneumoconiosis and healthy volunteers were not different in age, length, weight and smoking history. Written informed consent was obtained from all participants. The study was approved by the local medical ethics committee.

Occupational history data were obtained from questionnaires and confirmed by personal interviews. The number of years underground in coal miners with a normal chest radiograph was significantly lower ( $p < 0.005$ ) compared to the number of years underground of coal miners with coal worker's pneumoconiosis. The cumulative dust exposure was calculated as the sum of the products of the yearly mean dust concentration for the colliery where the miner had worked and the average time worked underground during that year. The resulting individual units were expressed as gram-hours per cubic meter of sampled air (21).

### *Pulmonary function studies*

Pulmonary function tests were performed at the day of CT densitometry. Spirometric measurements were obtained by means of a wet spirometer (Gould Pulmonet III; Sennormedics, Bithoven, the Netherlands): FEV<sub>1</sub> was expressed as a percentage of the reference values (25). Lung volumes were measured by whole-body plethysmography and were again expressed as a percentage of the reference values (25). The diffusing capacity was measured by the single-breath method (MasterLab; Jaeger, Würzburg, Germany). K<sub>CO</sub> was calculated as diffusing capacity divided by the alveolar volume.

### *Visual assessment of CT scans*

In each person, four thin-section CT scans were obtained (Somatom Plus; Siemens, Erlangen, Germany) within two year of the chest radiograph, at end-inspiratory lung volume with the person in supine position; two scans of the upper zones, 3 and 5 cm above the carina, and two scans of the lower zones, 3 and 5 cm below the carina. Scan-

ning parameters were 1.0-mm collimation, 137 kVp, 220 mA, 1.0 second scanning time, high-resolution reconstruction algorithm. Images were photographed at window level and width appropriate for lung detail (-800, 1600 HU). Each slice was scored by two thoracic radiologists (R.J.S.L., J.M.A.v.E.), separately, for the presence of non-calcified parenchymal opacities and categorized using the same principles as the ILO system for pulmonary disease on chest radiographs (1). This approach was used previously (8). Four profusion scores were defined: 0, no abnormalities; 1, few nodules, normal lung markings visible; 2, moderate opacities, normal lung markings partially obscured; 3, numerous opacities, normal lung markings totally obscured. The profusion score was noted as follows and converted to a linear scale from 0 to 10: 0/0 = 0, 0/1 = 1, 1/0 = 2, 1/1 = 3, 1/2 = 4, 2/1 = 5, 2/2 = 6, 2/3 = 7, 3/2 = 8, 3/3 = 9, 3/4 = 10. In the profusion score the first digit represents the final score and the digit behind the slash the alternative score the observer doubted. This classification represents a continuum of change from no opacity to the most advanced category. The score of the eight lung areas - four CT slices multiplied by two lungs - was summed and a total score was calculated, which could range from zero to 80. The coal worker's pneumoconiosis score for the whole lung as well as for the upper and the lower zones of the lungs were determined by each of the two observers and these scores were averaged. Both radiologists were blinded to the chest radiograph results and the exposure history when interpreting thin-section CT's. CT scans were also scored for the presence or absence of progressive massive fibrosis or post-tuberculous scars as well as for the presence of emphysematous changes. The CT diagnosis of emphysema was based on the presence of areas of abnormally low attenuation as determined visually (26).

### *Quantitative assessment of CT scans*

The CT scans of the lungs for quantitative assessment of lung density patterns were obtained in supine position. Scanning parameters were 1.0-mm collimation, 137 kVp, 220 mA and 1.0-second scanning time. Scans were reconstructed in the standard-resolution mode. No contrast medium was injected. In order to control the level of inspiration during scanning, the patient was asked to breathe through a small handheld spirometer (Micro Medical Instruments, Rochester, England), which was connected with the CT scanner (20). At user-selected levels of inspiration air flow was interrupted mechanically by a closing valve at what time a trigger signal was generated to start the scanner. The level of inspiration was constant for the duration the CT scan was made (20). Two anatomical levels were selected from the topogram: 5 cm above and 5 cm below the level of the carina. At each level two scans at 90% and 10 % inspiratory vital capacity, respectively, were obtained. The CT data were digitally transferred for analysis to a workstation (Sun SPARCstation 1+; SUN Microsystems, Mountain View, Calif). After the parenchyma of both lungs was delineated automatically by a

density-discriminating computer program, three densitometric parameters were derived: the mean lung density, the cut-off point of the frequency distribution (Hounsfield unit number) that defines the lowest 10th percentile, and the cut-off point that defines the highest 10th percentile. Apart from nodules, the physical density of the lung in coal worker's pneumoconiosis is determined by three other components: lung tissue, blood vessels, and air. Silicotic nodules, blood vessels and airway walls are densitometrically reflected by the Hounsfield number defining the highest 10th percentile of the frequency distribution of Hounsfield numbers whereas the Hounsfield number defining the lowest 10th percentile is more likely to represent air containing tissue.

### *Statistical analysis*

Results of visual assessment of both radiologists were compared with the Spearman rank correlation coefficient. The Student *t* test with a two-tailed significance level of 0.05 was used to evaluate the intergroup differences in parameters from spirometrically controlled CT lung densitometry and pulmonary function tests. Correlations between the coal worker's pneumoconiosis score for the upper and the lower zones and quantitative lung density parameters as well as the correlation between the coal worker's pneumoconiosis score of the whole lung and cumulative dust exposure were described by the Pearson correlation coefficient. For their correlation coefficients one-tailed *p* values were calculated.

## RESULTS

Cumulative dust exposure of coal miners with a normal chest radiograph was  $84 \pm 51$  gh/m<sup>3</sup> and tended to be lower in comparison to coal miners with coal worker's pneumoconiosis ( $122 \pm 58$  gh/m<sup>3</sup>). No significant differences in pulmonary function tests were observed between coal miners with a normal chest radiograph, coal miners with a chest radiograph showing nodular opacities consistent with coal worker's pneumoconiosis and healthy volunteers (Table 1).

Visual assessment of thin-section CT scans showed a good interreader correlation for the presence of nodular infiltration ( $r = 0.80$ ,  $p < 0.0001$ ). The median coal worker's pneumoconiosis score of the whole lung of coal miners with a normal chest radiograph was 7 (range, 0-39) and of coal miners with a chest radiograph showing nodules consistent with coal worker's pneumoconiosis 22 (range, 2-51). The median coal worker's pneumoconiosis score for the upper zones of the lungs in the whole coal miners population ( $n = 46$ ) was 7 (range, 0-35.5) and for the lower zones of the lungs 5 (range, 0-20.5). Since CT images allow a better stratification of parenchymal opacities

**Table 1.** Subjects Characteristics.

Parameter	Coal miners without CWP (ILO $\leq$ 0/1) (n = 35)			Coal miners with CWP (ILO > 0/1) (n = 11)		Healthy volunteers (n = 20)	
	Mean	SD	p*	Mean	SD	Mean	SD
Age (Y)	47	8		51	5	53	12
Length (cm)	170	8		173	6	175	10
Weight (kg)	77	11		84	11	78	10
Years underground	22	3	<0.005	26	3	0	
Cig. cons. (pack years)	23	23		31	21	17	12
FEV <sub>1</sub> (% predicted)	106	16		100	15	110	18
TLC (% predicted)	101	13		97	11	100	11
DL <sub>co</sub> (% predicted)	117	22		109	38	111	19
K <sub>co</sub> (% predicted)	88	15		84	27	90	9

Note. CWP = coal worker's pneumoconiosis, ILO = International Labor Organisation, values represent mean  $\pm$  standard deviation; \* Coal miners ILO  $\leq$  0/1 versus coal miners ILO > 0/1.

than chest radiographs, a comparison of densitometric and visual assessment of pneumoconiosis should preferably rely on visual scores from the CT modality. Our study population (n=66) was therefore arbitrarily subdivided into three groups; group 1, normal thin-section CT scan (coal worker's pneumoconiosis score = 0), n = 27; group 2, mild abnormal thin-section CT suggestive of coal worker's pneumoconiosis (coal worker's pneumoconiosis score  $0 < X \leq 15$ ), n = 22; and group 3, more severe abnormal thin-section CT consistent with coal worker's pneumoconiosis (coal worker's pneumoconiosis score > 15; range, 16-52), n = 17. The median of the coal worker's pneumoconiosis score for the upper zones of the lungs of group 2 was 3.5 (range, 0-10.5) and 12 (range, 2-35.5) in group 3. The median of the coal worker's pneumoconiosis score for the lower zones of the lungs of both groups was 1 (range, 0-6.5) and 12 (range, 4-20.5) respectively. Coalescence of opacities or large opacities were not observed. Two coal miners, one with a coal worker's pneumoconiosis score of 0, and one with coal worker's pneumoconiosis of 14, showed mild changes of centriacinar emphysema at thin-section CT.

Pulmonary function tests in the 3 groups were within normal limits (Table 2). Lung function tests gradually decreased with increasing coal worker's pneumoconiosis score of the whole lung, though not significant except for K<sub>CO</sub> between group 1 and group 3 (p < 0.05).

The results of the densitometric readings in the three groups are summarized in Table 3. All three densitometric parameters increase with increasing coal worker's pneumoconiosis score. At 90% vital capacity, the mean lung density, the lowest 10th percentile

**Table 2.** Results of Pulmonary Function Tests for Study Population Subdivided According to the Coal Worker’s Pneumoconiosis Score of the Whole Lung.

CWP score	Group 1 (n = 27)		Group 2 (n = 22)		Group 3 (n = 17)		
	0		0 < X ≤ 15		> 15		
	Mean	SD	Mean	SD	Mean	SD	p*
FEV1 (% predicted)	110	15	104	16	103	18	
TLC (% predicted)	104	13	100	11	98	13	
DL <sub>CO</sub> (% predicted)	114	17	111	30	103	24	
Kco (% predicted)	90	9	92	22	81	16	<0.05

Note. CWP score = coal worker’s pneumoconiosis score, values represent mean ± standard deviation;  
\* group 3 versus group 1.

**Table 3.** Densitometric Results in the Study Population Subdivided According to the Coal Worker’s Pneumoconiosis Score of the Whole Lung at 90% and 10% Vital Capacity.

CWP score	Group 1 (n = 27)			Group 2 (n = 22)			Group 3 (n = 17)		
	0			0 < X ≤ 15			> 15		
Vital Capacity	Mean	SD	p*	Mean	SD	p†	Mean	SD	p‡
<b>Upper lung zones</b>									
Mean lung density									
- 90	-856	26		-842	17	<0.005	-803	48	<.0005
- 10	-788	49		-772	58		-751	72	
Highest 10th percentile									
- 90	-751	51		-731	31	<0.005	-671	49	<0.001
- 10	-642	74		-627	84		-593	93	
Lowest 10th percentile									
- 90	-939	35		-927	12	<0.01	-908	27	<0.05
- 10	-896	42		-883	50		-869	47	
<b>Lower lung zones HU</b>									
Mean lung density									
- 90	-844	30	<0.005	-817	23		-804	30	<0.001
- 10	-776	57		-768	59		-742	85	
Highest 10th percentile									
- 90	-693	58		-666	42		-641	58	<0.01
- 10	-569	101		-564	95		-556	85	
Lowest 10th percentile									
- 90	-948	20	<0.001	-925	17		-920	18	<0.001
- 10	-910	38		-898	30		-891	38	

Note. CWP score = coal worker’s pneumoconiosis score, values represent mean ± standard deviation and are expressed in Hounsfield units; p\* Group 1 versus group 2; p† Group 2 versus group 3; p‡ Group 3 versus group 1.

of the frequency distribution, and the highest 10th percentile were in group 1 significantly lower than in group 3 in both zones of the lungs. At 10% vital capacity no statistically significant differences between the two groups were observed. All three densitometric parameters were statistically different between the groups 2 and 3 if the measurements were performed at 90% vital capacity in the upper zones of the lungs (all  $p < 0.05$ ). In the lower zones of the lungs the mean lung density as well as the lowest 10th percentile were significantly lower in group 1 compared with the two other groups, once again only at 90% vital capacity.

The best correlations between visual assessment of thin-section CT scans and CT lung densitometry at the same anatomical level were found in the upper zones of the lungs at 90% vital capacity (Table 4). In the lower lung zones correlations were moderate but significant. the mean lung density was the densitometric parameter that correlated best with the coal worker's pneumoconiosis score ( $r = 0.76$ ,  $p < 0.001$ ;  $r = 0.53$ ,  $p < 0.001$  respectively). At 10% vital capacity correlations between results of visual assessment of thin-section CT scans and CT lung densitometry were poor. Within individual groups, the best correlations between densitometry and visual assessment were observed in coal miners with a more severe abnormal thin-section CT consistent with coal worker's pneumoconiosis at 90% vital capacity (Table 5). There was no significant correlation between CT lung densitometry and visual assessment at 10% vital capacity (all  $p > 0.05$ ).

There was a tendency to higher coal worker's pneumoconiosis score of the whole lung with increasing cumulative dust exposure. Cumulative dust exposure of coal miners with a normal thin-section CT ( $n=7$ ) was  $66 \pm 45$  gh/m<sup>3</sup> and significantly different ( $p < 0.05$ ) from cumulative dust exposure of coal miners with a more severe abnormal thin-section CT consistent with coal worker's pneumoconiosis ( $121 \pm 44$  gh/m<sup>3</sup>,  $n=17$ ). Cumulative dust exposure of coal miners with a mild abnormal thin-section CT suggestive of coal worker's pneumoconiosis ( $86 \pm 58$  gh/m<sup>3</sup>,  $n=22$ ) differed not significantly from both groups of coal miners. In the whole coal miner population, a moderate correlation was present between the coal worker's pneumoconiosis score of the whole lung and the cumulative dust exposure ( $r = 0.45$ ,  $p < 0.005$ ). However, there was no significant correlation between CT lung densitometry and cumulative dust exposure (all  $p > 0.05$ ).



**Table 4.** Correlation between Objective and Subjective Parameters of Coal Worker’s Pneumoconiosis in 46 Coal Miners at the same Anatomical Level at 90% and 10% Vital Capacity.

	Mean lung density r	Highest 10th percentile r	Lowest 10th percentile r
<b>Upper lung zones</b>			
90% vital capacity	0.76	0.71	0.69
10% vital capacity	0.38	0.31	0.27
<b>Lower lung zones</b>			
90% vital capacity	0.53	0.46	0.45
10% vital capacity	0.28	0.26	0.27

Note. All correlations are statistically significant ( $p < 0.05$ ; one tailed).

**Table 5.** Correlation between Objective and Subjective Parameters of Coal Worker’s Pneumoconiosis in Two Groups of Coal Miners with Coal Worker’s Pneumoconiosis as Assessed with Thin-Section CT at 90% Vital Capacity.

CWP score	Group 2 (n = 22) 0 < X ≤ 15		Group 3 (n = 17) > 15	
	r	p	r	p
<b>Upper zones</b>				
Mean lung density	0.32	N.S.	0.72	<0.005
Highest 10th percentile	0.35	N.S.	0.62	<0.001
Lowest 10th percentile	0.17	N.S.	0.64	<0.05
<b>Lower zones</b>				
Mean lung density	0.11	N.S.	0.65	<0.001
Highest 10th percentile	-0.01	N.S.	0.58	<0.01
Lowest 10th percentile	0.16	N.S.	0.56	<0.001

Note. CWP score = coal worker’s pneumoconiosis score, N.S. = not significant.

DISCUSSION

Our study in a coal miner population demonstrates that progression of coal workers pneumoconiosis is associated with increasing attenuation values in both lung zones and at both levels of inspiration. At 90% vital capacity (VC), good correlations between objective and subjective indicators of coal worker’s pneumoconiosis were observed in the upper zones, and moderate correlations in the lower zones of the lungs. At 10% vital capacity the correlations in both lung zones were poor. The mean lung density was the densitometric parameter which correlated best with visual assessment of thin-section CT. With increasing extent of coal worker’s pneumoconiosis, correla-

tions between CT lung densitometry and visual assessment improved considerably. No significant correlations between CT lung densitometry and visual assessment were observed in early stages of coal worker's pneumoconiosis.

At both levels of inspiration and in both zones of the lungs we found higher densitometric values with increasing extent of coal worker's pneumoconiosis. At 90% vital capacity, the densitometric parameters of subjects with a normal and a more severe abnormal thin-section CT consistent with coal worker's pneumoconiosis differed significantly in both lung zones. At 10% vital capacity a similar densitometric pattern was observed. However, at 10% vital capacity, differences between mean densitometric parameters in the three groups were less pronounced and never statistically significant. This finding is in contrast to findings observed in patients with chronic obstructive pulmonary disease (COPD) where the analysis of CT slices obtained at 10% vital capacity was an essential part in the differentiation between patients with COPD and healthy persons (27,28). Lung function impairment in patients with COPD results in air-trapping at lower lung volumes and as a consequence significant differences in density between COPD patients and healthy volunteers can be observed. No lung function impairment in coal miners and healthy volunteers was seen, nor any difference in lung function between the three subgroups arbitrarily constituted on the basis of the coal worker's pneumoconiosis score of the whole lung.

At increasing extent of coal worker's pneumoconiosis, correlations between CT lung densitometry and visual assessment of thin-section CT improved considerably. Early detection of coal worker's pneumoconiosis would be, in our opinion, the most useful clinical application of CT lung densitometry. Although visual assessment of thin-section CT is considered to be the standard of reference for the depiction of fine parenchymal opacities, it may be difficult in the early stages of coal worker's pneumoconiosis, to differentiate blood vessels on end from micronodular infiltration at thin-section CT (8). We also encountered difficulties in this group of coal miners in confident assessment of micronodules. Correlations between CT densitometry and visual assessment of thin-section CT in coal miners with a mild abnormal thin-section CT suggestive of coal worker's pneumoconiosis were poor. The present findings are consistent with previous reports showing that correlation between antemortem radiographic findings in coal worker's pneumoconiosis was substantially better for the more severe categories of disease (30,31).

On the basis of recent work we think that our scan technique and data analysis are amenable for improvements. A sliding-thin-slab maximal intensity projection technique was reported to detect more accurately mild forms of micronodular infiltration (31). Further, density measurements are strongly dependent on section thickness and reconstruction kernel. For instance, thin-section densitometry using 1-mm sections in combination with high resolution kernels was not recommended for determining CT number histogram related parameters other than average density (32). In the pres-

ent study the mean lung density was the densitometric parameter which correlated best with visual assessment of thin-section CT, but the correlation of the other two densitometric parameters might improve when density resolution is better.

CT densitometry is not likely to be able to distinguish coal worker's pneumoconiosis from most other conditions that cause increased lung density. A shift towards higher densitometric values is not uniquely due to coal worker's pneumoconiosis since also other interstitial and alveolar lung diseases (33-35), panbronchiolitis (36), and postirradiation effects (37) are manifested by similar changes in physical density. For an ultimate diagnosis of coal worker's pneumoconiosis a key position remains to be reserved for visual assessment of thin-section CT scans.

The issue of emphysema in coal miners is controversial and subject to debate in the literature. A necropsy study has shown that emphysema is more common in coal worker's pneumoconiosis than in a population of non-dust exposed controls (38). Focal emphysema is commonly found in pneumoconiosis with p-type changes and is related to dust exposure (39,40). Other authors have concluded that progressive massive fibrosis is a crucial factor in determining the presence of emphysema (41), and that in simple coal worker's pneumoconiosis, emphysema is hardly seen (9,42). If pneumoconiosis with p-type changes and emphysema are associated it is expected that with progression of both disorders, the highest 10th percentile increases, and the lowest 10th percentile of the frequency distribution decreases in attenuation. Both changes would then nullify mean lung density changes. However, all the three parameters showed comparable changes in density with progression of coal worker's pneumoconiosis.

The overall extent of coal worker's pneumoconiosis in the lung, visually assessed at thin-section CT was found to be related to exposure to respirable dust. There was no significant correlation between cumulative dust exposure and the various densitometric parameters at both levels of inspiration. A possible explanation for this difference is the fact that the visual coal worker's pneumoconiosis score is based on the sum of the results of four CT slices whereas our densitometric results are based on the analysis of one CT slice only, which could give rise to sample error and statistically less robust estimates. A spiral volumetric CT technique would enable anatomically contiguous scanning and analysis of scans of the whole lung will probably more reliably reproduce coal worker's pneumoconiosis changes in the lung than the data of one single CT slice.

Longitudinal studies have demonstrated a significant negative relation between cumulative dust exposure and forced expiratory volume in one second ( $FEV_1$ ) (43-45). Loss of  $FEV_1$  is independent of the presence of pneumoconiosis (43,44). In our study  $FEV_1$  and  $K_{CO}$  values tended to decrease with cumulative dust exposure and mean coal worker's pneumoconiosis scores. However, all values are still normal and  $FEV_1$  differences were not statistically significant, probably due to the relatively small study population and the relatively low cumulative dust exposure as well.  $K_{CO}$  was the

only pulmonary function test which was, although in the normal range, significantly lower in workers with a more severely abnormal thin-section CT consistent with coal worker's pneumoconiosis than in subjects with a normal thin-section CT.

In conclusion, for the diagnosis of coal worker's pneumoconiosis, a history of extensive coal dust exposure, clinical and functional findings as well as nodular opacities assessed at chest radiography are required. CT scans obtained at 90% VC in the upper zones of the lungs are the best candidates for lung densitometric measurements in coal worker's pneumoconiosis. CT lung densitometry correlates well with visual assessment of thin-section CT of the lung provided that CT slices are obtained at 90% vital capacity. Further improvements of the technique are possible. Numbers of participating coal miners in this study were relatively small and further prospective studies need to be performed to assess the diagnostic accuracy and role of CT densitometry in coal worker's pneumoconiosis.

## REFERENCES

1. International Labour Office (1980). Guidelines for the use of ILO international classification of radiographs of pneumoconiosis, rev ed. International Labour Office Occupational and Health safety No. 22 (REV 1980) Geneva: International Labour Office
2. Rockoff SD, Schwartz A. Roentgenographic underestimation of early asbestosis by International Organization Classification. *Chest* 1988; 93:1088-1099.
3. Vallyathan V, Brower PS, Green FHY, Attfield MD. Radiographic and pathologic correlation of coal worker's pneumoconiosis. *Am J Respir Crit Care Med* 1996; 154: 741-748.
4. Nakata H, Kimoto T, Nakayama T, Kido M, Miyazaki N, Harada S. Diffuse peripheral lung disease: evaluation of high resolution computed tomography. *Radiology* 1985; 157:181-185.
5. Müller NL, Miller RR, Webb WR, Evans KG, Ostrow DN. Fibrosing alveolitis: CT- pathologic correlation. *Radiology* 1986; 160:585-588.
6. Mathieson JR, Mayo JR, Staples CA, Müller NL. Chronic diffuse infiltrative lung disease: comparison of diagnostic accuracy of CT and chest radiography. *Radiology* 1989; 171:111-116.
7. Staples CA, Gamsu G, Sue Ray C, Webb RW. High resolution computed tomography and lung function in asbestos-exposed workers with normal chest radiographs. *Am Rev Respir Dis* 1989; 139:1502-1508.
8. Remy-Jardin M, Degreiff JM, Beuscart R, Voisin C, Remy J. Coal worker's pneumoconiosis: CT assessment in exposed workers and correlation with radiographic findings. *Radiology* 1990; 177:363-371.
9. Bégin R, Ostiguy G, Fillion R, Colman N. Computed tomography scan in the early detection of silicosis. *Am Rev Respir Dis* 1991; 144:697-705.
10. Levi C, Gray JE, McCullough EC, Hattery RR. Variability of CT numbers as absolute values. *AJR* 1982; 139:443-447.
11. Zerhouni EA, Spivey JF, Morgan RH, Leo FP, Stitik FP, Siegelman SS. Factors influencing quantitative CT measurements of solitary pulmonary nodules. *J Comput Assist Tomogr* 1982; 6:1075-1087.
12. McCullough EC, Morin RL. CT-number variability in thoracic geometry. *AJR* 1982; 141:135-140.
13. Kemerink GJ, Lamers RJS, Thelissen GPR, van Engelshoven JMA. Scanner conformity in CT densitometry of the lungs. *Radiology* 1995; 197:749-752.

14. Kemerink GJ, Lamers RJS, Thelissen GRP, van Engelshoven JMA. CT-densitometry of the lungs: scanner performance. *J Comput Assist Tomogr* 1996; 20:24-33.
15. Müller NL, Staples CA, Miller RR, Abboud RT. "Density Mask": an objective method to quantitate emphysema using computed tomography. *Chest* 1988; 94:782-787.
16. Gould GA, MacNee W, McLean A, et al. CT density measurements of lung density in life can quantitate distal airspace enlargement: an essential defining feature of human emphysema. *Am Rev Respir Dis* 1988; 137:380-392.
17. Gevenois PA, de Martelaer V, De Vuyst P, Zanen J, Yernault JC. Comparison of computed density and macroscopic morphometry in pulmonary emphysema. *Am J Respir Crit Care Med* 1995; 151:653-657.
18. Hartley PG, Galvin JR, Hunninghake GW, et al. High-resolution CT derived measures of lung density are valid indexes of interstitial lung disease. *J Appl Physiol* 1994; 76:271-272.
19. Beinert T, Behr J, Mehnert F, et al. Spirometrically controlled quantitative CT for assessing diffuse parenchymal lung disease. *J Comput Assist Tomogr* 1995; 19:924-931.
20. Kalender WA, Rienmüller R, Seissler W, Behr J, Welke M, Fichte H. Measurement of pulmonary parenchymal attenuation: use of spirometric gating with quantitative CT. *Radiology* 1990; 175:265-268.
21. Schins RPF, Borm PJA. Epidemiological evaluation of monocyte-a release as an exposure marker in pneumoconiosis: a five year follow up study among coal workers. *Occup Environ Med* 1995; 52:441-450.
22. Rienmüller RK, Behr J, Kalender WA, et al. Standardized quantitative high resolution CT in lung disease. *J Comput Assist Tomogr* 1991; 15:742-749.
23. Borm PJA, Palmen N, Engelen JJM, Buurman WA. Spontaneous and stimulated release of tumor necrosis factor (TNF)- $\alpha$  from blood monocytes of miners with coal workers' pneumoconiosis. *Am Rev Respir Dis* 1988; 138:1589-1594.
24. Engelen JJM, Borm PJA, van Sprundel M, Lenaerts L. Blood-anti-oxidant parameters at different stages of pneumoconiosis. *Env Health Persp* 1990; 84:165-172.
25. Quanjer PH. Standardized lung function testing. *Bull Eur Physiopathol Respir* 1983; 19:7-44.
26. Foster WL, Pratt PC, Roggli VL, Godwin JD, Halvorsen RA, Putman CE. Centrilobular emphysema: CT-pathologic correlation. *Radiology* 1986; 159:835-837.
27. Lamers RJS, Thelissen GRP, Kessels AG, Wouters EFM, van Engelshoven JMA. Chronic obstructive pulmonary disease: evaluation with spirometrically controlled CT lung densitometry. *Radiology* 1994; 193:109-113.
28. Gevenois PA, De Vuyst P, Sy M, et al. Pulmonary emphysema: quantitative CT during expiration. *Radiology* 1996; 199:825-829.
29. Caplan A. Correlation of radiological category with lung pathology in coal workers' pneumoconiosis. *Br J Radiol* 1961; 19:171-179.
30. Fernie JM, Ruckley VA. Coalworkers' pneumoconiosis: correlation between opacity profusion and number and type of dust lesions with special reference to opacity type. *Br J Ind Med* 1987; 44:273-277.
31. Remy-Jardin M, Remy J, Artaud D, Deschildre F, Duhamel A. Diffuse infiltrative lung disease: clinical value of sliding-thin-slab maximum intensity projections CT scans in the detection of mild micronodular patterns. *Radiology* 1996; 200:333-339.
32. Kemerink GJ, Kruize HH, Lamers RJS, van Engelshoven JMA. Density resolution in quantitative computed tomography of foam and lung. *Med Phys* 1996; 23:1697-1708.
33. Gilman MJ, Laurens RG, Somogyi JW, Honig EG. CT attenuation values of lung density in sarcoidosis. *J Comput Assist Tomogr* 1983; 7:407-410.
34. Bellamy EA, Nicholas D, Husband JE. Quantitative assessment of lung damage due to bleomycin using computed tomography. *Br J Radiol* 1987; 60:1205-1209.
35. Hedlund LW, Effman EL, Bates WM, Beck JW, Goulding PL, Putman CE. Pulmonary edema: a CT study of regional changes in lung density following oleic acid injury. *J Comput Assist Tomogr* 1982; 6:939-946.

36. Maruta K, Itoh H, Senda M, et al. Stratified impairment of pulmonary ventilation in 'diffuse panbronchiolitis': PET and CT studies. *J Comput Assist Tomogr* 1989; 13:48-53.
37. Van Dyk J, Hill RP. Post-irradiation lung density changes as measured by computerized tomography. *Int J Radiat Oncol Biol Phys* 1983; 9:847-852.
38. Cockcroft A, Wagner JC, Ryder R, Seal RME, Lyons JP, Andersson A. Post-mortem studies of emphysema in coal workers and non-coal workers. *Lancet* 1982; ii: 600-603.
39. Leigh J, Outhred KG, McKenzie HI, Glick M, Wiles AN. Quantified pathology of emphysema, pneumoconiosis, and chronic bronchitis in coal workers. *Br J Ind Med* 1983; 40:258-263.
40. Akira M, Higashihara T, Yokoyama K, et al. Radiographic type p pneumoconiosis: high-resolution CT. *Radiology* 1989; 171: 117-123.
41. Ruckley VA, Gauld SJ, Chapman JS. Emphysema and dust exposure in a group of coal workers. *Am Rev Respir Dis* 1984; 129:528-532.
42. Kinsella M, Müller N, Vedal S, Staples C, Abboud RT, Chan-Yeung M. Emphysema in silicosis: a comparison of smokers with nonsmokers using pulmonary function testing and computed tomography. *Am Rev Respir Dis* 1990; 141:1497-1500.
43. Soutar CA, Hurley JF. Relation between dust exposure and lung function in miners and ex-miners. *Br J Ind Med* 1996; 43:307-320.
44. Attfield MD, Hodous TK. Pulmonary function of U.S. coal miners related to dust exposure estimates. *Am Rev Respir Dis* 1992; 145:605-609.
45. Oxman AD, Muir DCF, Shannon HS, Stock SR, Hnizdo E, Lange HJ. Occupational dust exposure and chronic obstructive pulmonary disease: a systematic overview of the evidence. *Am Rev Respir Dis* 1993; 148:38-48.



## CHAPTER 10

---

# Summary and conclusions

Since its introduction, computed tomography (CT) densitometry has been promoted as a useful method for determining the regional and global density of the lung. The X-ray attenuation of soft tissue as measured by CT has a linear relationship to the soft tissue density ( $\text{g}/\text{cm}^3$ ) and therefore densitometry of the lungs has the potential to provide non-invasively objective information about lung density, its spatial distribution and its changes over time. The aim of this thesis is to determine the inter- and intrascanner conformity of various CT scanners for lung densitometry purposes, to standardize the technique of post-processing and to determine the reproducibility of this method in a clinical setting. Furthermore we applied CT lung densitometry to clinical studies of chronic obstructive pulmonary disease (COPD) and silicosis pulmonum.

**Chapter 2** gives a brief overview of several aspects of chronic obstructive pulmonary disease (COPD): definition, pathologic characterization, clinical features, pulmonary function tests, and radiological diagnosis. COPD severity can be staged on the basis of the degree of airflow obstruction. The test is not suitable to distinguish between chronic bronchitis and emphysema. Disturbance of gas exchange manifested by reduced single-breath carbon monoxide diffusing capacity ( $\text{DL}_{\text{CO}}$ ), have been proposed as the most accurate and specific pulmonary function tests for pulmonary emphysema. High resolution CT (HRCT) has also proven to be an accurate noninvasive technique to diagnose emphysema in vivo, and high correlations between visual CT emphysema scores and pathological grades have been reported (0.57 - 0.91).

Comparison of densitometric results obtained on different scanners has proved difficult for various reasons. Most CT scanners were not optimized for low-attenuation studies and nearly all densitometric studies published so far were deficient in their attention to analysis protocols and applied methodology. An additional problem is the influence of level of inspiration on lung density. Changes by more than a factor of two between full inspiration and expiration are possible. Therefore, control of the level of inspiration is mandatory to obtain reproducible results. Another problem is that the numeric analysis of CT data of lung tissue is operator dependent and very time consuming. Support by an automatic evaluation method is necessary to achieve high precision and to reduce operator's influence.



We assessed the performance of our CT scanner at air density. It proved to have a stability within 1 HU and a reproducibility for density of lung tissue within 2-3%. Additionally we implemented a spirometric CT triggering technique, as described by Kalender and coworkers, to get the possibility to scan at defined levels of inspiration. To ensure reproducibility and objectivity, an automatic evaluation procedure for CT densitometry of the lungs has been developed. This computer program, using a segmentation threshold in a contour tracking algorithm, isolates both lungs automatically after which all relevant CT parameters are calculated.

**Chapter 3** gives an overview of the literature of CT densitometry of the lungs and describes the CT protocol, the technique of respiratory gating of the CT scanner and dosimetrical aspects.

In **chapter 4** the issue of conformity between the various scanners on the market is addressed. A systematic comparison of lung densitometry as calculated with six CT scanners was performed; GE Highlight, Picker PQ-2000, Philips scanners SR 7000 and LX, and two Siemens Somatom Plus systems. All CT scanners had an acceptable calibration of water density. The scanners were well designed with respect to CT number sensitivity to reconstruction filter, zoom factor, table height and slice thickness, with the exception of the two Philips systems in regard to sensitivity to slice thickness. CT numbers from the GE Highlight and Picker PQ-2000 scanner showed some sensitivity to phantom size and composition. The Siemens Somatom Plus systems were well calibrated and not very sensitive to phantom size or composition. After correcting for poor air calibration the conformity of all scanners in the low density range was fair: at a density of about  $100 \text{ kg/m}^3$  the standard deviation of the average over all scanners is less than 3 HU, and the maximum observed inter-scanner difference is 7 HU.

In **chapter 5** a contribution is given to optimize the method of image analysis. An image analysis program uses a segmentation threshold which discriminates soft tissue from lung by fast contour tracking. In addition, outer pixels that are still affected by the thoracic wall or larger vessels are excluded by shrinking the contour to obtain truly lung parenchyma related data. This process is called 'erosion'. Subsequently, CT number histograms of both lungs are determined and the densitometric parameters are calculated automatically. Changing segmentation threshold and number of erosions affect strongly the number of pixels that belong to the high density part of the CT number histogram of the lung.

Most previous authors paid little attention to the analysis protocol and were not aware of the large differences in densitometric parameters which are introduced by changing segmentation threshold and numbers of erosions. The segmentation procedure is usually poorly described and often there is no mention whether erosions have been applied. A low threshold is well suited for segmentation along thin septa but a too low threshold can lead to exclusion of parts of the lungs. For comparability of results, the same evaluation protocols should be applied. From our experiments it was con-

cluded that for densitometry a segmentation threshold of -400 HU combined with two erosions should be applied. For volumetry, the same threshold combined with zero erosions should be adequate.

In **chapter 6** the reproducibility of spirometrically controlled CT lung densitometry at defined levels of inspiration in a clinical setting was assessed. CT sections were obtained on two separate days from 20 hospitalized patients. Various lung density parameters, reflecting the shape of the CT number histogram were calculated and results of corresponding CT sections were compared. The most reproducible CT lung density measurements were obtained at 90% vital capacity. At this level of inspiration, reproducibility was of the order of 3-14 HU. At 10% vital capacity, however, reproducibility was worse by a factor of three. If CT scans at residual volume are used for diagnosis and follow-up, respiratory control is mandatory. Reproducibility of lung density measurements was not influenced by severe respiratory insufficiency.

In **chapter 7** CT lung densitometry results at defined levels of inspiration from 3 groups of 20 individuals each were compared: a group consisting of patients who fulfilled the functional criteria of emphysema; a group who met the clinical and functional criteria of chronic bronchitis, and a group of persons who had no pulmonary symptoms and normal results of lung function tests. This study confirmed the value of spirometrically controlled CT densitometry in the quantitative assessment of lung density at selected levels of inspiration. Three densitometric parameters, namely mean lung density, percentage of pixels in the -910 to -1024 HU range (pixel index), and the cut-off point that defines the lowest 10th percentile of the frequency distribution of HU numbers, were compared. Regardless of the level of inspiration, significant differences were found between patients who had emphysema, healthy persons and patients who had chronic bronchitis. Differences between healthy subjects and patients with chronic bronchitis were only significant at 10% vital capacity. On the basis of these results, we concluded that two sections obtained at the same level - one at 90% vital capacity and one at 10% vital capacity - are sufficient for the classification of subjects into one of the three groups.

In **chapter 8** we assessed the association of emphysema with airflow limitation in patients with advanced COPD, and studied the point of debate whether  $DL_{CO}$  can be used as an indicator for emphysema in advanced COPD. In a study of 100 patients with COPD we used high resolution CT of the lungs in combination with CT lung densitometry, as the gold standard for the diagnosis of emphysema and for assessment of its severity. Using a visual grading method, CT-scored significant emphysema was found mainly in patients with stage II or stage III COPD ( $FEV_1 < 50\%$  predicted). Lung density measurements confirmed visual observations. With progression of airflow limitation, the lung density in patients with COPD obtained at 90% vital capacity and at 10% vital capacity decreased as expected. Results suggest a distinct presence of emphysema in patients with advanced COPD. The  $DL_{CO}$  proved to be a useful test to

separate emphysema from chronic bronchitis types of COPD. The vast majority of patients with COPD (93%) and a  $DL_{CO}$  % predicted of less than 50 % showed emphysematous changes at CT, and 56 % of these patients suffered from significant emphysema. In contrast with this, only 23 % of patients with COPD and  $DL_{CO}$  % predicted of equal to or more than 50 showed emphysema on CT, and only a small minority of patients (4%) showed significant emphysematous parenchymal changes on CT. We found a good correlation between  $DL_{CO}$  and the severity of emphysema independent of the degree of airflow limitation. However in patients with  $DL_{CO}$  less than 50 % predicted, the correlation between  $DL_{CO}$  and the severity of emphysema was poor.  $DL_{CO}$  measurements cannot be relied on for quantitative assessment of severity and extent of emphysema, but  $DL_{CO}$  measurements are valuable for selection of patients for radiologic emphysema assessment.

The usefulness of CT lung densitometry in the assessment of interstitial lung disease was investigated in **chapter 9**. Thin-section CT scans were obtained of a group of 66 persons consisting of 35 coal miners with a normal chest radiograph, 11 coal miners with a chest radiograph showing nodular opacities consistent with coal worker's pneumoconiosis, and 20 healthy volunteers. All scans were visually assessed for the presence and extent of coal worker's pneumoconiosis. In addition, spirometrically gated CT sections of the upper and the lower zones of the lungs were obtained at 90% and 10% vital capacity. Based on results of visual assessment, subjects were divided into three subsets. Densitometric parameters of coal worker's pneumoconiosis obtained from the three groups were compared and correlated with results of visual assessment of CT scans. Progression of coal worker's pneumoconiosis was associated with increasing attenuation values in both lung zones and at both levels of inspiration. Densitometric parameters between groups differed significantly only in the upper zones at 90% vital capacity. CT densitometry correlated well with visual assessment of thin-section CT of the lung provided that the CT sections were obtained at 90% vital capacity. At 10% vital capacity correlations were always poor. CT scans obtained at 90% vital capacity in the upper zones of the lungs are the best candidates for lung densitometric measurements in coal worker's pneumoconiosis.

### *In conclusion*

Modern CT scanners that are properly calibrated are well suited for densitometric studies of the lung, but to attain generally comparable results the same scan and analysis protocols should be applied. For the study of the lungs at intermediate levels of inspiration, gated triggering of the CT scanner is required. Reproducibility of densitometric results using this technique was shown to be satisfactory. Densitometry proved to be useful in the assessment of pulmonary emphysema and might also be helpful in the diagnosis and follow-up of interstitial lung disease

### *Future developments*

The development of very fast volume scanning makes possible the investigation of the whole lung within a single breath-hold period. Using this technique it is likely that total lung mass *in vivo* can be determined much more accurately than was previously possible. With suitable software for the analysis of the large datasets obtained, volume scanning might then find application in the field of lung volume reduction surgery and in longitudinal studies of various forms of lung disease.

Surgical resection of nonfunctioning areas of lung tissue - lung volume reduction surgery- is emerging as a promising option for the treatment of selected patients with severe debilitating emphysema. Volumetric CT densitometry may be helpful in selecting candidates who will benefit from lung volume reduction surgery. From a surgical point of view, assessment of the relative severity and location of emphysematous lung may be useful so that the most emphysematous section of the lung can be removed. In conjunction with clinical findings and pulmonary function tests, these densitometric data will improve our understanding of the full mechanisms responsible for the improvement after lung volume reduction surgery as well as of the long-term outcome.

CT can be used to quantify the progression of the pathology in emphysema. Longitudinal studies of lung mass might be very rewarding if combined with metabolic studies. There is a growing interest in the relationship between the nutritional status and lung structure. Food deprivation alters the architecture of terminal air spaces in a manner similar to that which occurs in emphysema. Studies mainly performed in animals have repeatedly shown that lung weight is decreased in starvation. A substantial number of patients suffering from COPD also experience gradual and significant weight loss during the course of their illness yet the potential effect on lung weight is unknown. The significance of *in vivo* determination of lung density could be of particular interest from the point of view of understanding the pathophysiology of starvation-induced changes in pulmonary structure, but also to evaluate the effectiveness of therapeutic strategies to improve nutritional status.



## Samenvatting

Al sedert de introductie van computertomografie (CT) is densitometrie gebruikt om op niet-invasieve wijze de regionale en gemiddelde dichtheid van de longen te bepalen. CT densitometrie is gebaseerd op het feit dat de door de CT scanner in wekdelen gemeten verzwakking van de röntgenbundel een lineaire relatie kent met de dichtheid ( $\text{g/cm}^3$ ). De techniek biedt de mogelijkheid om objectieve informatie te verschaffen omtrent de dichtheid van de longen en eventuele veranderingen daarin.

Doelen van dit proefschrift zijn: het vergelijken van de prestaties van verschillende CT scanners op het gebied van longdensitometrie, het bepalen van de variabiliteit van één en dezelfde scanner, het leveren van een bijdrage aan de standaardisering van zowel de scantechniek als de post-processing van CT beelden, het bepalen van de reproduceerbaarheid van spirometrisch gecontroleerde longdichtheidsmetingen in de dagelijkse praktijk, en tenslotte het toepassen van spirometrisch gecontroleerde CT triggering in enkele pulmonologische klinische studies.

In **hoofdstuk 2** worden verscheidene aspecten van chronisch obstructief longlijden (COPD) belicht: definities, pathologische karakterisering, klinisch beeld, longfunctieonderzoek en radiologisch onderzoek. Een sterk verlaagde expiratiesnelheid is een spirometrisch ventilatoire bevinding wijzend op bronchusobstructie, terwijl de diffusiecapaciteit van koolmonoxyde ( $\text{DL}_{\text{CO}}$ ) meer specifieke informatie geeft omtrent het al dan niet aanwezig zijn van emfyseem.

Hoge resolutie CT wordt als de meest betrouwbare onderzoeksmethode beschouwd om emfyseem op een niet-invasieve manier in vivo te diagnostiseren en te kwantificeren. Correlaties tussen visuele CT emfyseemscores en pathologische emfyseemscores liggen in de orde van grootte van 0.57 tot 0.91.

In het verleden is vergelijking van densitometrische resultaten, verkregen met verschillende CT scanners, om verschillende redenen niet mogelijk gebleken. De meetresultaten van veel CT scanners bleken in lage-dichtheidstudies onvoldoende nauwkeurig en daarnaast werd in vrijwel alle tot op heden gepubliceerde CT densitometrische studies geen aandacht geschonken aan acquisitie- en analyseprotocollen. Een ander belangrijk probleem was de invloed van de mate van inspiratie op de longdichtheid: veranderingen in de orde van grootte van een factor 2 tussen inspiratie en expiratie zijn mogelijk. Controle van het inspiratieniveau tijdens het scannen is dus een eerste vereiste voor reproduceerbaarheid van metingen. Ook was de handmatig

uitgevoerde analyse van de CT data afhankelijk van de onderzoeker. Bovendien was deze analyse zeer tijdrovend. Automatische evaluatieprogrammatuur lijkt noodzakelijk om binnen acceptabele tijd een hoge mate van precisie te bereiken en om de invloed van de onderzoeker op het uiteindelijke meetresultaat te elimineren.

We hebben de prestaties van onze CT scanner ten aanzien van luchtdichtheidsmetingen bepaald. Het systeem bleek correcte resultaten te leveren (CT-waarde:  $1000 \pm 1$  Hounsfield Unit, HU) en toonde over een periode van meer dan een jaar een verloop van hooguit 1 HU. De reproduceerbaarheid van metingen aan longweefsel lag in de orde van 2 tot 3 %.

Daarnaast hebben wij een door Kalender en medewerkers beschreven spirometrische 'triggering techniek' geïmplementeerd, teneinde de mogelijkheid te verkrijgen om op vooraf in te stellen inspiratieniveaus te scannen.

Om objectiviteit van de analyse van CT data te waarborgen werd speciale, in hoge mate geautomatiseerde evaluatieprogrammatuur ontwikkeld ten behoeve van CT longdensitometrie. Deze programmatuur maakt gebruik van een algoritme dat automatisch de longwand zoekt, en deze op een in te stellen CT waarde (de segmentatiedrempel) volgt zodat het longparenchym van het andere thoraxweefsel gescheiden wordt. Na deze automatische segmentering, die met de hand nog gecorrigeerd kan worden, worden alle relevante densitometrische parameters berekend.

In **hoofdstuk 3** wordt een kort literatuuroverzicht gegeven inzake CT longdensitometrie, gevolgd door een beschrijving van het scan protocol, de spirometrische 'CT triggering techniek' en de wijze waarop de analyse van CT data geschiedt. Tenslotte komen dosimetrische aspecten van het gebruikte CT scanprotocol aan de orde.

In **hoofdstuk 4** worden de densitometrische prestaties van een zestal CT scanners vergeleken. In het onderzoek zijn betrokken: GE Highlight, Picker PQ-2000, de Philips scanners SR 7000 en LX, en 2 Siemens Somatom Plus systemen. Alle CT scanners toonden een acceptabele kalibratie voor water, terwijl de kalibratie voor lucht voor sommige scanners enigszins te wensen overliet. De scanners konden de toets der kritiek wat betreft de gevoeligheid voor reconstructiefilter, vergrotingsfactor, tafelhoogte en snededikte goed doorstaan, met uitzondering van de twee Philips systemen die een grote gevoeligheid voor coupedikte aan de dag legden. De CT-waarden van de GE Highlight en Picker PQ-2000 scanner bleken enigszins gevoelig voor fantoomgrootte en -samenstelling. Na correctie van de luchtkalibratie waren de meetresultaten van de diverse scanners vergelijkbaar. Voor dichtheden rond  $0.1 \text{ g/cm}^3$  bedroeg de standaarddeviatie van de resultaten van alle scanners minder dan 3 HU, terwijl het maximale gemeten verschil tussen twee scanners 7 HU bedroeg.

In **hoofdstuk 5** wordt een bijdrage geleverd aan de optimalisatie van de analysemethodieken van CT data. Er is een computerprogramma ontwikkeld waarin een segmentatiedrempel kan worden ingesteld die in een contourdetectiealgoritme wordt gebruikt om longparenchym te scheiden van het de longen omhullende wekeweefsel.

Na segmentatie kunnen de buitenste pixels, die mogelijk nog beïnvloed zijn door de thoraxwand of de grote vaten, geëxcludeerd worden om data te verkrijgen die louter met longparenchym gerelateerd zijn. Het excluseren van de buitenste pixels, dus het 'krimpen' van de contour, heet erosie. Vervolgens worden automatisch CT-waarden histogrammen van beide longen berekend, en hieruit alle gewenste densitometrische parameters.

Veranderingen in segmentatiedrempel en aantal erosies beïnvloeden wezenlijk het aantal pixels dat behoort tot het hoge-dichtheidsdeel van het CT-waarden histogram. In het verleden hebben de meeste auteurs aan analyseprotocollen weinig aandacht geschonken. De segmentatieprocedure is gewoonlijk slecht beschreven en vaak wordt zelfs niet vermeld of, dan wel hoeveel, erosies er zijn toegepast. Een lage segmentatiedrempel is weliswaar geschikt om nog succesvol langs dunne septae te segmenteren, maar een te lage segmentatiedrempel kan resulteren in uitsluiting van longparenchym. Om vergelijkbare resultaten te verkrijgen dienen dezelfde acquisitie- en evaluatieprotocollen te worden toegepast. Uit onze experimenten kan worden geconcludeerd dat voor longdensitometrie een segmentatiedrempel van -400 HU, gecombineerd met 2 erosies, meestal optimaal is. Voor volumetrie is dezelfde segmentatiedrempel, maar nu gecombineerd met nul erosies, het meest geschikt.

In **hoofdstuk 6** wordt bestudeerd hoe het met de reproduceerbaarheid van spirometrisch gecontroleerde CT densitometrie gesteld is in de dagelijkse praktijk. Op twee opeenvolgende dagen werden op twee spirometrisch gecontroleerde inspiratieniveaus (90% en 10% van de inspiratoire vitale capaciteit) bij 20 gehospitaliseerde patiënten CT opnames gemaakt van zowel de boven- als de ondervelden van de long. Densitometrische parameters, die de vorm van het CT-waarden histogram reflecteerden, werden berekend en vergeleken voor corresponderende CT coupes. De meetresultaten verkregen op 90% van de vitale capaciteit bleken het beste reproduceerbaar te zijn, met gevonden verschillen in de orde van grootte van 3-14 HU. De reproduceerbaarheid was een factor 3 slechter indien werd gescand op 10% van de vitale capaciteit. Geconcludeerd werd, dat als CT scans op residuaal volume nodig zijn voor diagnostiek of het vervolgen van respiratoire aandoeningen, deze onder spirometrische controle uitgevoerd dienen te worden. De reproduceerbaarheid van longdichtheidsmetingen bleek niet te worden beïnvloed door de ernst van de respiratoire insufficiëntie van patiënten.

In **hoofdstuk 7** werden densitometrische meetresultaten vergeleken afkomstig van 3 groepen personen, waarbij elke groep bestond uit 20 individuen. Eén groep was samengesteld uit patiënten die voldeden aan de functionele criteria van emfyseem, de tweede groep uit patiënten die voldeden aan de klinische en functionele criteria van chronische bronchitis, en de derde groep uit personen zonder pulmonale symptomen en met een normaal longfunctieonderzoek. De CT scans werden wederom spirometrisch getriggerd op 90% en 10% van de inspiratoire vitale capaciteit in zowel de



boven- als de ondervelden. Deze studie bevestigde de waarde van spirometrisch gecontroleerde CT densitometrie in de kwantitatieve vaststelling van longdichtheid op vastgestelde inspiratieniveaus. Ongeacht het niveau van inspiratie werden significante verschillen in dichtheid gevonden tussen patiënten met emfyseem enerzijds, en patiënten met chronische bronchitis en gezonde personen anderzijds. De longdichtheid van gezonde personen en patiënten met chronische bronchitis verschilde alleen significant op 10% van de vitale capaciteit. De gemiddelde veranderingen in densitometrische parameters tussen 90 en 10% vitale capaciteit waren bij gezonde personen aanzienlijk groter dan bij patiënten met COPD. Op basis van deze resultaten hebben wij geconcludeerd dat het goed mogelijk is om op basis van de meetresultaten van twee op het zelfde scanniveau verkregen CT sneden, één op 90% en één op 10% van de vitale capaciteit, personen in te delen bij één van deze 3 groepen.

In **hoofdstuk 8** werd bij een groep van 100 patiënten met COPD onderzocht of emfyseem geassocieerd is met luchtwegobstructie. Daarnaast werd nagegaan of  $DL_{CO}$  metingen gebruikt kunnen worden als indicator voor emfyseem. De mate van emfyseem werd met behulp van hoge-resolutie CT en een visueel graderingssysteem vastgesteld. De resultaten suggereerden een uitgesproken aanwezigheid van emfyseem in patiënten met gevorderd COPD. Significante emfyseem werd voornamelijk aangetroffen bij patiënten met stadium II of III COPD ( $FEV_1$  kleiner dan 50 % van de gemiddelde normale waarde). Visuele observaties werden door longdichtheidsmetingen bevestigd. De dichtheid van de longen nam met progressie van luchtwegobstructie significant af, zowel in scans op 90% als 10% van de inspiratoire vitale capaciteit.

$DL_{CO}$  bleek bij patiënten met COPD een nuttige longfunctietest te zijn om emfyseem te onderscheiden van chronische bronchitis. De overgrote meerderheid van patiënten met COPD (93%) en een  $DL_{CO}$  kleiner dan 50% van de gemiddelde normale waarde, *toonde emfysemateuze veranderingen op CT, en 56% van deze patiënten leden aan ernstig emfyseem*. Daarentegen vertoonden slechts 23 % van de patiënten met COPD, en een  $DL_{CO}$  groter of gelijk dan 50% van de gemiddelde normale waarde, emfysemateuze veranderingen, waarvan bij een kleine minderheid (4%) ernstige emfysemateuze veranderingen werden vastgesteld. Er bestond een goede correlatie tussen  $DL_{CO}$  en de ernst van emfyseem, onafhankelijk van de mate van luchtwegobstructie. Daarentegen werd bij patiënten met een  $DL_{CO}$  kleiner dan 50% van de gemiddelde normale waarde geen verband aangetoond tussen  $DL_{CO}$  en de ernst van emfyseem.  $DL_{CO}$  metingen zijn dus nuttig om emfyseem bij patiënten met COPD vast te stellen, maar voor emfyseemkwantificering zijn ze niet geschikt. Het is aan te bevelen om bij patiënten met  $DL_{CO}$  waarden kleiner dan 50 % van de gemiddelde normale waarde de ernst van emfyseem vast te stellen met aanvullende HRCT.

Het nut van CT densitometrie bij de vaststelling van interstitiële longziekten, waarvan stoflongen er één is, was onderwerp van studie in **hoofdstuk 9**. Van een groep van 66 personen, bestaande uit 35 mijnwerkers met een normale thoraxfoto, 11 mijnwer-

kers met een thoraxfoto die nodulaire afwijkingen vertoonde wijzend op stoflongen, en 20 gezonde vrijwilligers werden 5 hoge-resolutie CT scans gemaakt. Alle scans werden visueel beoordeeld op de aanwezigheid en uitgebreidheid van interstitiële noduli. Vervolgens werden van iedere persoon spirometrisch gecontroleerde CT sneden van de boven- en de ondervelden gemaakt op respectievelijk 90% en 10 % van de inspiratoire vitale capaciteit. Gebaseerd op de resultaten van de visuele beoordeling werden de personen naar ernst onderverdeeld in drie groepen. De densitometrische parameters van de groepen werden onderling vergeleken en op correlatie met de visuele beoordelingsresultaten onderzocht. Progressie van stoflongen ging op beide inspiratieniveaus gepaard met hogere dichtheidswaarden in zowel boven- als ondervelden. De densitometrische parameters van de groepen verschilden alleen significant op 90 % van de vitale capaciteit. CT longdensitometrie correleerde goed met de visuele score, wederom alleen op 90 % van de vitale capaciteit. CT sneden van de bovenvelden van de long zijn het meest geschikt ter vaststelling van stoflongen.

### *Conclusie*

De huidige CT scanners zijn, mits goed gekalibreerd, uitermate geschikt voor densitometrische studies van de long. Echter, om algemeen vergelijkbare resultaten te verkrijgen is het van groot belang eenzelfde scan- en analyse protocol te hanteren. Voor densitometrisch onderzoek van de long op intermediaire inspiratieniveaus is spirometrische controle een vereiste. CT densitometrie kan nuttig zijn voor de diagnostisering, kwantificatie en het vervolgen van emfyseem en interstitiële longziekten.

### *Toekomstige ontwikkelingen*

De ontwikkeling van snelle volumescanning maakt het mogelijk gedurende één periode van ademinhouden de gehele thorax te scannen. Gebruik makend van deze techniek kan men het longvolume en de longmassa bepalen met een nauwkeurigheid die veel groter is dan in het verleden haalbaar was. Met geschikte software voor de analyse van de zo verkregen omvangrijke datasets kan volumescanning wellicht van nut zijn in het kader van volumereductiechirurgie en longitudinale studies van verscheidene vormen van longziekten.

Resectie van niet functionerende gebieden van longweefsel - volumereductiechirurgie - is inmiddels uitgegroeid tot een veelbelovende therapie voor een kleine groep van geselecteerde patiënten met ernstig invaliderend emfyseem. Volumetrische CT densitometrie kan behulpzaam zijn bij het selecteren van kandidaten die van deze behandeling kunnen profiteren. Voor de chirurg kan objectieve vaststelling van de locatie en de ernst van emfyseem nuttig zijn zodat hij het meest emfysemateuze longweefsel kan reseceren. Samen met klinische bevindingen en longfunctie-onder-

zoek kunnen densitometrische data mogelijk helpen inzicht te verschaffen in de mechanismen die verantwoordelijk zijn voor verbetering na behandeling en langere termijn ontwikkeling van de aandoening.

Longitudinale studies van longmassa kunnen erg de moeite waard zijn in combinatie met metabole studies. Er is groeiende interesse in de relatie tussen de voedingsstatus en longarchitectuur. Langdurige ondervoeding en emfyseem veranderen de structuur van de luchthoudende ruimten distaal van de bronchiolus terminalis op min of meer overeenkomstige wijze. Dierexperimenteel onderzoek heeft herhaaldelijk aangetoond dat het gewicht van de long tijdens langdurig vasten vermindert. Een groot aantal patiënten dat lijdt aan COPD ondergaat een geleidelijk maar significant gewichtsverlies gedurende het beloop van hun ziekte. Het potentiële effect op het longgewicht is onbekend. De *in vivo* bepaling van de longdichtheid is dan interessant in het kader van de begripsvorming omtrent de pathofysiologie van door vasten geïnduceerde veranderingen in de pulmonale architectuur, alsook om de effectiviteit van therapeutische strategieën ter verbetering van de voedingstatus te evalueren.

---

# Acknowledgments

I feel greatly indebted to many persons who have contributed to the realization of this thesis.

Review of the manuscript: Prof dr J.M.A. van Engelshoven  
Dr G.J. Kemerink  
Prof dr E.F.M. Wouters

CT scan acquisitions: G.G.H. Wijnhoven

Secretarial help: H.M.J.C. Kengen

Statistical help: Drs A.G.H. Kessels

Software development: Dr G.J. Kemerink, B.J. Pellis, Ir G.R.P. Thelissen

Data analysis: Drs H.H. Kruize

Correction and translation: Dr G.J. Kemerink, Prof dr J.T. Wilmink

Coordination of patients: Drs M.P.K.J. Engelen, H.M.J.C. Kengen, Dr R.P.F. Schins

Referral of patients: Drs J.D. Does, Drs R. Mostert



---

## Curriculum vitae

Rob J.S. Lamers

1958	Geboren te Leiden
1978	Eindexamen Atheneum- $\beta$ Coriovallum College Heerlen
1979	Studie geneeskunde Rijks Universitair Centrum Antwerpen
1980-1986	Studie geneeskunde Universiteit van Utrecht
1986-1991	Opleiding radiologie Academisch Ziekenhuis Maastricht Opleider: Prof dr B.K. Janevski
1991-	Werkzaam als radioloog Academisch Ziekenhuis Maastricht Hoofd: Prof dr J.M.A. van Engelshoven